THE UNIVERSITY OF MICHIGAN

INDUSTRY PROGRAM OF THE COLLEGE OF ENGINEERING

ULTRASONIC-INDUCED CAVITATION STUDIES IN MERCURY AND WATER

R. Garcia
R. E. Nystrom
F. G. Hammitt

February, 1966

IP-731

ACKNOWLEDGMENTS

Financial support for this investigation was provided by a grant from the National Science Foundation. Mechanical properties data supplied by Pratt & Whitney Aircraft (CANEL) and the University of Michigan Department of Chemical & Metallurgical Engineering is also gratefully acknowledged.

Special thanks are also due Dr. Clarence A. Siebert, Professor of Chemical and Metallurgical Engineering, and Dr. M. John Robinson, Lecturer in Nuclear Engineering, for many helpful suggestions and continuing interest in this project; Mr. Richard L. Crandall, Research Assistant, Computing Center, for much assistance in the proper use of the Least Mean Squares Regression Program used for data correlation and the proper interpretation of results; Mr. Edward Rupke, Instrument Shop Supervisor, Mr. William Rekewitz, Instrument Shop Foreman, and Mr. John Love, Instrument Maker, for many helpful suggestions and prompt service in fabricating all of the test specimens and special hardware required; and Mr. Allen R. Schaedel, Research Assistant in the Department of Nuclear Engineering, for many helpful suggestions, stimulating conversation, and continuing interest in this project.

TABLE OF CONTENTS

TABLE OF CONTENTS CONT'D

LIST OF FIGURES

LIST OF FIGURES CONT'D

LIST OF TABLES

LIST OF TABLES CONT'D

CHAPTER I

INTRODUCTION

A. Importance of Cavitation Studies

Cavitation can be described as a hydrodynamic phenomenon which relates to the formation and collapse of vapor bubbles in a liquid. In general terms, these bubbles form in regions where the local pressure is reduced below the vapor pressure at that temperature and start to collapse as soon as the local pressure exceeds the vapor pressure. The bubble collapse can be considered as giving rise either to a shock wave which is propagated through the fluid, or to a small high-velocity liquid jet, in either case terminating at the wall of the fluid container. The effects produced as a consequence of cavitation are twofold. First, for flow processes, it generally decreases the transferable energy, and hence causes a loss in efficiency. Secondly, destruction (damage) of the material may take place at the point at which the shock wave or liquid jet terminates. Thus, it becomes necessary to investigate carefully those conditions resulting in cavitation and the damage suffered by various materials.

Since the cavitation damage process is apparently very closely related to damage from droplet or particle impingement or conventional erosion*, the damage data so obtained for various structural materials is

---

* Reference 1 includes many papers on the relations between these various forms of attack, including one by one of the present authors. Also ASTM Committee G-2 , of which one of the authors is the present vice-chairman, has recently been formed to attempt to relate these various phenomena and form applicable test standards.

also to some extent applicable to the resistance of these materials to these other forms of attack, so that the fields of droplet erosion in wet vapor streams (as in turbines or other two-phase flow passages), rain erosion of high-speed aircraft, micrometeorite bombardment of space vehicles, etc., are involved.

The successful pumping and handling of high-temperature liquid metals, wherein cavitation itself is a problem, is of considerable importance in the present and future space program, particularly from the viewpoint of power generation using nuclear heat sources and liquid-metal Rankine cycle power-conversion equipment. As has been recently demonstrated, damaging cavitation attack can occur in bearings[2], close-clearance passages[3], etc., as well as pumps[4],[5]. Recent theoretical studies[6] emphasize, in addition, a form of microcavitation that may also occur in many high-performance bearing applications and even in components such as gear teeth, so that the pitting which is often found in such units may well be a result of a form of cavitation. The same problems are, of course, also important in the conventional nuclear power plant program[3], which includes several existing and projected reactor systems using liquid metals as the coolant.

In the SNAP application the minimization of size and weight and the maximization of temperature are of over-riding importance, so that the fluid-handling equipment must be designed to operate under conditions approaching cavitation or actually in a cavitating regime. Hence, it becomes necessary to know realistically under what conditions cavitation

can be anticipated, and the quantity and quality of damage to be expected for a given degree of cavitation, since it may not be possible or desirable to avoid the cavitating regime entirely by over-conservative design, as has been the practice for conventional applications.

B. Importance and Significance of Accelerated Cavitation Studies

In a prototype system, the damage due to cavitation appears usually only after fairly lengthy operation under design conditions. Hence, it is clear that if a systematic study is to be made, involving a variety of materials and numerous plant conditions, it will be necessary to expend large amounts of time and money. An alternate approach, sacrificing direct applicability to some extent in the interests of economy, is to accelerate the cavitation losses by employing any one of several laboratory techniques which have been developed for this purpose. One commonly-used method which is also employed in our own laboratory is a flowing tunnel system utilizing a venturi test section and a centrifugal pump to circulate the test fluid around a closed loop. This system has been described elsewhere.(7) The venturi is reasonably similar to actual flow systems, but at the same time damage occurs only rather slowly. As an alternative to a flowing system, various acoustic techniques have been used by researchers in the past to bring about accelerated cavitation.(8), (9), (10), (11) Presently, accelerated cavitation studies are conventionally conducted through the use of polarized magnetostrictive or polycrystalline piezoelectric materials. Various materials exhibit either the piezoelectric effect or the phenomenon of magnetostriction. Both effects are

reversible. The utilization of such acoustic techniques appears to allow economical screening of a wide variety of materials in various fluids under ambient and elevated temperatures. The method has been widely used in the past for cavitation studies in water and other ambient temperature fluids, but not until very recently have tests been conducted in high-temperature liquid metals as sodium[3], [12], [13] and lead-bismuth alloy[14], [15] and, of course, the present tests in mercury.

In the past, the utility of acoustic cavitation damage results has been limited because no direct correlation with cavitation in a flowing system has been available. However, if such a correlation could be formulated, it might be possible to substitute relatively economical acoustic testing for tests in a tunnel facility. Our own laboratory has conducted cavitation tests in both water and mercury in venturi facilities[16], [17], [18] for the past several years and has accummulated much useful data over this period of time. It is expected that the accelerated cavitation data obtained with the acoustic facility can be compared with the tunnel results, so that a correlation can be obtained, allowing a more direct application of the accelerated test results. In the meanwhile, it is our belief that the accelerated device provides a useful and economical screening test, but that final check tests of a few selected materials should be made in a flowing system such as the venturi facility.

It has been demonstrated[19] that a pulsing technique, whereby a short period of cavitation is followed by a longer non-cavitating interval, produces more meaningful results in cases where corrosion is important. The accumulated non-cavitating time allows a more realistic opportunity

for any corrosion mechanism to manifest itself on the test specimen. In a purely cavitating experiment of the accelerated type, the test time involved might be so short that the corrosion contribution to the total damage mechanism would be negligible as compared to field conditions, and hence the results obtained misleading. Such pulsing apparatus can be used for both steady and pulsed cavitation studies. Hence, the effect of corrosion damage can be quantitatively determined. Although the present facility has this capability, it has not been used in this fashion thus far, since, as discussed later, corrosion has apparently been quite negligible.

It is possible to measure the relative cavitation resistance to high-temperature liquid metals and water of numerous potentially useful alloys in a simple and economical test using the vibratory facility which has been developed by this laboratory. Almost any liquid metal of interest could be accommodated in the present facility. This initial screening of materials under relatively realistic fluid and temperature conditions would be of great value in choosing materials for those components susceptible to cavitation-erosion attack, or, as previously mentioned, droplet-impingement or pure erosion.

In addition to the cavitation testing program, it is essential to determine the applicable mechanical properties of the materials tested at the test temperatures so that a correlation between resistance to this form of two-phase attack and some combination of the mechanical properties can be obtained. Applicable mechanical properties certainly might include

the ultimate tensile strength, yield strength, hardness, strain energy to failure, elongation, reduction in area, impact resistance, etc. If such a correlation were available, it would be possible not only to choose intelligently materials for these various purposes, but also to specify the most desirable heat-treat program, surface treatment, etc. Such a procedure would eliminate the necessity for costly materials-screening programs such as have been necessary many times in the past after the construction of a particular facility. Further, it would be possible to specify materials in critical locations in advance so that more aggressive designs (and hence more economical designs, as for liquid metal pumps, etc.) could be used.

C. The University of Michigan High-Temperature Ultrasonic Cavitation Vibratory Facility

The University of Michigan high-temperature ultrasonic cavitation vibratory facility has been described elsewhere.[7], [20] However, the major features of the facility will be reviewed here. Figure 1 is a schematic block diagram of the high-temperature ultrasonic vibratory facility showing the audio-oscillator, power-amplifier, transducer-horn assembly, test specimen, oscilloscope, frequency counter, high-temperature furnace and cavitation vessel, and accelerometer. The signal supplied by the variable-frequency audio-oscillator is amplified and applied to the piezoelectric crystals. The resultant periodic motion of the crystals effectively constitutes a standing wave generator with the amplitude of the standing wave being increased as it traverses the exponential horn assembly. The use of exponential horns as velocity

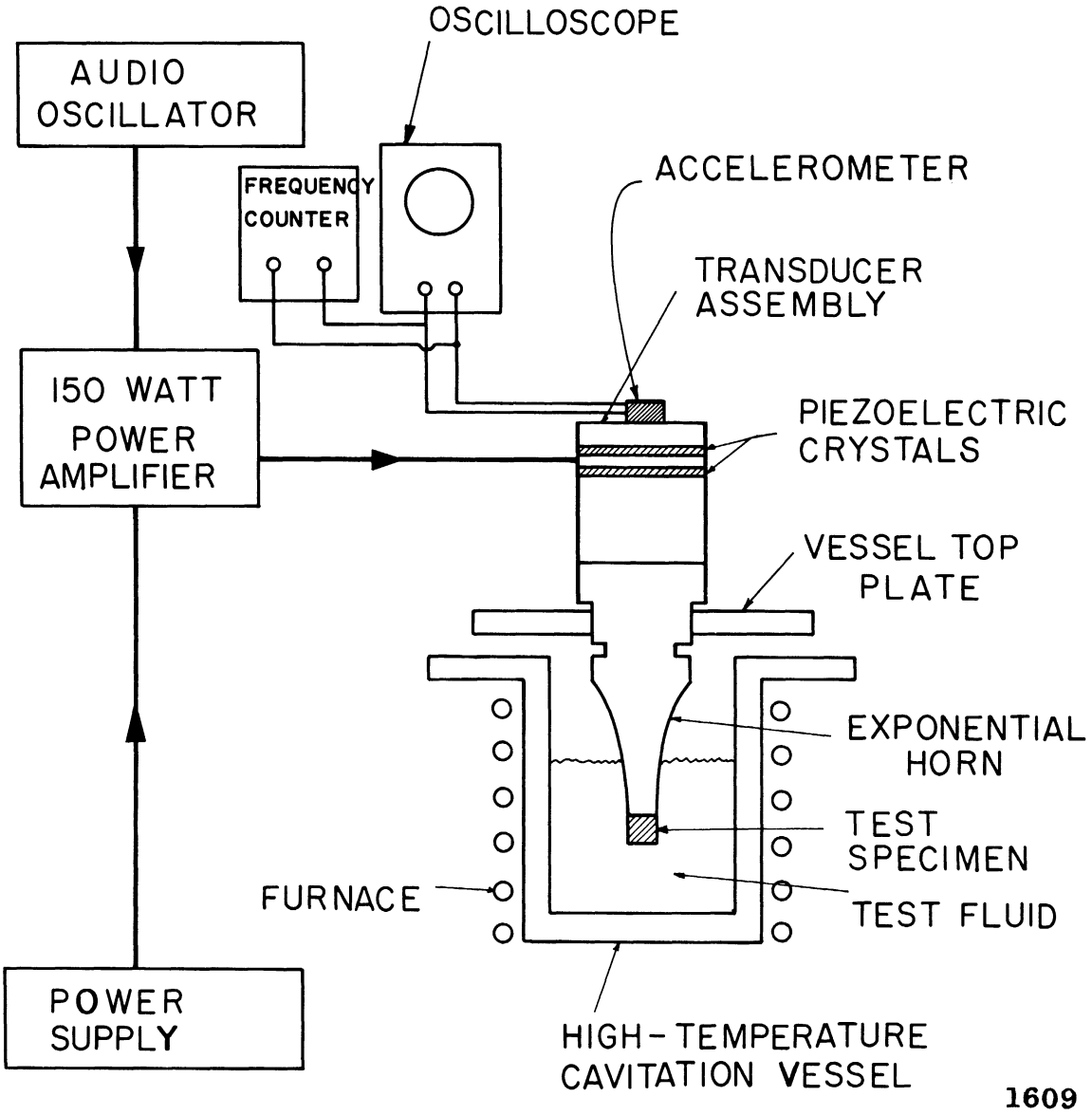

Figure 1. Block Diagram of the High-Temperature Ultrasonic Vibratory Facility.

transformers in this fashion was first suggested by Mason.[21] The movement of the horn tip, to which a test specimen has been attached, results in a rapid variation in local pressure, causing the periodic formation and collapse of an intense cavitation cloud. The final result is an accelerated erosion of the test specimens subjected to the collapsing bubble cloud. The materials of interest can be tested in a variety of fluids over a wide temperature range. For studies at elevated temperatures the transducer-horn assembly is attached to the special cavitation vessel which is filled with the appropriate fluid. Figure 2 is a photograph of the facility showing the audio-oscillator, power-amplifier, voltmeter, oscilloscope, timer, temperature controller, furnace, and the transducer-horn assembly installed in the high-temperature cavitation vessel. The vessel is inserted in the furnace. The line running to the vessel supplies argon as a cover gas for the fluid..

The cavitation facility has been completely calibrated and operated at fluid temperatures in excess of 1500°F at a frequency of $\sim$ 20 Kc./sec. and double amplitude of $\sim$ 2 mils. It is capable of operation with a variety of fluids.

D. Present Investigation

Recently cavitation-erosion data have been obtained in mercury at 70°F and 500°F and in water at 70°F for a variety of materials. This investigation is part of a continuing effort whose objectives are the determination of materials showing the greatest cavitation resistance in water at room temperature and in liquid metals at elevated temperatures; the determination of material-fluid parameters to correlate damage

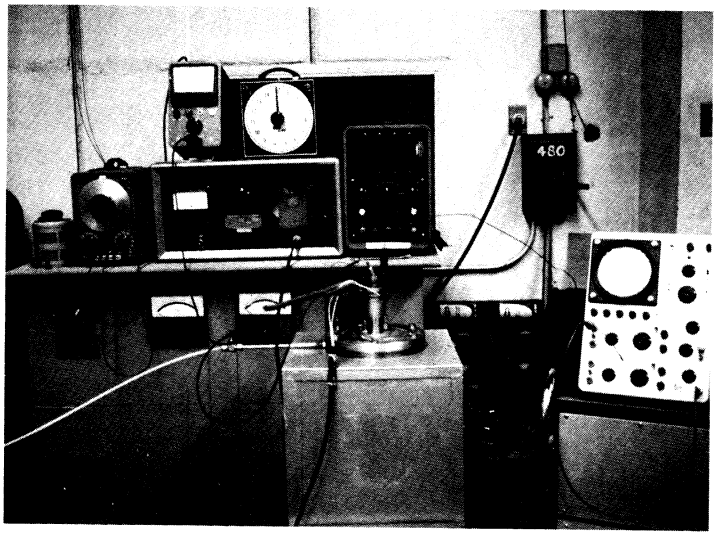

1767

Figure 2. Photograph of the High-Temperature Cavitation Facility.

and allow its á priori prediction; and the development of a relationship between the damage incurred in the venturi facilities operated by this laboratory and the damage noted in the present vibratory facility studies. Previously, cavitation-erosion results obtained in lead-bismuth alloy at 500°F and 1500°F utilizing the vibratory facility were reported.[22] The present investigation includes measurements of the cavitation resistance of several high-temperature refractory materials that were previously tested in the lead-bismuth program in addition to several other materials that were included because of availability of data from the venturi studies. These materials include various grades of aluminum, stainless steels, carbon steel, tantalum-base alloys, Mo-1/2Ti, Cb-1Zr, Cb-1Zr(A), Plexiglas, and various heat-treats of Cu, Cu-Zn, Cu-Ni, and Ni alloys. Table I summarizes the specimen material-fluid-temperature combinations which were studied in this investigation.

TABLE I

SPECIMEN MATERIAL-FLUID-TEMPERATURE COMBINATIONS INVESTIGATED

Material \ Fluid	Water 70°F	Mercury 70°F	Mercury 500°F
1100-0 Al (U-M)	X	---	---
2024-T351 Al (U-M)	X	---	---
6061-T651 Al (U-M)	X	---	---
304 Stainless Steel (U-M)	X	X	X
316 Stainless Steel (U-M)	X	X	X
Hot-Rolled Carbon Steel (U-M)	X	X	X
T-111 (Ta-8W-2Hf) (P & W)	X	X	X
T-222 (Ta-9.5W-2.5Hf-.05C) (P & W)	X	X	---
T-222 (A) (P & W)	---	---	X
Mo-1/2Ti (P & W)	X	X	X
Cb-1Zr (P & W)	X	X	X
Cb-1Zr (A) (P & W)	X	X	X
Plexiglas (U-M)	X	X	---
Cu (60% cold-worked) (U-M)	X	---	---
Cu (900°F anneal, 1 hour) (U-M)	X	---	---
Cu (1500°F anneal, 1 hour) (U-M)	X	---	---
Cu-Zn (60% cold-worked) (U-M)	X	---	---
Cu-Zn (850°F anneal, 1 hour) (U-M)	X	---	---
Cu-Zn (1400°F anneal, 1 hour) (U-M)	X	---	---
Cu-Ni (60% cold-worked) (U-M)	X	---	---
Cu-Ni (1300°F anneal, 1 hour) (U-M)	X	---	---
Cu-Ni (1800°F anneal, 1 hour) (U-M)	X	---	---
Ni (75% cold-worked) (U-M)	X	---	---
Ni (1100°F anneal, 1 hour) (U-M)	X	---	---
Ni (1600°F anneal, 1 hour) (U-M)	X	---	---

NOTES:

1. "X" indicates test conducted for this specimen material-fluid-temperature combination.

2. The notations (U-M) and (P & W) following the specimen materials indicate the source of the material, namely, The University of Michigan and Pratt & Whitney Aircraft (CANEL), respectively; whereas the notation (A) denotes an annealed condition of the material.

CHAPTER II

CAVITATION STUDIES IN MERCURY AT 500°F

A. Experimental Procedure

The eight materials tested in mercury at 500°F were 304 stainless steel (U-M), 316 stainless steel (U-M), hot-rolled carbon steel (U-M), T-111(Ta-8W-2Hf) (P & W), T-222(A) (Ta-9.5W-2.5Hf-.05C) (P & W), Mo-1/2Ti(P & W), Cb-1Zr(P & W), and Cb-1Zr(A) (P & W) . Standard cavitation test specimens, as shown in Figure 3, were machined from available bar stock. The required dimensions "A" and "B" for the eight materials tested are listed in Table II. The required dimensions for other materials tested in mercury and water at 70°F are also listed in Table II.

TABLE II

SPECIMEN DIMENSIONS

Material	"A"	"B"
304 Stainless Steel	.250"	.625"
316 Stainless Steel	.250"	.625"
Hot-Rolled Carbon Steel	.250"	.625"
T-111	.085"	.460"
T-222	.085"	.460"
T-222(A)	.085"	.460"
Mo-1/2Ti	.175"	.550"
Cb-1Zr	.220"	.595"
Cb-1Zr(A)	.220"	.595"
1100-0 Aluminum	.820"	1.195"
2024-T351 Aluminum	.820"	1.195"
6061-T651 Aluminum	.820"	1.195"

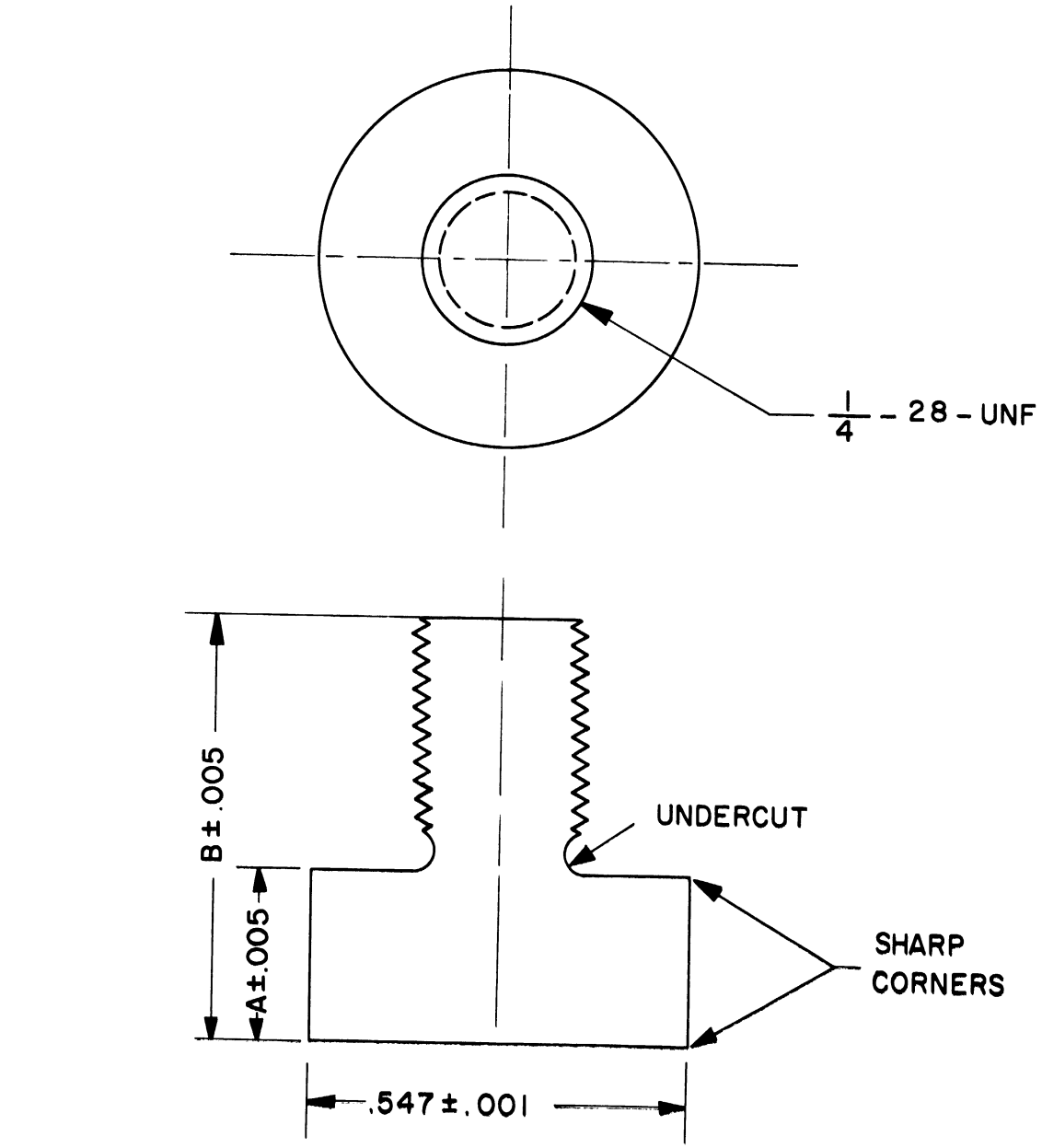

Figure 3. Standard Cavitation Test Specimen.

These dimensions provide a standard specimen weight of 9.4 ± .1 g. Initially, each of the specimens was weighed on a precision balance to an accuracy of 0.01 mg., and then attached to the tip of the stainless steel exponential horn, whereupon the unit was assembled. The mercury test fluid is maintained at the required test temperature of 500°F throughout the test with a suitable temperature controller. Variations in temperature during the test amounted to less than 5°F. The test specimens are oscillated by a pair of lead-zirconate-titanate piezoelectric crystals at ~ 20 Kc./sec. with the horn tip immersed ~ 1 1/2 inches into the mercury. The double amplitude at the specimen was ~ 2 mils and the argon cover gas over the mercury was maintained at 2.4 psig throughout the 500°F investigations. The value of argon cover gas pressure is chosen for a given fluid-temperature combination such that the difference between local pressure at the specimen and vapor pressure of the fluid is approximately constant for all investigations involving a variety of fluid-temperature combinations.* Total test duration varied for the different materials, ranging from 8 to 12 hours, with frequent inspections and weighings monitoring the specimen surface. Prior to each weighing any excess mercury adhering to the specimen surface was removed by heating in a vacuum furnace so as to eliminate oxidation of the specimen.

B. Experimental Results

The cavitation results obtained at 500°F in mercury will be

---

* The facility limitations are such that it is not possible to maintain a constant NPSH at the horn tip.

displayed as accumulative weight loss versus test duration, and also as accumulative mean depth of penetration (MDP) versus test duration. The mean depth of penetration, computed assuming that the weight loss is smeared uniformly over the cavitated specimen surface, is felt to be more physically meaningful than weight loss, since it is generally the total penetration of a particular component by cavitation erosion that would render it unfit for service. Of course, neither weight loss nor MDP is sensitive to damage distribution and form, i.e., damage may vary from isolated deep pits to relatively uniform wear, depending on material-fluid combination. Obviously, a "figure of merit" such as MDP takes into account the large variation in density that may occur within a set of test materials.

The appropriate expression for computing the MDP of a given material is of the form:

$$MDP(\text{mils}) = C \cdot W$$

where W is the weight loss expressed in mg. and C is a constant for the given material. Values of the constant C for computing the MDP of all the materials tested, along with their densities, are presented in Table III.

Table IV summarizes the cavitation results obtained in mercury at 500°F. Figure 4 is a plot of accumulative weight loss versus test duration, while Figure 5 is the corresponding plot of accumulative MDP versus test duration for the eight materials tested.

TABLE III

RELATION BETWEEN WEIGHT LOSS AND MDP

(MDP = C·W)

Material	Density	Constant, C*
1100-0 Al	2.77 g/cc.	.0935
2024-T351 Al	2.77	.0935
6061-T651 Al	2.77	.0935
304 Stainless Steel	7.85	.033
316 Stainless Steel	7.85	.033
Hot-Rolled Carbon Steel	7.85	.033
T-111	17.66	.0147
T-222	17.66	.0147
T-222(A)	17.66	.0147
Mo-1/2Ti	10.22	.0253
Cb-1Zr	8.72	.0296
Cb-1Zr(A)	8.72	.0296
Plexiglas	1.23	.210
Cu(60% cold-worked)	8.97	.0288
Cu(900°F anneal, 1 hour)	9.04	.0287
Cu(1500°F anneal, 1 hour)	9.06	.0286
Cu-Zn(60% cold-worked)	8.61	.0300
Cu-Zn(850°F anneal, 1 hour)	8.62	.0300
Cu-Zn(1400°F anneal, 1 hour)	8.62	.0300
Cu-Ni(60% cold-worked)	9.05	.0287
Cu-Ni(1300°F anneal, 1 hour)	9.05	.0286
Cu-Ni(1800°F anneal, 1 hour)	9.02	.0287
Ni(75% cold-worked)	8.97	.0288
Ni(1100°F anneal, 1 hour)	9.00	.0288
Ni(1600°F anneal, 1 hour)	9.00	.0288

* Valid when MDP is expressed in mils and W is expressed in mg.

On the basis of either average weight loss rate or average MDP rate it is clear that the T-111 is the most cavitation resistant of the materials tested, while the T-222(A) is about 7% less resistant. These materials exhibited average MDP rates of .43 mils/hour and .46 mils/hour, respectively. The hot-rolled carbon steel, 316 stainless steel, and 304 stainless steel rank third, fourth, and fifth, respectively, with average MDP rates of .61 mils/hour, .63 mils/hour, and .69 mils/hour, respectively. Three refractory materials: Mo-1/2Ti, Cb-1Zr, and Cb-1Zr(A) were the least resistant to cavitation damage, with the Cb-1Zr(A) suffering gross damage and ranking last among the materials tested. These three materials suffered damage ranging from 3X to 8X greater than that suffered by the tantalum-base alloys, T-111 and T-222(A). It is clear from Figures 4 and 5 that the rate of erosion for each individual material is approximately constant for all the materials tested for the duration of the test.

TABLE IV

SUMMARY OF CAVITATION RESULTS IN MERCURY AT 500°F

Material	Avg. Wt. Loss Rate	Avg. MDP Rate
T-111(P & W)	29.48 mg./hr.	.43 mils/hr.
T-222(A) (P & W)	31.52	.46
Hot-Rolled Carbon Steel (U-M)	18.60	.61
316 SS (U-M)	19.01	.63
304 SS (U-M)	20.83	.69
Mo-1/2Ti(P & W)	43.16	1.09
Cb-1Zr (P & W)	81.85	2.43
Cb-1Zr(A) (P & W)	125.78	3.73

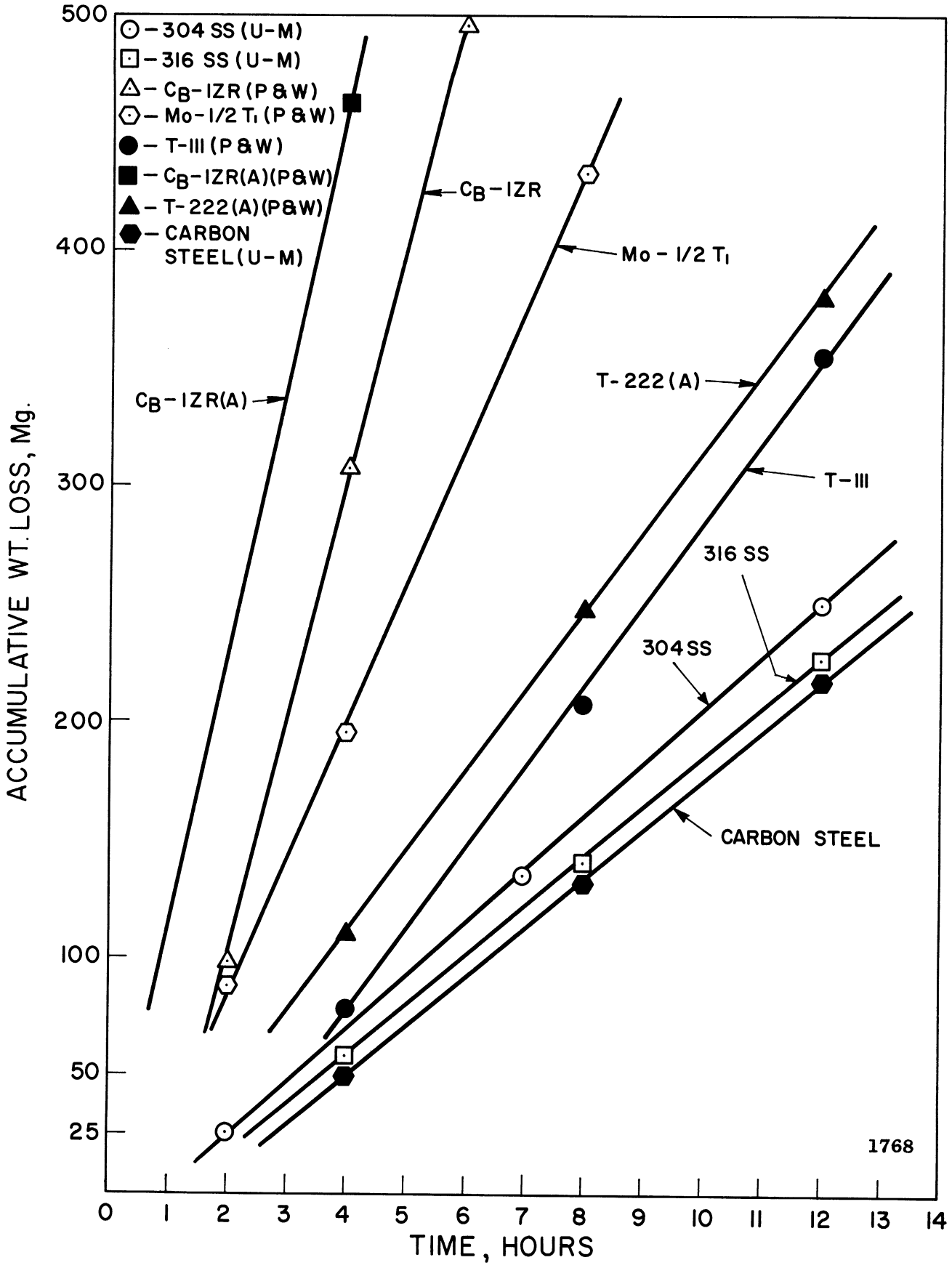

Figure 4. Effect of Cavitation Test Duration on Weight Loss at 500°F in Mercury.

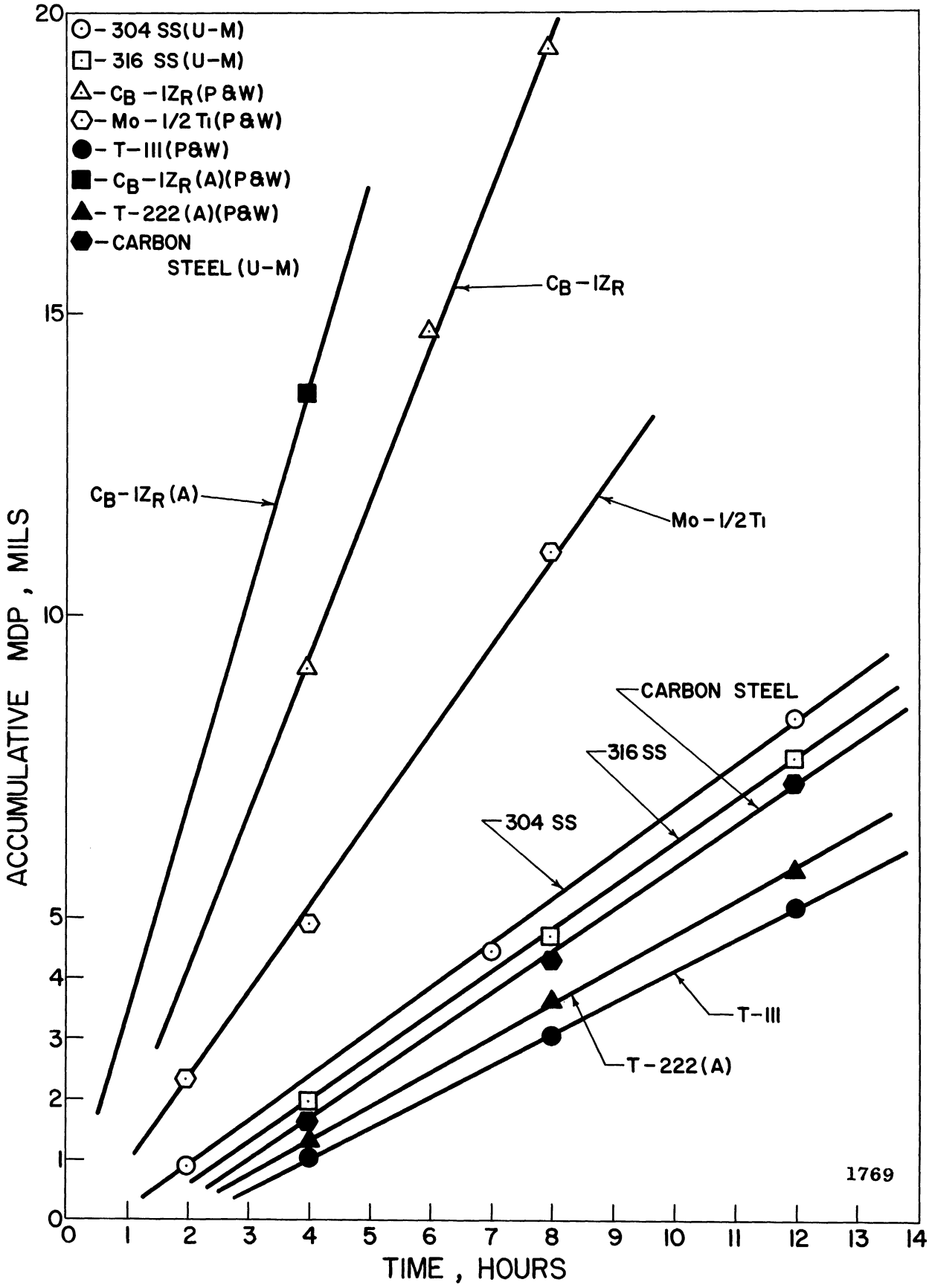

Figure 5. Effect of Cavitation Test Duration on MDP at 500°F in Mercury.

Photographs of the test specimens at the conclusion of the cavitation experiment are presented in Figure 6. The materials are arranged in order of decreasing resistance to cavitation damage. Note the severe pitting of the Mo-1/2Ti, Cb-1Zr, and Cb-1Zr(A) surfaces. In all cases the damage is relatively uniform over the specimen face as opposed to individual isolated, deep pitting. It is felt that the approximately constant rate of erosion noted for all the materials tested in mercury at 500°F is due to this uniform damage pattern, and the fact that the area presented to the collapsing bubble cloud is approximately constant for the duration of the test. A photograph of a 304 stainless steel specimen before exposure is included in Figure 6 and serves to indicate a representative initial surface condition for all the specimens tested.

Detailed examination of the 303 stainless steel exponential horn, the 316 stainless steel container vessel, and the sides of the various test specimens, all of which are <u>not</u> subject to cavitation, but <u>are</u> submerged in the test fluid, indicates that corrosion effects in the absence of cavitation in these investigations were negligible. Hence, one might assume that the damage suffered by the test specimens was due almost completely to the cavitation erosion process and not to chemical corrosion by the mercury test fluid.

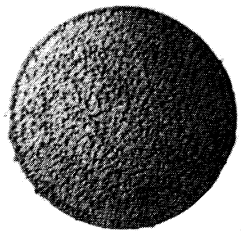

(1) T-111(P & W)
12 Hour Exposure

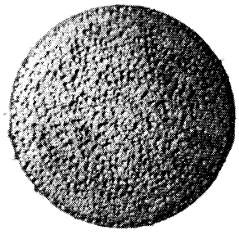

(2) T-222(A)(P & W)
12 Hour Exposure

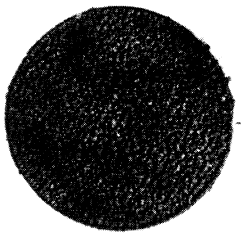

(3) Carbon Steel(U-M)
12 Hour Exposure

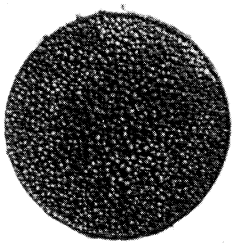

(4) 316 SS(U-M)
12 Hour Exposure

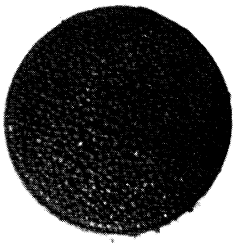

(5) 304 SS(U-M)
12 Hour Exposure

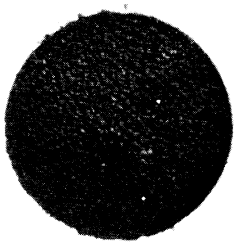

(6) Mo-1/2Ti(P & W)
12 Hour Exposure

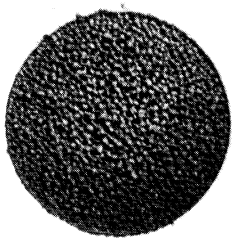

(7) Cb-1Zr(P & W)
8 Hour Exposure

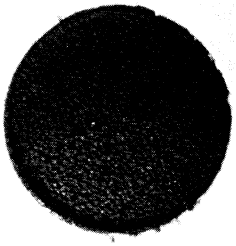

(8) Cb-1Zr(A)(P & W)
8 Hour Exposure

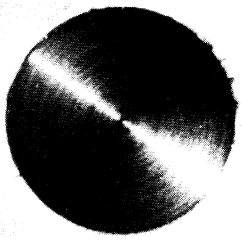

304 SS(U-M)
Before Exposure

Figure 6. Photographs of Specimens Subjected to Cavitation Damage in Mercury at 500°F.

CHAPTER III

CAVITATION STUDIES IN MERCURY AT 70°F

A. Experimental Procedure

The materials tested in mercury at 70°F were identical to those tested at 500°F and listed previously in Table I, with the exception of T-222 which was substituted for T-222(A) due to a shortage of the annealed stock. In addition Plexiglas was also tested at 70°F because of availability of cavitation data for this material from the venturi tests. Standard cavitation test specimens of T-222 have the same dimensions as given previously for the annealed stock (see Table II).

Due to the low density of the Plexiglas (compared to the other materials tested) and its brittle nature, it was completely impractical to fabricate standard cavitation test specimens as shown in Figure 3. The low density would result in an unusually large "A" dimension, while the brittle nature of the material made it impossible to firmly affix a specimen to the ultrasonic horn without damage to the threaded portion. It is necessary that the specimen be firmly and tightly attached to the horn tip so that the ultrasonic energy is properly transmitted across the interface for efficient operation. Hence the design shown in Figure 7 consisting of a Plexiglas test specimen with internal thread and a separate stainless steel mounting stud was adopted and proved to be satisfactory. The mounting stud results in a firm attachment of the Plexiglas cylinder to the horn tip without damage to the Plexiglas internal threads. This design overcomes all of the problems encountered with the standard cavitation test specimen.

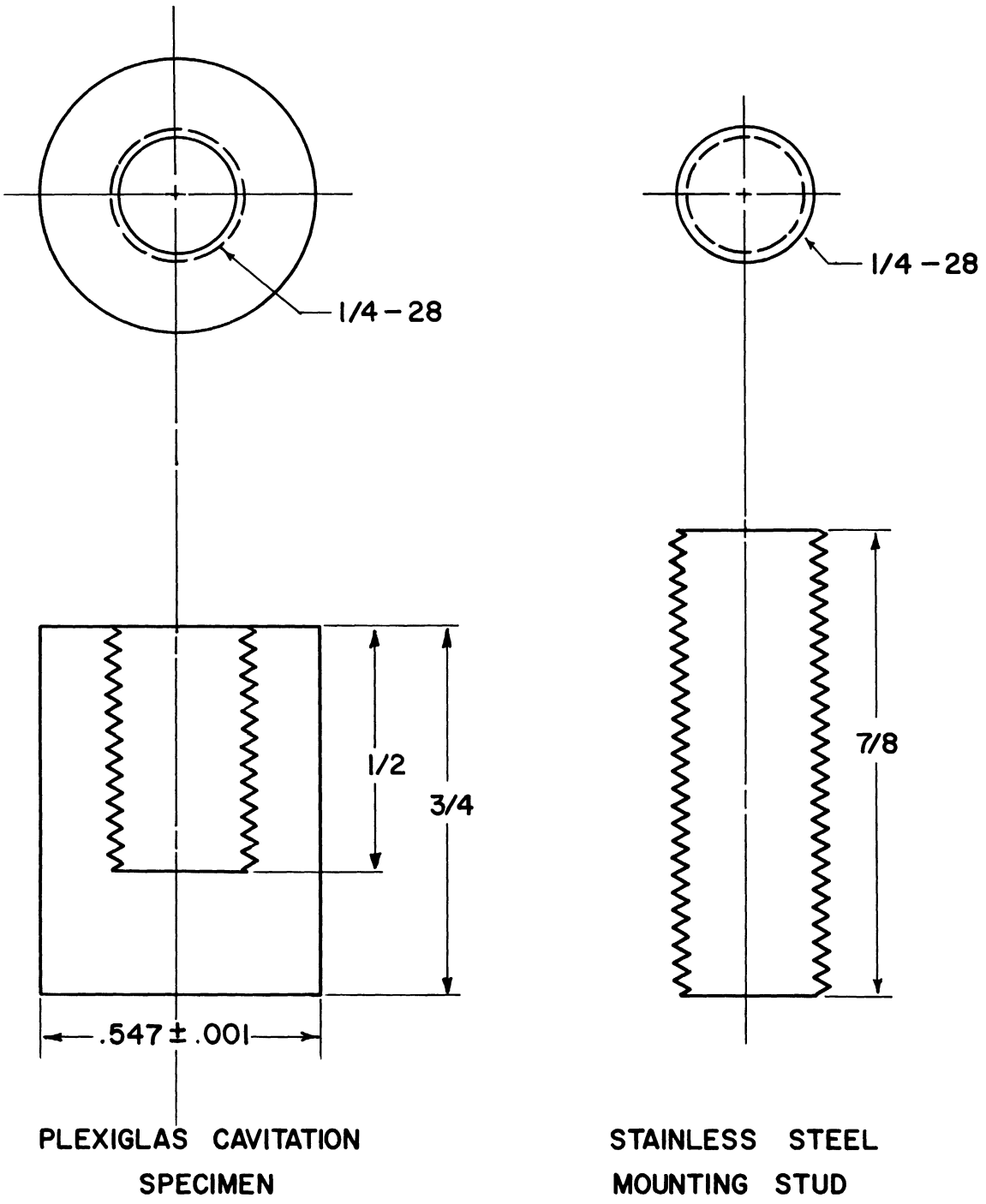

Figure 7. Special Plexiglas Cavitation Test Specimen and Mounting Stud.

The experimental procedure employed for the testing of the nine materials in mercury at 70°F closely parallels that used for the 500°F tests discussed previously. However, for the 70°F tests the argon cover gas pressure was maintained at 0.5 psig throughout the investigations. Total test duration varied for the different materials, ranging from 8 to 12 hours, with the exception of the Plexiglas which was tested for only one hour due to mechanical problems. Frequent inspections and weighings monitored the specimen surface. Prior to each weighing any excess mercury adhering to the specimen surface was removed by heating in a vacuum furnace (except for the Plexiglas) so as to eliminate oxidation of the specimen.

B. Experimental Results

The cavitation results obtained at 70°F in mercury will be displayed as accumulative weight loss versus test duration, and also as accumulative mean depth of penetration (MDP) versus test duration.

Table V summarizes the cavitation results obtained in mercury at 70°F. Figure 8 is a plot of accumulative weight loss versus test duration, while Figure 9 is the corresponding plot of accumulative MDP versus test duration for the nine materials tested.

The 304 stainless steel and 316 stainless steel were the most resistant to cavitation at 70°F based either on average weight loss rate or average MDP rate, differing by only 3%. These materials exhibited average MDP rates of .32 mils/hour and .33 mils/hour, respectively. The alloys T-111 and T-222 were 6% and 30% less resistant

TABLE V

SUMMARY OF CAVITATION RESULTS IN MERCURY AT 70°F

Material	Avg. Wt. Loss Rate	Avg. MDP Rate
304 SS (U-M)	9.82 mg./hr.	.32 mils/hr.
316 SS (U-M)	9.88	.33
T-111 (P & W)	23.71	.35
T-222 (P & W)	28.92	.43
Mo-1/2Ti (P & W)	22.58	.57
Cb-1Zr (P & W)	31.04	.92
Hot-Rolled Carbon Steel (U-M)	31.17	1.03
Cb-1Zr(A) (P & W)	54.22	1.61
Plexiglas (U-M)	19.00	3.99

than the stainless steels, respectively, while the Mo-1/2Ti was 80% less resistant. The Cb-1Zr, hot-rolled carbon steel, and Cb-1Zr(A) all suffered heavy damage in the cavitation environment at 70°F. The appropriate MDP rates for these materials were approximately 3X to 5X greater than for the stainless steels and the T-111. The Plexiglas suffered the most severe damage in terms of average MDP rate with a value of 3.99 mils/hour. It is clear from Figures 8 and 9 that the rate of erosion for each individual material is approximately constant for all the materials tested for the duration of the test.

Photographs of the test specimens at the conclusion of the cavitation experiment are presented in Figure 10. The materials are arranged in order of decreasing resistance to cavitation damage. Note the severe pitting of the Cb-1Zr, hot-rolled carbon steel, Cb-1Zr(A), and Plexiglas. In all cases the damage noted is relatively uniform over the specimen face as opposed to individual isolated, deep pitting. This was also the case for the 500°F tests in mercury as previously

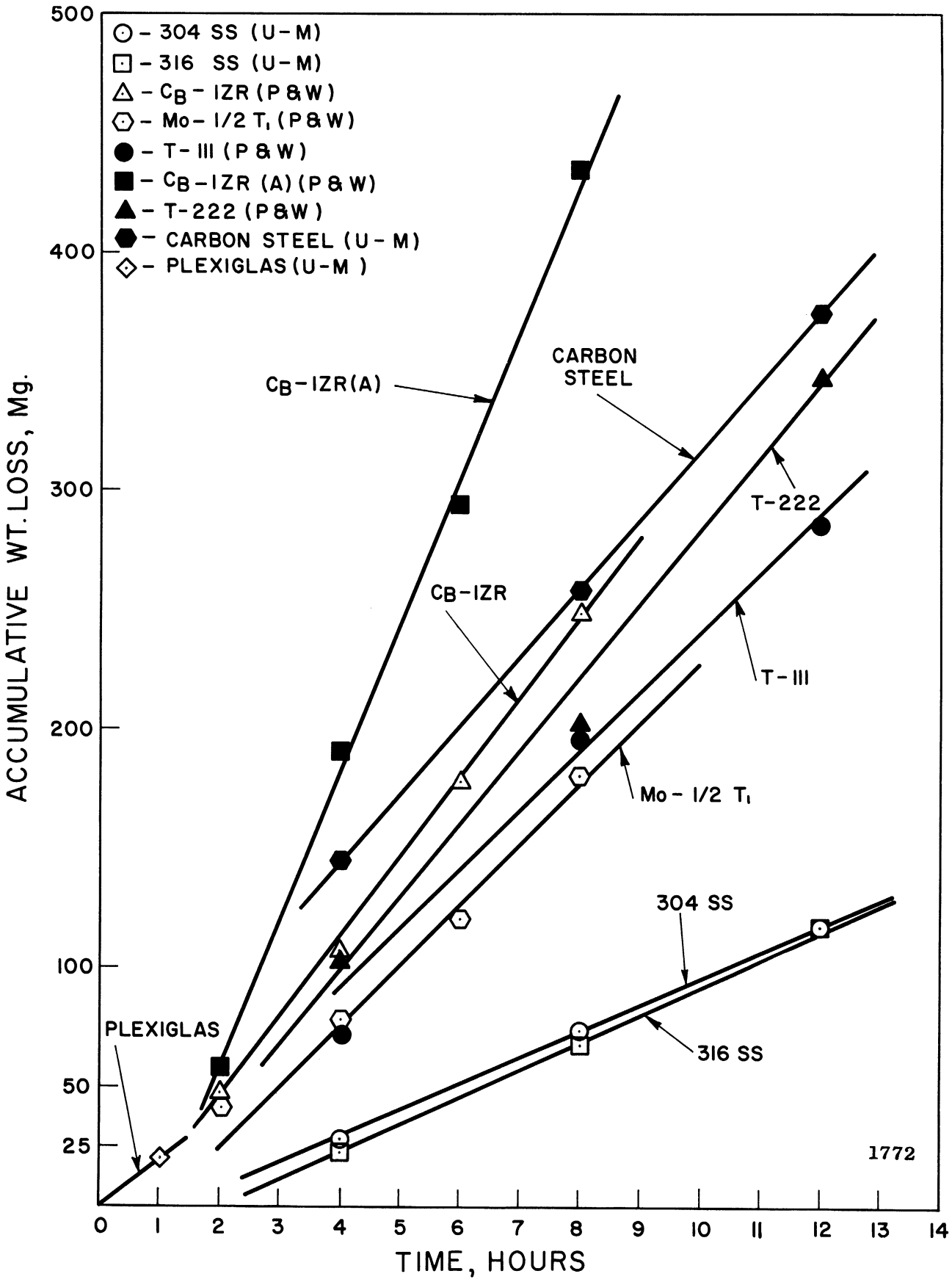

Figure 8. Effect of Cavitation Test Duration on Weight Loss at 70°F in Mercury.

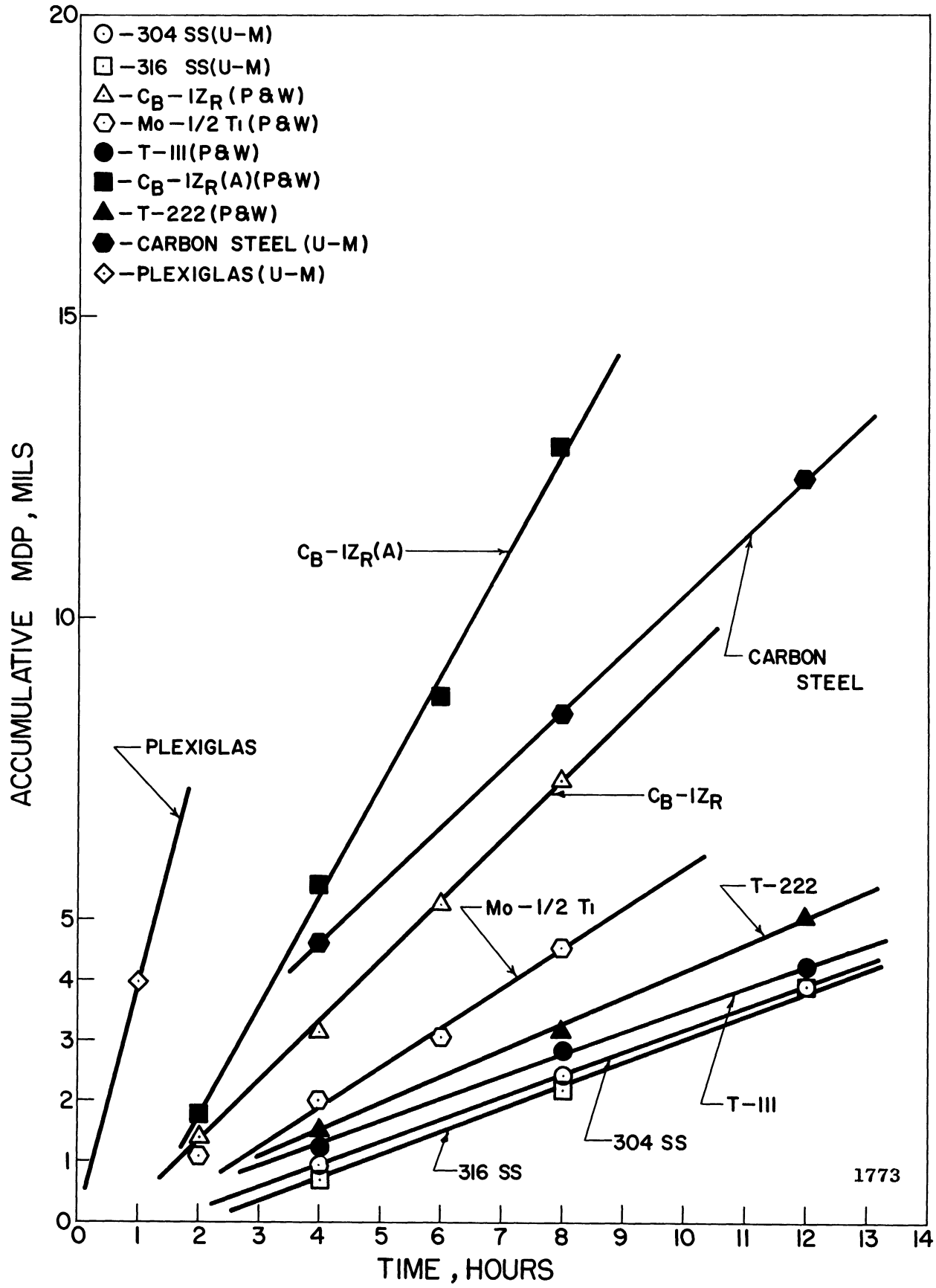

Figure 9. Effect of Cavitation Test Duration on MDP at 70°F in Mercury.

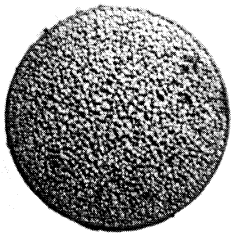

(1) 304 SS(U-M)
12 Hour Exposure

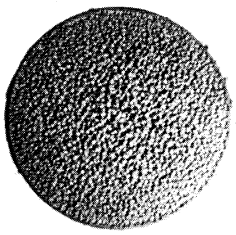

(2) 316 SS(U-M)
12 Hour Exposure

(3) T-111(P & W)
12 Hour Exposure

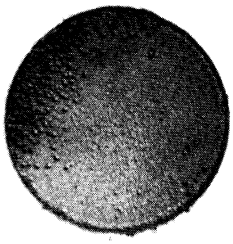

(4) T-222(P & W)
12 Hour Exposure

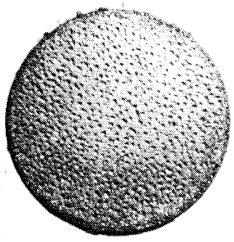

(5) Mo-1/2Ti(P & W)
8 Hour Exposure

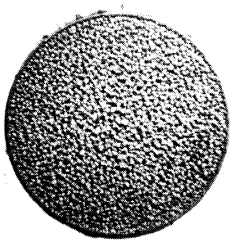

(6) Cb-1Zr(P & W)
8 Hour Exposure

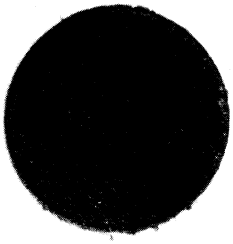

(7) Carbon Steel(U-M)
12 Hour Exposure

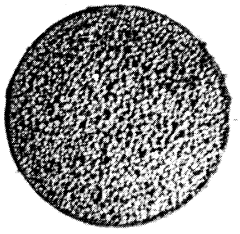

(8) Cb-1Zr(A)(P & W)
8 Hour Exposure

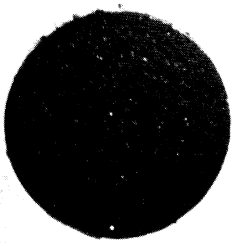

(9) Plexiglas(U-M)
1 Hour Exposure

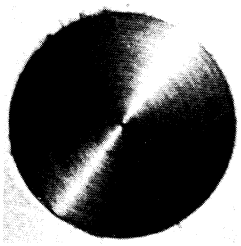

304 SS(U-M)
Before Exposure

1774

Figure 10. Photographs of Specimens Subjected to Cavitation Damage in Mercury at 70°F.

noted. It is felt that the approximately constant rate of erosion noted for all the materials tested in mercury at 70°F is due to this uniform damage pattern, and the fact that the area presented to the collapsing bubble cloud is approximately constant for the duration of the test. A photograph of a 304 stainless steel specimen before exposure is included in Figure 10 and serves to indicate a representative initial surface condition for all the specimens tested.

Detailed examination of the 303 stainless steel exponential horn, the 316 stainless steel container vessel, and the sides of the various test specimens, all of which are not subject to cavitation, but are submerged in the test fluid, indicates that corrosion effects in the absence of cavitation in these investigations were negligible. Hence, one might assume that the damage suffered by the test specimens was due almost completely to the cavitation erosion process and not to chemical corrosion by the mercury test fluid. This was also the case for the 500°F tests.

C. Comparison with Venturi Facility Mercury Results

It was noted earlier that the utility of acoustic cavitation damage results has been limited because no direct correlation with cavitation in a flowing system was available. However, if such a correlation could be formulated, it might be possible to substitute relatively economical acoustic testing for tests in a tunnel facility. This laboratory has conducted cavitation tests in both water and mercury for the past several years[23,24,25] and has accumulated much useful data

over this period of time. Now that data in mercury at 70°F has been obtained with the ultrasonic (acoustic) facility, it is possible to qualitatively compare the data from both facilities for similar materials.

Table VI is a tabulation of the available data in mercury at 70°F for the two facilities. The wear in the venturi loop is given in terms of MDP after 50 hours of testing, whereas in the case of the acoustic facility, the average MDP rate is listed. The stainless steels tested in the venturi are similar to the 304 SS and 316 SS tested in the ultrasonic facility, but not identical. The composition of the T-111 is Ta-8W-2Hf, so that the corresponding specimens in both facilities are of the same composition. The composition of the T-222 is Ta-9.5W-2.5Hf-.05C and differs slightly from the Ta-10W tested in the venturi. The carbon steels tested are not identical but have similar carbon content and hardness values. The remainder of the materials investigated in both facilities are nearly identical in composition.

In both facilities the materials have been listed in order of decreasing cavitation resistance, or increasing susceptibility to cavitation-erosion attack. It is clear from Table VI that the first five materials have identical rankings in each facility with the stainless steels being the most resistant to cavitation-erosion attack. The Cb-1Zr, carbon steel, and Cb-1Zr(A) occupy the next three places in this qualitative ranking for both facilities, but their rankings do not agree in detail. In the case of the venturi tests the Cb-1Zr ranks eighth, while it ranks sixth in the ultrasonic facility. The order of

ranking of the carbon steel and Cb-1Zr(A) is preserved in both facilities. It was noted in the venturi investigations that the damage sustained by the Cb-1Zr apparently indicated a thin multi-layer-like (laminated) structure. This could easily lead to greater damage and weight losses if one speculated that large sections of the Cb-1Zr outer layer were being removed by the cavitation action as opposed to the normal minute pitting mechanism that would be expected. The unusual structure of the Cb-1Zr tested in the venturi is as yet unexplained, but could account for the poor showing of this material in that facility. No such observation was made in the case of the acoustic facility. The Plexiglas was the least resistant to cavitation damage by far in both facilities and attained ninth ranking.

TABLE VI

COMPARISON OF CAVITATION EROSION DATA IN MERCURY AT 70°F - VENTURI AND ULTRASONIC FACILITIES

Venturi Data		Ultrasonic Data	
Material	MDP at 50 Hours	Material	Avg. MDP Rate
Stainless Steel	$.28 \times 10^{-2}$ mils	304 SS	.32 mils/hr.
		316 SS	.33
Ta-8W-2Hf	$.85 \times 10^{-2}$	T-111	.35
Ta-10W	1.71×10^{-2}	T-222	.43
Mo-1/2Ti	2.10×10^{-2}	Mo-1/2Ti	.57
Carbon Steel	2.94×10^{-2}	Cb-1Zr	.92
Cb-1Zr(A)	5.87×10^{-2}	Carbon Steel	1.03
Cb-1Zr	29.0×10^{-2}	Cb-1Zr(A)	1.61
Plexiglas	225×10^{-2} *	Plexiglas	3.99

* MDP at 25 hours

It is clear that with the exception of the Cb-1Zr the qualitative rankings of the materials tested in the venturi and ultrasonic facilities agree very well. This agreement offers hope that a quantitative correlation could be developed that would couple the results of the two facilities. Such a correlation must await the generation of more complete data in both facilities for a variety of test fluids and temperatures.

It is interesting to note from Table VI that the intensity of damage in the acoustic facility is approximately 1000X greater than that in the venturi loop, and also that the ratios of damage between various materials in the venturi facility is much greater even though the rankings are similar.

CHAPTER IV

COMPARISON OF CAVITATION RESULTS IN MERCURY AT 70°F AND 500°F IN VIBRATORY FACILITY

Table VII summarizes the cavitation data obtained in mercury at 70°F and 500°F. The eight materials tested have been rated on the basis of cavitation resistance as determined by MDP, with a rating of "1" indicating the most cavitation resistant material while a rating of "8" would denote that material most susceptible to cavitation damage.

The most cavitation-resistant materials at 70°F were the stainless steels with the tantalum-base alloys ranking third and fourth. At 500°F the superior mechanical properties of the tantalum-base alloys at even a very moderate elevated temperature are already evident as the T-111 and T-222(A) rank first and second, respectively. The hot-rolled carbon steel, 316 stainless steel, and 304 stainless steel rank third, fourth, and fifth, respectively, at 500°F. The Mo-1/2Ti, Cb-1Zr, and Cb-1Zr(A) all maintained the same relative position at both test temperatures. The hot-rolled carbon steel which had fared well at 500°F with a rating of "3" was damaged almost 70% more at 70°F. This supposedly anomalous behavior is easily explained by the fact that the mechanical properties of the hot-rolled carbon steel such as tensile strength and yield strength are greater at 500°F than at 70°F. This phenomenon is termed "strain aging". Eventually the strength properties pass through a maximum and then decrease with further increase in temperature. Very few materials possess this rather unique property.

TABLE VII

COMPARISON OF CAVITATION RESULTS IN MERCURY
AT 70°F AND 500°F - VIBRATORY FACILITY

Material	70°F		500°F	
	Avg. MDP Rate	Rating	Avg. MDP Rate	Rating
304 SS	.32 mils/hr.	1	.69 mils/hr.	5
316 SS	.33	2	.63	4
T-111	.35	3	.43	1
T-222 *	.43	4	.46*	2
Mo-1/2Ti	.57	5	1.09	6
Cb-1Zr	.92	6	2.43	7
Carbon Steel	1.03	7	.61	3
Cb-1Zr(A)	1.61	8	3.73	8
Plexiglas	3.99	9	----	-

* T-222(A) was tested at 500°F

It is further noted that with the exception of the hot-rolled carbon steel, all of the materials tested sustained greater damage at 500°F than at 70°F. The stainless steels were damaged about 100% more and the T-111 about 23% more, while the damage rates for the Mo-1/2Ti, Cb-1Zr, and Cb-1Zr(A) were 2X to 3X greater at 500°F than at 70°F. No direct comparison is possible in the case of the T-222 and T-222(A) as the mechanical properties of these materials are not comparable.

The effect of temperature on the cavitation results in mercury is further displayed in Figure 11 which is a plot of average MDP rate versus temperature for the eight materials tested. The effect of temperature on the T-111 and T-222 is almost negligible, while the effect on all of the other materials is quite dramatic, as evidenced by the slopes of the appropriate curves. The behavior of the hot-rolled carbon steel is once again noted. Later discussion shows that the

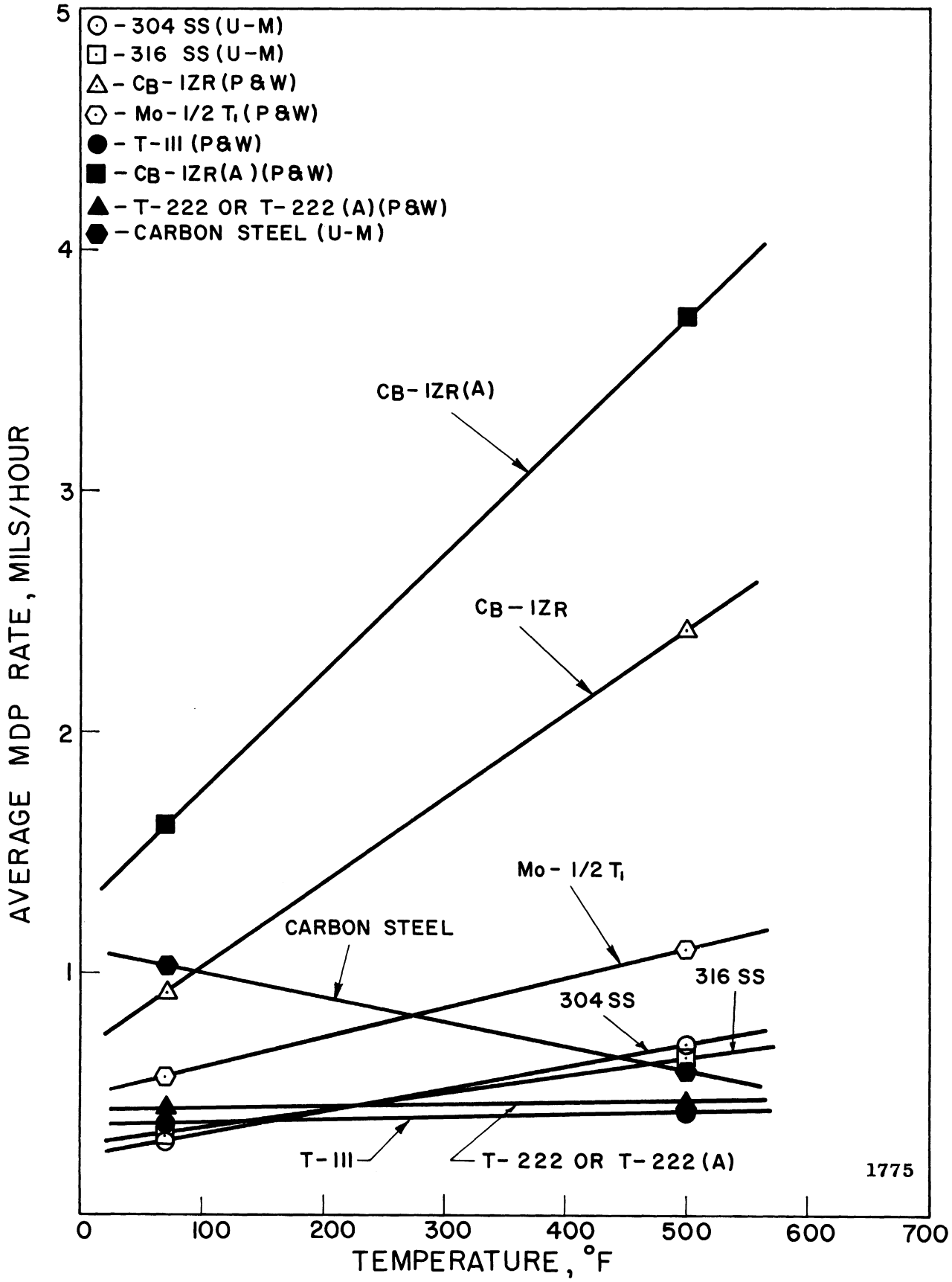

Figure 11. Effect of Temperature on Cavitation Resistance in Mercury.

temperature-dependent behavior of the cavitation resistance of these materials can be explained on the basis of the variation of mechanical properties data with temperature. It is further shown that the mechanical properties of the tantalum-base alloys are weak functions of temperature, whereas those of the other materials vary considerably from 70°F to 500°F.

CHAPTER V

CAVITATION STUDIES IN WATER AT 70°F

A. Experimental Procedure

The 24 materials tested in water at 70°F are listed in Table I (previously cited). The three grades of aluminum and the various heat-treats of Cu, Cu-Zn, Cu-Ni, and Ni were included in the vibratory cavitation program in water because extensive results from the venturi program are available for these materials in water. Standard cavitation test specimens, as shown in Figure 3 (previously cited), were machined from available bar stock of the three grades of aluminum. The appropriate "A" and "B" dimensions for aluminum were given in Table II.

It was desired to test in the vibratory facility the identical heat-treats of Cu, Cu-Zn, Cu-Ni, and Ni that had been previously tested in the venturi loop facility. Since these materials were available only in sheet stock 1/16" thick, it was necessary to design a special specimen consisting of an adaptor of a suitable material and a disc of the desired material. Means of attaching the disc to the adaptor had to be provided so that a firm bond would result. This is necessary so that the ultrasonic energy is efficiently transferred across the interface. Hence the design shown in Figure 12, consisting of a brass adaptor and a disc of the desired material, was adopted and proved to be satisfactory. The disc is fastened to the adaptor with soft solder. Various epoxies and cements were attempted as a bonding material, but the bond was immediately destroyed upon initiation of the test. The acoustic impedance of the soft solder is on the order

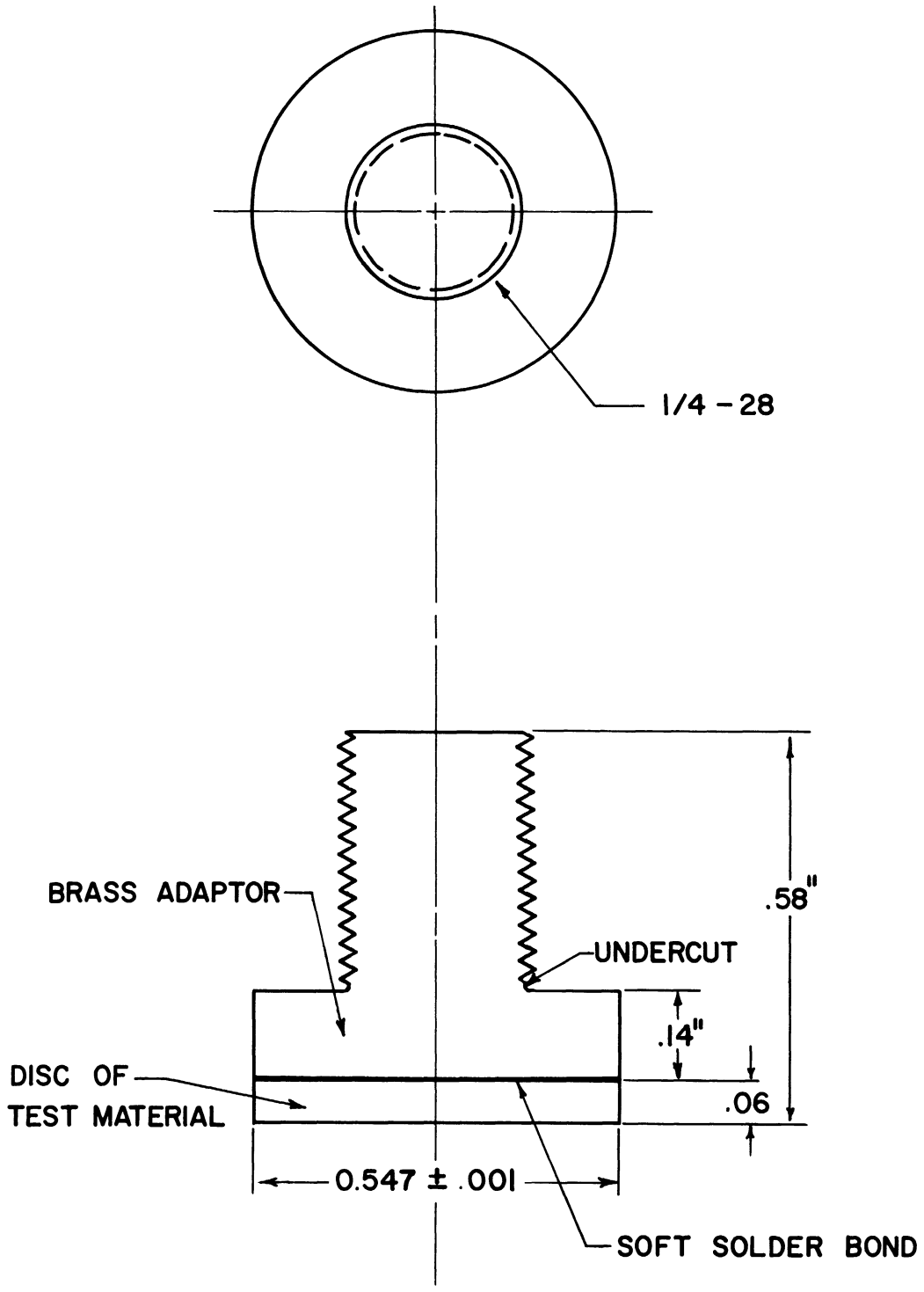

Figure 12. Special Cavitation Test Specimen for Cu, Cu-Zn, Cu-Ni, and Ni.

of that of both the brass adaptor and disc materials, while the epoxies and cements possessed a very low acoustic impedance due to negligible elastic properties. The arrangement shown in Figure 12 results in a standard specimen weight of 9.4 ± .1 g.

The Plexiglas specimens tested in water were fabricated as per Figure 7 (previously cited).

The water tests were conducted in a Plexiglas cavitation vessel whose dimensions are identical to those of the 316 stainless steel container previously employed for the mercury tests. The Plexiglas vessel permits visual observation of the bubble cloud and continuous monitoring of the condition of the specimen surface during a test. All other equipment is identical to that previously used in the mercury investigation.

The test specimens are oscillated by a pair of lead-zirconate-titanate piezoelectric crystals at ~ 20 Kc/sec with the horn tip immersed ~ 1 1/2 inches into the water. The double amplitude at the specimen was ~ 2 mils and the argon cover gas over the water was maintained at 1.1 psig throughout the investigations. Total test duration varied for the different materials, ranging from 1 hour for the very soft 1100-0 aluminum to 36 hours for the stainless steels and the refractory materials. The Cu, Cu-Zn, Cu-Ni, and Ni specimens were tested for 6 hours. Frequent inspections and weighings monitored the specimen surface.

B. Experimental Results

The cavitation results obtained in water at 70°F will be displayed as accumulative weight loss versus test duartion, and also as accumulative mean depth of penetration (MDP) versus test duration.

The appropriate expressions for computing the MDP of the aluminum, Cu, Cu-Zn, Cu-Ni, and Ni alloys were presented in Table III.

The 24 materials tested in water at 70°F have been divided into three subsets for data display purposes. One subset consists of those materials that have also been tested in mercury and lead-bismuth[22], namely 304 SS, 316 SS, T-111, T-222, Mo-1/2Ti, hot-rolled carbon steel, Cb-1Zr, and Cb-1Zr(A). The second subset consists of the three aluminum alloys and Plexiglas, while the third subset includes the 12 alloys of Cu, Cu-Zn, Cu-Ni, and Ni. The second and third subsets contain materials that have been tested only in water (with the exception of the Plexiglas that was tested in mercury at 70°F).

Table VIII summarizes the cavitation results obtained in water at 70°F for the materials in the first two subsets. Figure 13 is a plot of accumulative weight loss versus test duration while Figure 14 is the corresponding plot of accumulative MDP versus test duration for the eight materials contained in Subset 1. Figures 15 and 16 are the corresponding plots for Subset 2 which consists of the aluminum alloys and the Plexiglas.

On the basis of either average weight loss rate or average MDP rate it is clear that the T-222 is the most cavitation resistant of the materials contained in Subsets 1 and 2. The T-111 which ranked second suffered about 3X more damage than the T-222, while the Mo-1/2Ti and 316 stainless steel were equally damaged and ranked third and fourth. The 304 stainless steel in fifth place sustained 5X more damage than the T-222. The Cb-base alloys, Cb-1Zr and Cb-1Zr(A),

and the hot-rolled carbon steel ranked sixth through eighth, respectively, and suffered damage 7 to 12X more severe than the T-222, based on average MDP rate. The aluminum alloys and the Plexiglas were the least resistant to cavitation-erosion attack among the materials in Subsets 1 and 2. Considering only the three aluminum alloys, the 2024-T351 alloy was the most resistant while the very soft 1100-0 alloy sustained the greatest damage.

TABLE VIII

SUMMARY OF CAVITATION RESULTS IN WATER - SUBSETS 1 AND 2

Material	Avg. Wt. Loss Rate	Avg. MDP Rate
T-222(P & W)	1.05 mg./hr.	.02 mils/hr.
T-111(P & W)	4.33	.06
Mo-1/2Ti(P & W)	3.49	.09
316 SS (U-M)	2.81	.09
304 SS (U-M)	3.04	.10
Cb-1Zr(P & W)	5.10	.15
Cb-1Zr(A)(P & W)	6.10	.18
Carbon Steel(U-M)	7.08	.23
2024-T351 Al(U-M)	6.13	.57
6061-T651 Al(U-M)	7.73	.72
Plexiglas (U-M)	6.60	1.39
1100-0 Al (U-M)	28.90	2.70

An examination of Figures 13 and 14 indicates that the rate of erosion for the T-222, T-111, Mo-1/2Ti, 316 SS, and 304 SS is approximately constant for the duration of the test, while the rate of erosion for the Cb-1Zr, Cb-1Zr(A), and the hot-rolled carbon steel is approximately constant during the early stages of the test and then begins to decrease as the accumulative weight loss and the accumulative MDP increase to larger values. Examination of the specimens generally indicated that those materials showing a linear response rate exhibit a

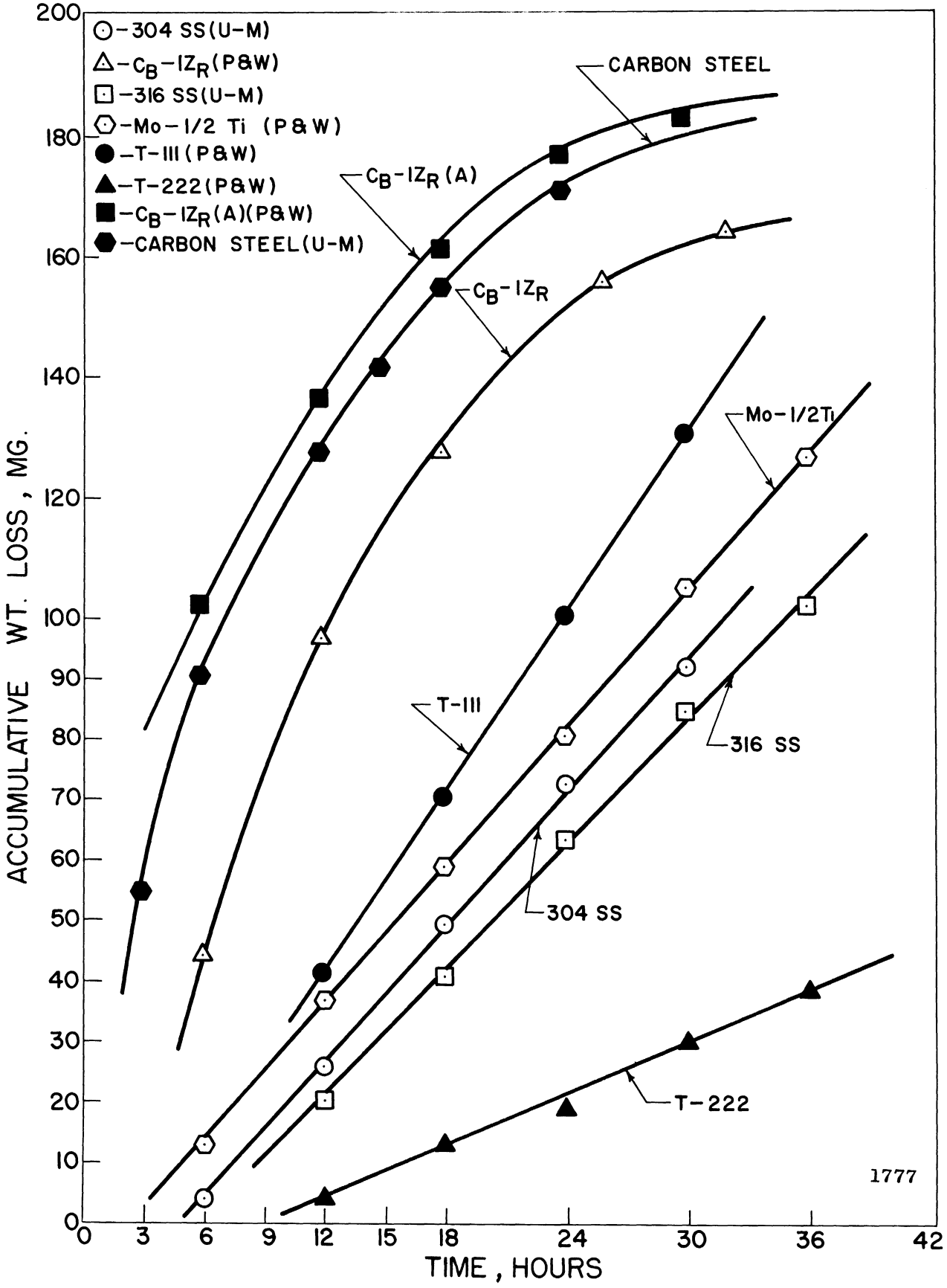

Figure 13. Effect of Cavitation Test Duration on Weight Loss at 70°F in Water - Subset 1.

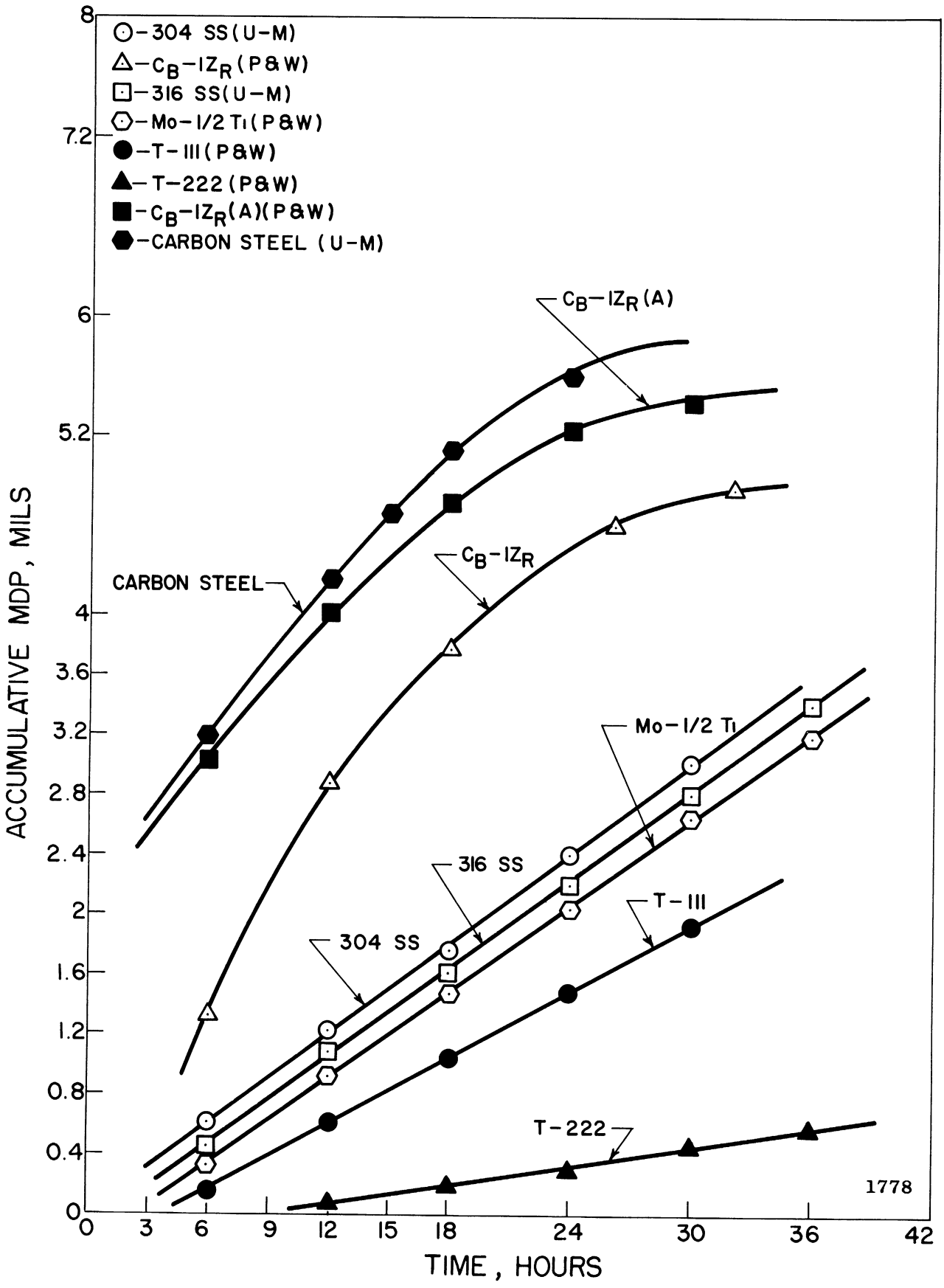

Figure 14. Effect of Cavitation Test Duration on MDP at 70°F in Water - Subset 1.

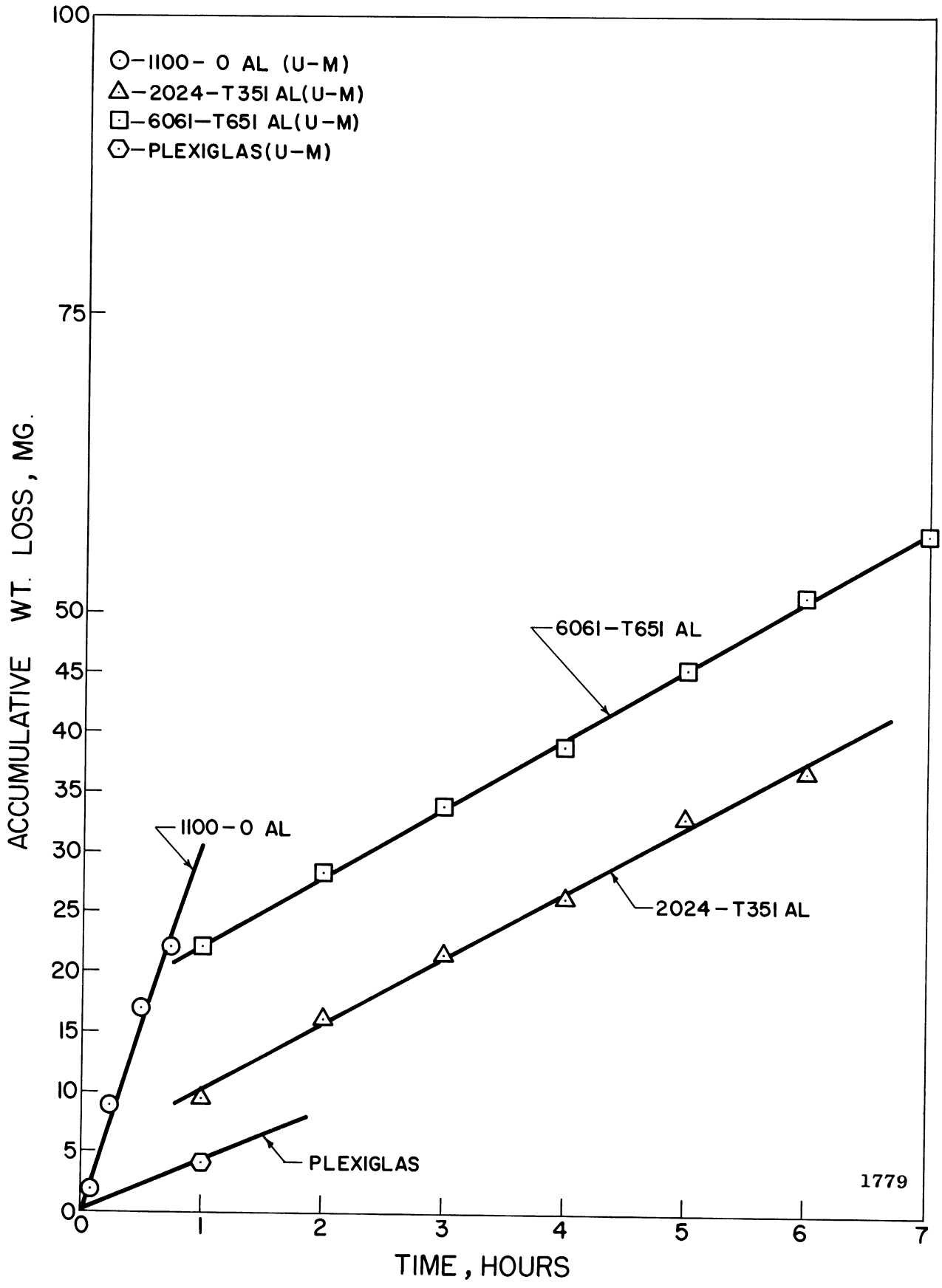

Figure 15. Effect of Cavitation Test Duration on Weight Loss at 70°F in Water - Subset 2.

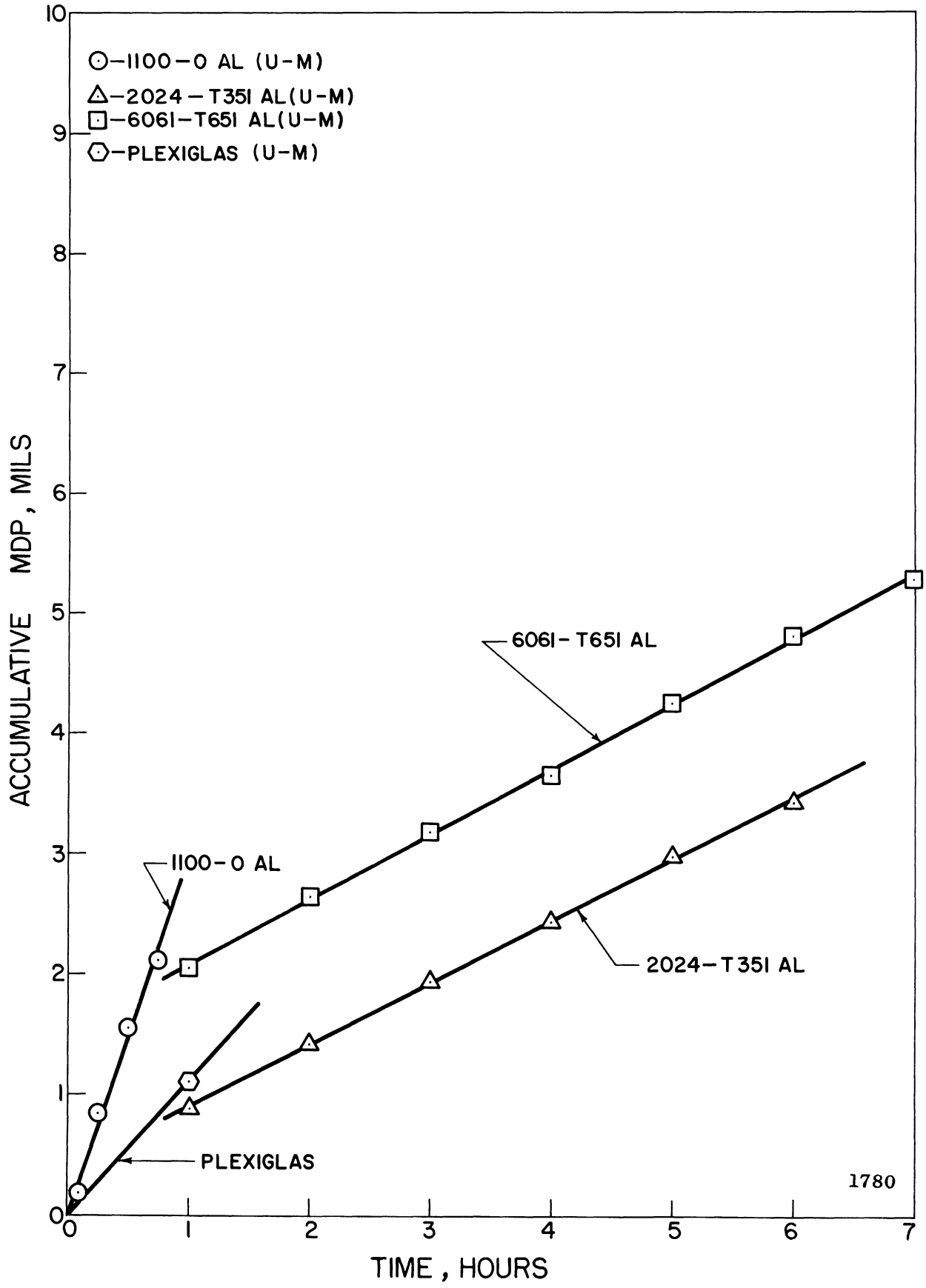

Figure 16. Effect of Cavitation Test Duration on MDP at 70°F in Water - Subset 2.

fairly uniform surface damage pattern, whereas those showing a non-linear response are characterized by surface damage consisting primarily of heavy, isolated, deep pitting. This latter pattern would result in a reduced surface area being presented to the collapsing bubble cloud since the area surrounding the very deep isolated pits has been shown to produce relatively few cavitation bubbles.[26] Hence one would expect the erosion rate to decrease as the total weight loss or MDP increased, as clearly pointed out in a recent paper by Plesset.[26]

Photographs of the test specimens in Subset 1 at the conclusion of the cavitation experiment are presented in Figure 17. The materials are arranged in order of decreasing resistance to cavitation damage. Note the severe pitting of the Cb-1Zr, Cb-1Zr(A), and hot-rolled carbon steel surfaces. A photograph of a 304 stainless steel specimen before exposure is included in Figure 17 and serves to indicate a representative initial surface condition for all the specimens tested.

It is clear from Figures 15 and 16 that the rate of erosion for the three aluminum alloys is approximately constant for the duration of the test, in spite of the deep, isolated pitting of the type which in the previous materials corresponded to a non-linear damage rate. The explanation for this anomaly is not at present known.

Photographs of the test specimens in Subset 2 at the conclusion of the cavitation experiment are presented in Figure 18. A photograph of a 2024-T351 aluminum specimen before exposure is included for comparison.

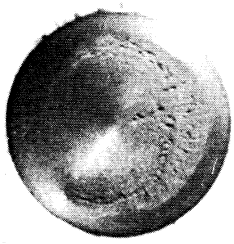

(1) T-222(P & W)
36 Hour Exposure

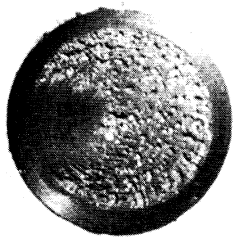

(2) T-111(P & W)
30 Hour Exposure

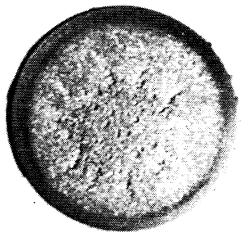

(3) Mo-1/2Ti(P & W)
36 Hour Exposure

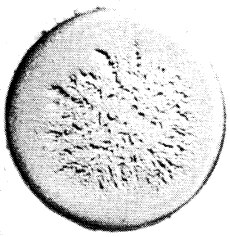

(4) 316 SS(U-M)
36 Hour Exposure

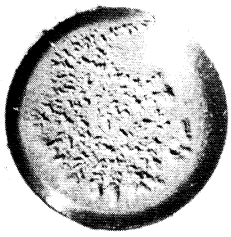

(5) 304 SS(U-M)
30 Hour Exposure

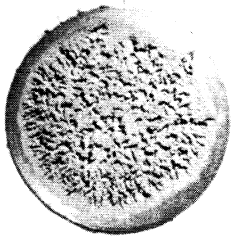

(6) Cb-1Zr(P & W)
32 Hour Exposure

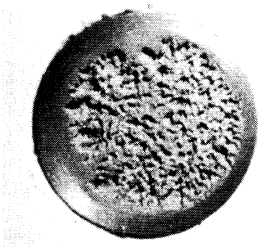

(7) Cb-1Zr(A)(P & W)
30 Hour Exposure

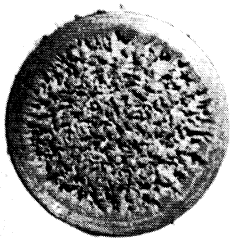

(8) Carbon Steel(U-M)
21 Hour Exposure

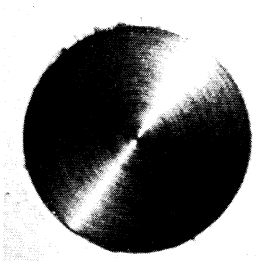

304 SS(U-M)
Before Exposure

Figure 17. Photographs of Specimens Subjected to Cavitation Damage in Water at 70°F - Subset 1.

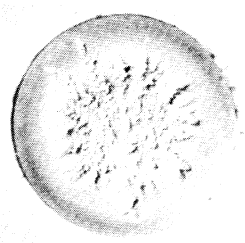

(1) 2024-T351 Al(U-M)
6 Hour Exposure

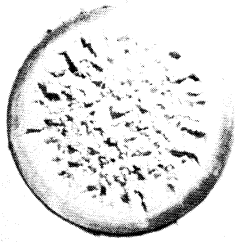

(2) 6061-T651 Al(U-M)
8 Hour Exposure

(3) 1100-0 Al(U-M)
45 Minute Exposure

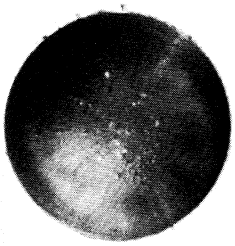

Plexiglas(U-M)
30 Minute Exposure

2024-T351 Al(U-M)
Before Exposure

1782

Figure 18. Photographs of Specimens Subjected to Cavitation Damage in Water at 70°F - Subset 2.

Table IX summarizes the cavitation results obtained in water at 70°F for the materials in Subset 3, namely the 12 Cu, Cu-Zn, Cu-Ni, and Ni alloys. The various heat-treats of a given material are grouped together for purposes of comparison. Figure 19 is a plot of accumulative weight loss versus test duration, while Figure 20 is the corresponding plot of accumulative MDF versus test duration for the 6 Cu and Ni alloys in Subset 3. Figures 21 and 22 are the corresponding plots for the 6 Cu-Zn and Cu-Ni alloys in Subset 3.

On the basis of either average weight loss rate or average MDP rate the Cu-Zn (60% cold-worked) was the most cavitation resistant among the 12 materials contained in Subset 3 with an average MDP rate of .38 mils/hour. The Ni (75% cold-worked) ranked second with an average MDP rate of .44 mils/hour, while the Cu-Ni (1800°F anneal, 1 hour) and Ni (1600°F anneal, 1 hour) were third and fourth with erosion rates of .47 mils/hour and .48 mils/hour, respectively. The three copper heat-treats were the least resistant to cavitation damage in Subset 3 with the Cu (900°F anneal, 1 hour) ranking last with an erosion rate of 1.02 mils/hour. This specimen suffered approximately 3X as much damage as the most resistant material, Cu-Zn.

Considering only the three copper specimens tested, the cold-worked material was most cavitation resistant while the high-temperature heat-treat ranked second and the low-temperature heat-treat was last. Identical rankings apply to the three Cu-Zn specimens and the three Ni specimens. For Cu-Ni the high-temperature heat-treated specimen was the most cavitation resistant followed by the low-temperature

heat-treated material and the cold-worked specimen in that order. It may be possible to explain the order of ranking of the materials contained in Subset 3 after a consideration of the applicable mechanical properties data that will be presented in Chapter VIII.

TABLE IX

SUMMARY OF CAVITATION RESULTS IN WATER - SUBSET 3

Cu, Cu-Ni, Cu-Zn, & Ni

Material	Avg. Wt. Loss Rate	Avg. MDP Rate
Cu-cold-worked	32.83 mg./hour	.95 mils/hour
Cu-900°F anneal	35.37	1.02
Cu-1500°F anneal	33.32	.95
Cu-Ni-cold-worked	24.18	.70
Cu-Ni-1300°F anneal	21.97	.63
Cu-Ni-1800°F anneal	16.25	.47
Cu-Zn-cold-worked	12.74	.38
Cu-Zn-850°F anneal	23.88	.72
Cu-Zn-1400°F anneal	22.78	.68
Ni-cold-worked	15.27	.44
Ni-1100°F anneal	20.25	.58
Ni-1600°F anneal	16.69	.48

An examination of Figures 19, 20, 21, and 22 indicates that the rate of erosion for the materials contained in Subset 3 is generally not constant. This is probably due to the pattern of the surface damage which is again characterized by heavy, isolated, deep pitting. Such a condition would result in changes in flow geometry and a reduced effective surface area being presented to the collapsing bubble cloud, i.e., the intensity of attack in a deep pit may become attenuated as the pit deepens and the bubbles are not generated over that portion of the surface.[26] This preferential damage of the surface may be caused by non-uniformity of applicable mechanical properties. However, it is

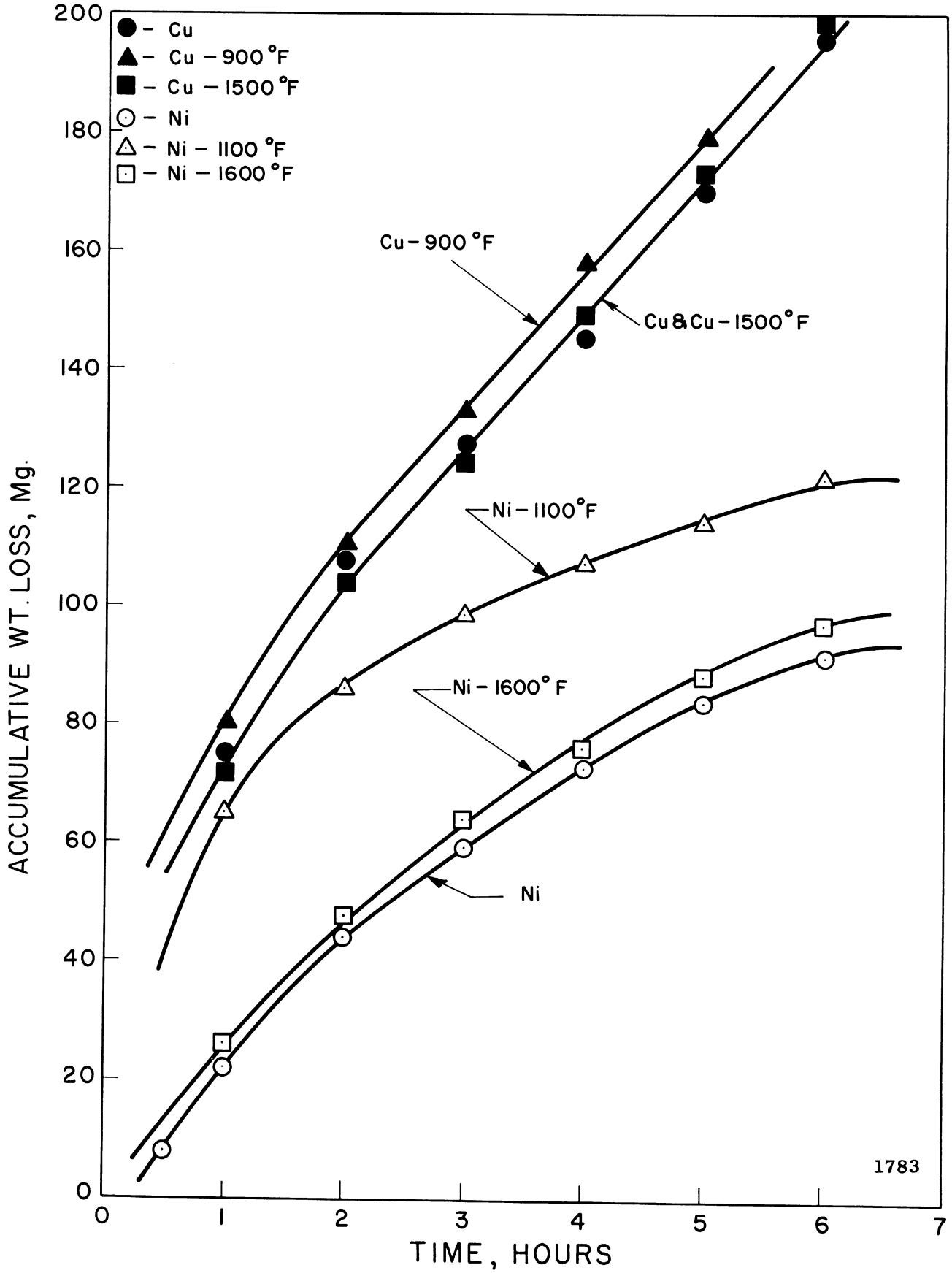

Figure 19. Effect of Cavitation Test Duration on Weight Loss at 70°F in Water - Cu and Ni (Subset 3).

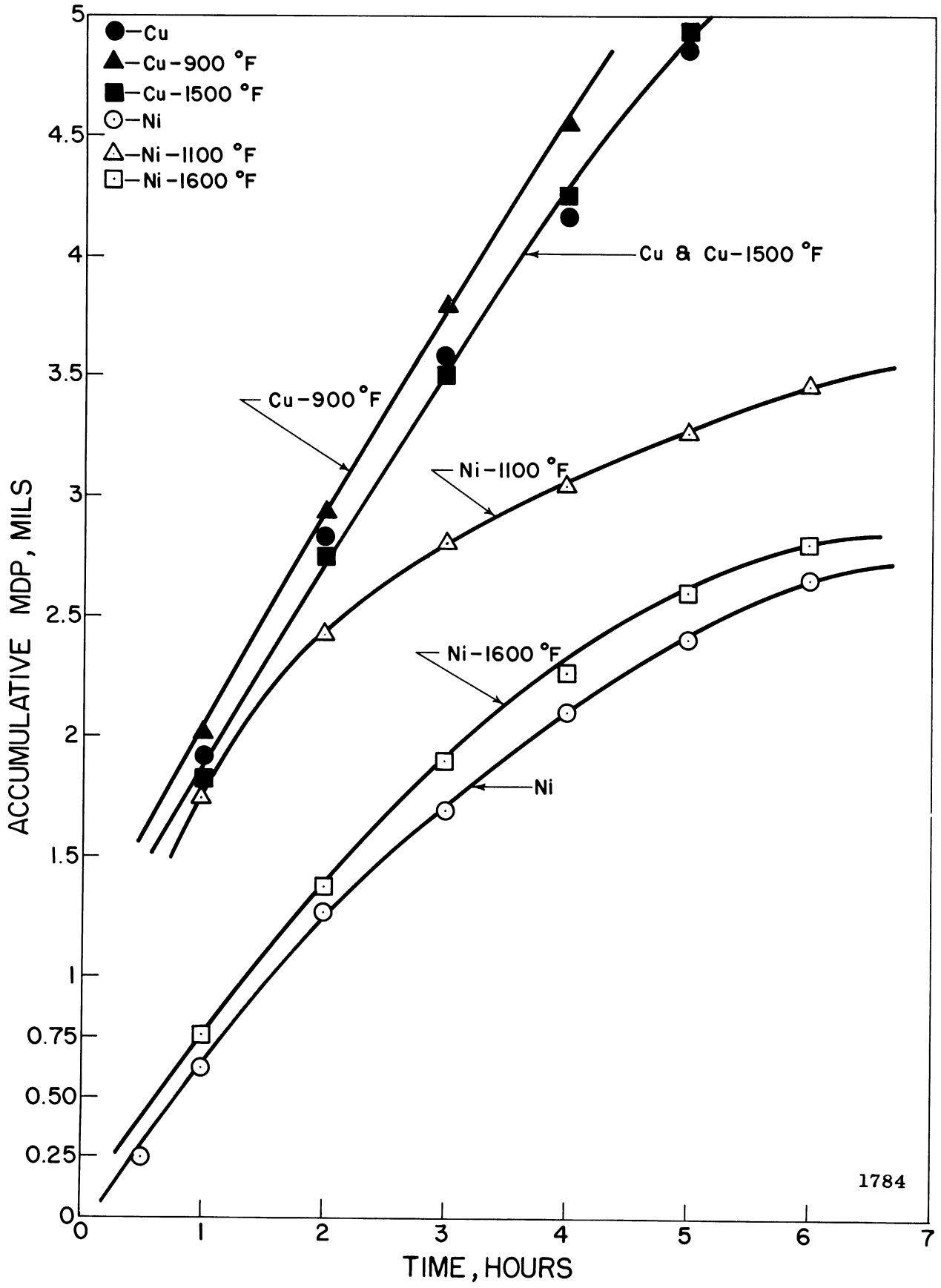

Figure 20. Effect of Cavitation Test Duration on MDP at 70°F in Water - Cu and Ni (Subset 3).

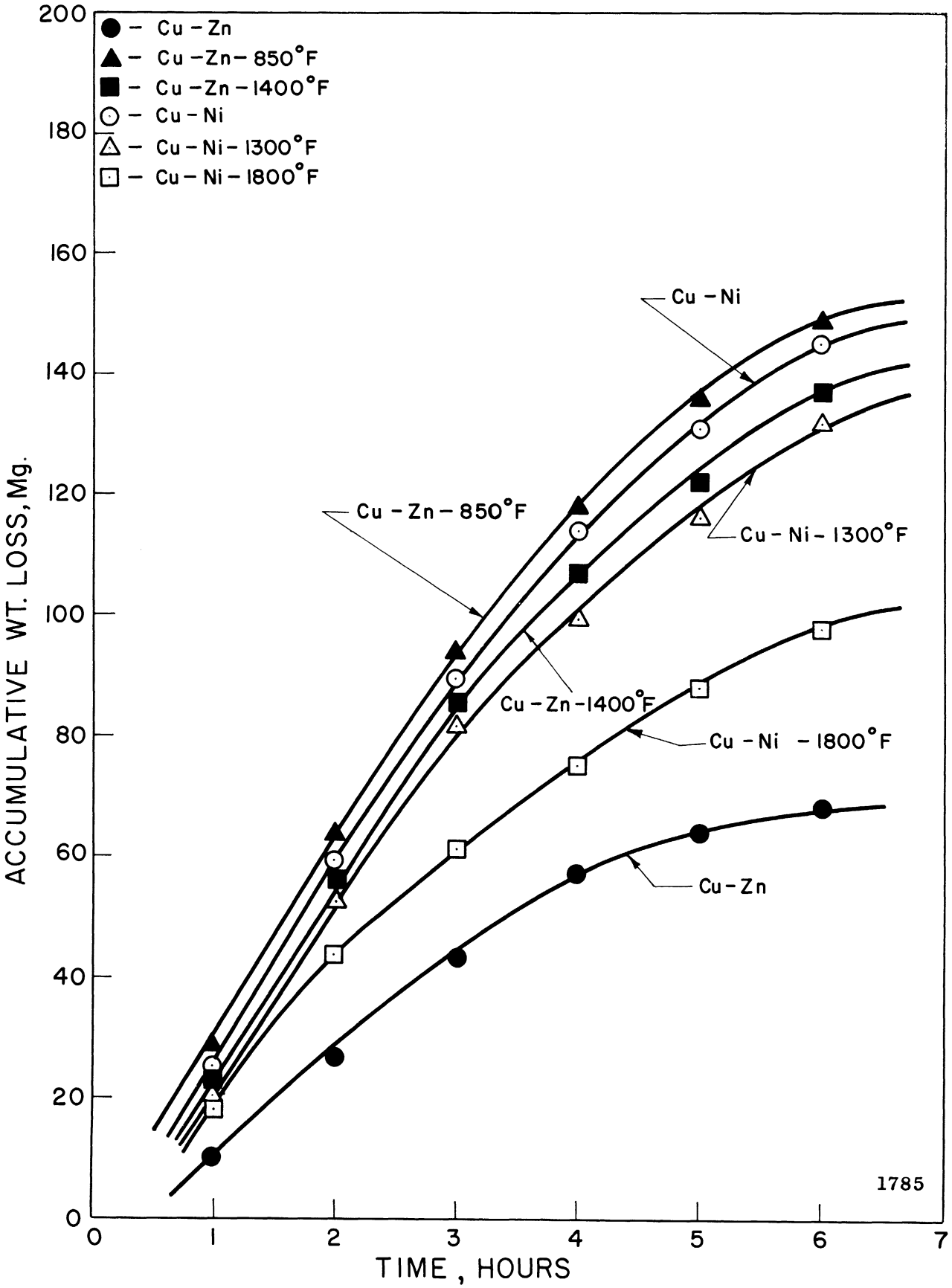

Figure 21. Effect of Cavitation Test Duration on Weight Loss at 70°F in Water - Cu-Ni and Cu-Zn (Subset 3).

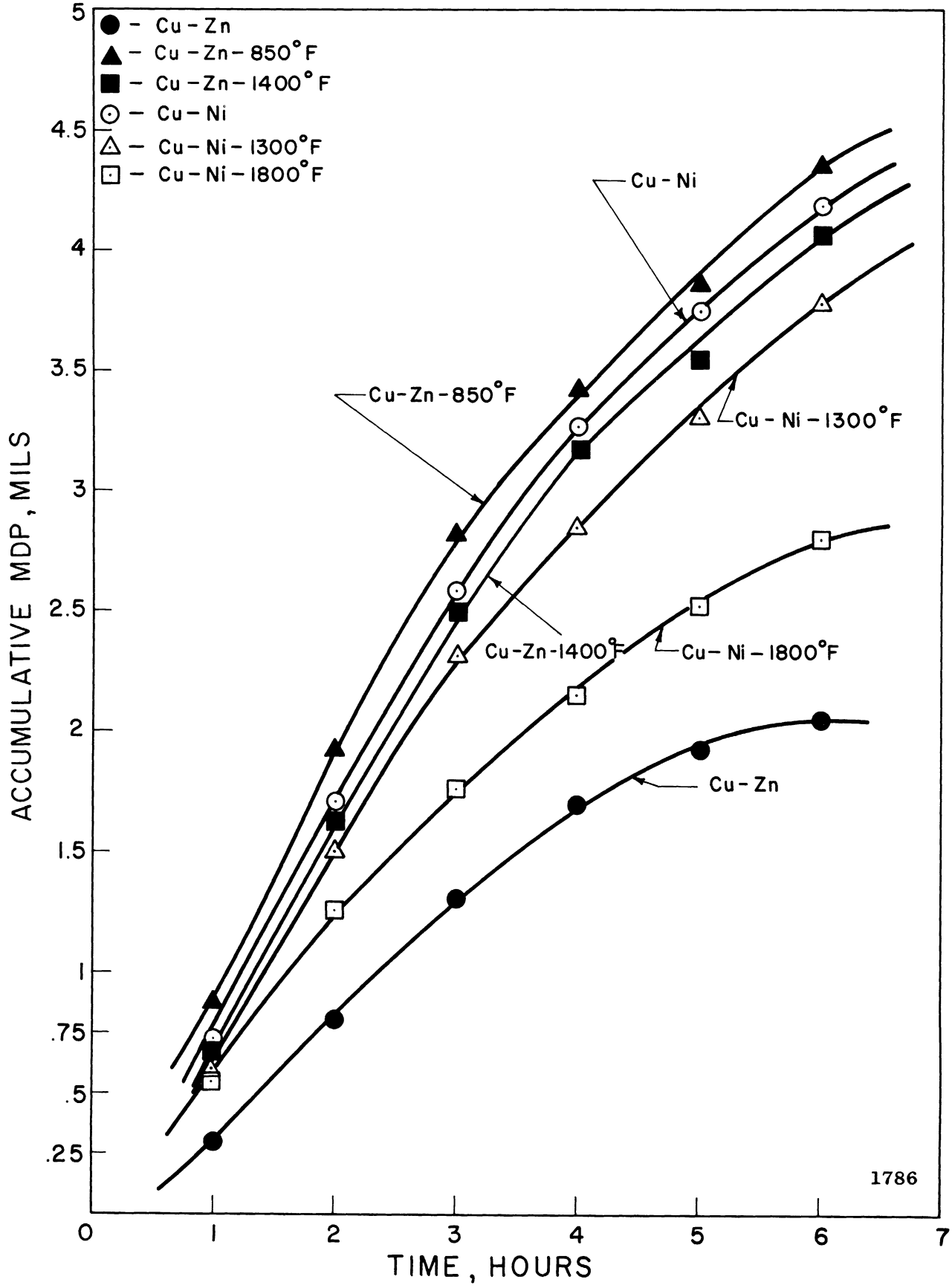

Figure 22. Effect of Cavitation Test Duration on MDP at 70°F in Water - Cu-Ni and Cu-Zn (Subset 3)

curious that for materials as stainless steel, the character of the damage in mercury or lead-bismuth is a uniform distribution, while in water it is composed of the previously discussed deep, isolated pitting. This lack of similarity in damage pattern may be due to the fact that the NPSH has not been modeled between tests, and similarity of flow regime might not occur. This might also be related to the frequently occurring star pattern of bubble cloud as opposed to the uniform bubble cloud observed on other occasions. No theoretical explanation for predicting these observed flow patterns yet exists to our knowledge.

Typical photographs of the test specimens in Subset 3 at the conclusion of the cavitation experiment are presented in Figure 23. Note the heavy, isolated, deep pitting that has developed.

In all of the tests conducted in water, only the hot-rolled carbon steel specimen showed definite visual indications of having suffered corrosion damage. Hence, the results quoted for this material reflect damage caused both by the corrosion and erosion components. All other results can be attributed solely to the cavitation-erosion mechanism.

C. Comparison with Venturi Facility Water Results

Cavitation data from the venturi water facility operated by this laboratory was previously obtained for all of the materials that were tested in the ultrasonic facility in water. Hence, as was the case in mercury at 70°F, it is now possible to qualitatively compare

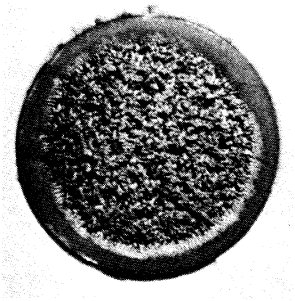

Cu(60% cold-worked)(U-M)
6 Hour Exposure

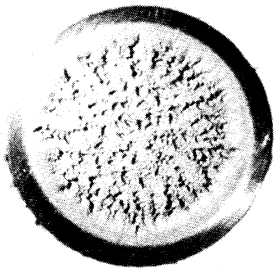

Ni(75% cold-worked)(U-M)
6 Hour Exposure

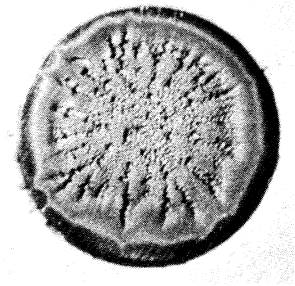

Cu-Ni(1300°F anneal)(U-M)
6 Hour Exposure

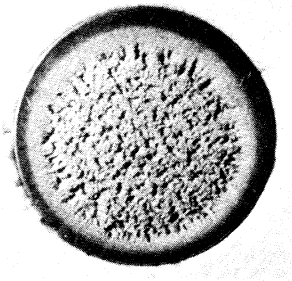

Cu-Zn(1400°F anneal)(U-M)
6 Hour Exposure

Figure 23. Photographs of Selected Specimens Subjected to Cavitation Damage in Water at 70°F - Subset 3.

the data from both facilities and hopefully be able to eventually arrive at a quantitative relationship coupling the results. Table X is a tabulation of the data available in water for the two facilities for the materials contained in Subsets 1 and 2. Table XI is a similar tabulation for the materials contained in Subset 3, namely the Cu, Cu-Ni, Cu-Zn, and Ni alloys. The wear in the venturi loop is given in terms of MDP after 50 hours of testing, whereas in the case of the acoustic facility, the average MDP rate is listed. The stainless steels tested in the two facilities are comparable as are the T-111 and the Ta-8W-2Hf. The T-222 and the Ta-10W are similar as are the carbon steels. The remainder of the materials investigated in both facilities are nearly identical in composition.

TABLE X

COMPARISON OF CAVITATION EROSION DATA IN WATER AT 70°F - VENTURI AND ULTRASONIC FACILITIES (SUBSETS 1 & 2)

Venturi Data		Ultrasonic Data	
Material	MDP at 50 Hours	Material	Avg. MDP Rate
Cb-1Zr	3.50×10^{-3} mils	T-222	.02 mils/hr.
Stainless Steel	5.27×10^{-3}	T-111	.06
		Mo-1/2Ti	.09
Ta-8W-2Hf	7.62×10^{-3}	316 SS	.09
Ta-10W	11.11×10^{-3}	304 SS	.10
Cb-1Zr(A)	20.29×10^{-3}	Cb-1Zr	.15
Plexiglas	67.25×10^{-3} *	Cb-1Zr(A)	.18
Mo-1/2Ti	99.72×10^{-3}	Carbon Steel	.23
Carbon Steel	769.2×10^{-3}	2024 Al	.57
2024 Al	1618×10^{-3}	6061 Al	.72
6061 Al	1976	Plexiglas	1.39
1100-0 Al	2451×10^{-3}	1100-0 Al	2.70

*MDP at 4 hours

TABLE XI

COMPARISON OF CAVITATION EROSION DATA IN WATER AT 70°F - ULTRASONIC AND VENTURI FACILITIES (SUBSET 3)

Material	Ultrasonic MDP Rate		Venturi MDP at 50 Hours	
Cu-Zn	.38 mils/hr.	(1)	39.77×10^{-3} mils	(12)
Ni	.44	(2)	14.85×10^{-3}	(5)
Cu-Ni-1800°F anneal	.47	(3)	8.58×10^{-3}	(2)
Ni-1600°F anneal	.48	(4)	4.04×10^{-3}	(1)
Ni-1100°F anneal	.58	(5)	14.63×10^{-3}	(4)
Cu-Ni-1300°F anneal	.63	(6)	13.29×10^{-3}	(3)
Cu-Zn-1400°F anneal	.68	(7)	25.09×10^{-3}	(9)
Cu-Ni	.70	(8)	19.23×10^{-3}	(6)
Cu-Zn-850°F anneal	.72	(9)	25.72×10^{-3}	(10)
Cu	.95	(10)	24.29×10^{-3}	(8)
Cu-1500°F anneal	.95	(11)	27.62×10^{-3}	(11)
Cu-900°F anneal	1.02	(12)	23.75×10^{-3}	(7)

In Table X the materials have been listed in order of decreasing cavitation resistance, or increasing susceptibility to cavitation erosion attack for both facilities. A certain amount of agreement is noted in Table X. In both facilities the stainless steels, the tantalum-base alloys, and the Cb-1Zr are among the most cavitation resistant materials. But the rankings do not agree in detail. Among the least resistant materials the carbon steel and the three aluminum alloys have indentical rankings in both facilities. It was noted in the venturi investigations that the damage sustained by the Cb-1Zr apparently indicated a thin laminated structure which could lead to erroneous results in this case.

The results presented in Table XI for the Cu, Cu-Ni, Cu-Zn, and Ni alloys agree only in a few respects. The rather general disagreement noted for this data subset cannot be fully explained at this time. However, it is noted that the damage rates for these materials differ by a much smaller factor than for those previously discussed, so that an upsetting of the ranking order would involve much smaller errors in damage rates. Nevertheless, as for the previous cases, the ratios between materials tested in the venturi are much greater than between materials tested in the vibratory facility.

Discrepancies in rankings between these two types of facilities may also be due to the greater influence of corrosion in the venturi tests where the damage proceeds at a much slower rate (factor of about 10^3 for all the data subsets). The effect of corrosion even in the vibratory type test has been previously examined by Plesset.[19]

CHAPTER VI

COMPARISON OF CAVITATION RESULTS IN MERCURY AND WATER AT 70°F

It is interesting to compare the results obtained in mercury and water at the same test temperature of 70°F in an effort to determine fluid effects on cavitation damage. Table XII summarizes the cavitation data obtained in mercury and water at 70°F. The nine materials tested in both fluids have been rated on the basis of cavitation resistance as determined by the average MDP rate, with a rating of "1" indicating the most cavitation resistant material, while a rating of "9" would denote that material most susceptible to cavitation damage.

TABLE XII

COMPARISON OF CAVITATION RESULTS IN MERCURY AND WATER AT 70°F

	Mercury		Water	
Material	Avg. MDP Rate	Rating	Avg. MDP Rate	Rating
304 SS	.32 mils/hr.	1	.10 mils/hr.	5
316 SS	.33	2	.09	4
T-111	.35	3	.06	2
T-222	.43	4	.02	1
Mo-1/2Ti	.57	5	.09	3
Cb-1Zr	.92	6	.15	6
Carbon Steel	1.03	7	.23	8
Cb-1Zr(A)	1.61	8	.18	7
Plexiglas	3.99	9	1.39	9

The following comments apply to the comparison:

(1) There are several differences in the comparative ratings of the materials in the two fluids. In mercury the stainless steels and the tantalum-base alloys were the most resistant to cavitation damage and only differed in this respect by about 25%. In the case of the water the tantalum-base alloys were the most resistant among the materials tested, while the stainless steels suffered damage 2X to 5X greater than the T-111 and T-222. The Mo-1/2Ti ranked third in water and fifth in mercury. However, the first five rankings were occupied by the same materials in both fluids. The Cb-1Zr, carbon steel, Cb-1Zr(A), and Plexiglas suffered the most damage and had comparable rankings in both fluids except for the carbon steel which ranked seventh in mercury and eighth in water. This could have been due to the additional corrosion suffered by the carbon steel in water.

(2) For any given material the damage suffered in mercury was 3X to 20X more severe than in water. Note that the comparison is on the basis of equal static suppression pressures rather than head. The stainless steels, in particular, suffered about 3X as much damage in mercury as in water.

(3) The stainless steels were the most cavitation resistant materials in mercury, while the tantalum-base alloys, T-111 and T-222, were far superior in water. The Plexiglas was the least resistant

in both fluids, as opposed to the venturi tests where it was quite resistant in water but poor in mercury. This may indicate that materials which rely to some extent on a superior yield deflection range for their protection (as rubberized coatings and also Plexiglas in the present tests) are suitable in relatively low intensity cavitation fields but fail under more intense attack. This observation, we believe, is consistent with much field experience. The Cb-1Zr, Cb-1Zr(A), and carbon steel also did not fare well in either fluid.

It is felt that the primary cause of the greater damage suffered by all the materials in mercury as opposed to water is its much greater density. The pressure generated by bubble collapse would be proportional to the fluid density if the suppression heads seen by the bubbles were the same. This may be approximately true in the present case since the major contribution to the suppression head at the start of collapse is the dynamic head caused by the horn motion. This portion would be the same for all tests, although the static heads differ by the density ratio since constant static suppression pressure was maintained. A more definite conclusion in this regard will have to await the accumulation of more complete cavitation erosion data in a variety of fluids.

In the venturi results previously presented, it is noted that the stainless steels were most resistant in mercury at 70°F, as is the case in the ultrasonic facility. In water the venturi results show the Cb-1Zr to be the most resistant, followed by the stainless steels.

CHAPTER VII

COMPARISON OF CAVITATION RESULTS IN MERCURY AND LEAD-BISMUTH AT 500°F

Previously[22], cavitation studies were carried out in this laboratory in lead-bismuth alloy at 500°F and 1500°F. It is interesting to compare the results obtained in lead-bismuth and mercury at the same test temperature of 500°F in a further effort to determine fluid effects on cavitation damage.

Table XIII summarizes the cavitation data obtained in lead-bismuth and mercury at 500°F. The seven materials tested in both fluids have been rated on the basis of cavitation resistance as determined by the average MDP rate, with a rating of "1" indicating the most cavitation resistant material, while a rating of "7" would denote that material most susceptible to cavitation damage. The following comments apply to the comparison:

(1) For both the lead-bismuth and the mercury tests the materials investigated had identical comparative ratings with the exception of the Mo-1/2Ti (P & W) which ranked third in lead-bismuth, but ranked fifth in mercury among the same materials tested in both fluids.

(2) Any given material tested in both fluids suffered damage which was of the same order of magnitude. This is not surprising considering the similarity of the fluids.

(3) The T-111 (P & W) and T-222(A) (P & W) were the most cavitation resistant materials in both fluids, while the Cb-1Zr(P & W) and Cb-1Zr(A) (P & W) were the least resistant in both fluids.

(4) The T-111, T-222(A), 316 SS, and 304 SS all suffered less damage in the mercury than in the lead-bismuth alloy.

(5) The Mo-1/2Ti, Cb-1Zr, and Cb-1Zr(A) all suffered more damage in the mercury than in the lead-bismuth alloy.

TABLE XIII

COMPARISON OF CAVITATION RESULTS
IN MERCURY AND LEAD-BISMUTH AT 500°F

	Mercury		Lead-Bismuth	
Material	Avg. MDP Rate	Rating	Avg. MDP Rate	Rating
T-111	.43 mils/hr.	1	.72 mils/hr.	1
T-222	.46	2	.76	2
Carbon Steel	.61	-	---	-
316 SS	.63	3	.88	4
304 SS	.69	4	.93	5
Mo-1/2Ti	1.09	5	.78	3
Cb-1Zr	2.43	6	1.63	6
Cb-1Zr(A)	3.73	7	3.54	7

The observations noted in items (4) and (5) above are not easily explained at this time. Intensive computer correlations are presently being undertaken in an effort to isolate the effect of different fluids on the cavitation damage of identical materials tested under similar experimental conditions. Fluid properties that have been given consideration

as possible coupling parameters include the density, surface tension, net positive suction head (NPSH), bulk modulus, kinematic viscosity, and ratio of the fluid acoustic impedance to test material acoustic impedance. It is hoped that these studies will result in a better understanding of the role of fluid properties on cavitation-erosion damage of materials.

CHAPTER VIII

MECHANICAL PROPERTIES DATA FOR THE TEST MATERIALS

In order to obtain a meaningful correlation between the cavitation resistance of the various materials tested, their mechanical properties, and suitable fluid coupling parameters, it is absolutely essential that the applicable mechanical properties such as tensile strength, yield strength, engineering strain energy, true strain energy, hardness, elongation, reduction in area, and elastic modulus be measured at the test temperatures using tensile bars machined from the same bar stock as were the cavitation specimens. Otherwise the variations between material lots due to differences in heat-treat, cold work, etc., are too large to allow useful results. Accordingly, all cavitation test specimens, tensile bars, and special hot hardness specimens for each material were machined from the same piece of bar stock. In the case of the Cu, Cu-Ni, Cu-Zn, and Ni alloys that were available only in sheet stock, flat tensile specimens were fabricated and tested.

The mechanical properties data for the stainless steels and refractory materials were determined at 70°F and 500°F at Pratt & Whitney Aircraft (CANEL) under the supervision of Mr. Henry P. Leeper, Project Metallurgist. Earlier, Pratt & Whitney Aircraft (CANEL) had supplied generous portions of all of the refractory materials tested in this program, whereas the stainless steels used were supplied by this laboratory. The results of the mechanical properties determination program were supplied

to this laboratory by private communication[27] and have become an integral part of the cavitation analysis and correlation effort.

The data supplied by Pratt & Whitney Aircraft (CANEL) at 70°F and 500°F is tabulated in Tables XIV and XV, respectively. Three values for strain energy to failure are listed: i.e., "engineering strain energy" which is based on the "approximate" or engineering stress-strain curve and is equal to the area under this curve, and two values for "true strain energy", which are based on approximations of the true stress-strain curve. The first value of true strain energy listed takes into account elongation of the test specimen in computing the strain, while the second value takes into account necking of the specimen, reduction in area after plastic deformation begins, and the resulting higher values for the local true breaking stress and strain in the actual failure region. The large discrepancies in some cases, as for highly ductile materials, between these strain energy values indicate the difficulties and uncertainties incurred in using this parameter. If it occurs that the engineering strain energy proves to be a better correlating parameter than the true strain energy based on reduction in area, then this may indicate that brittle rather than ductile failures are typical of cavitation damage. The remaining values listed in Tables XIV and XV are rather commonly reported metallurgical properties and need no further explanatory remarks. The hardness values listed were measured with a diamond pyramid indenter and 1.1 Kg. load.

TABLE XIV

MECHANICAL PROPERTIES DATA AT 70°F FROM PRATT & WHITNEY AIRCRAFT (CANEL)

Material	Tensile Strength psi	Yield Strength psi	Eng. Strain Energy psi	True Strain Energy psi		DPH Hardness 1.1 Kg.	Elongation %	Area Reduction %	Elastic Modulus psi
304 SS	94,500	64,700	57,300	41,300	47,500	237	63.8	77.9	29.0×10^6
316 SS	87,200	63,600	48,850	38,200	49,500	227	57.8	80.3	29.0×10^6
T-111	131,600	124,900	16,750	16,000	68,600	308	14.8	80.4	28.0×10^6
T-222	154,200	154,200	15,250	16,050	70,350	338	10.6	55.6	28.0×10^6
T-222(A)	108,900	91,100	23,950	22,180	52,350	288	23.1	61.1	28.0×10^6
Mo-1/2Ti	165,800	150,400	21,300	14,570	11,600	295	9.3	7.9	45.0×10^6
Cb-1Zr	59,200	59,000	6,650	6,300	29,600	151	14.3	88.4	15.0×10^6
Cb-1Zr(A)	36,300	19,200	13,200	7,050	12,110	99	41.9	91.4	15.0×10^6

TABLE XV

MECHANICAL PROPERTIES DATA AT 500°F FROM PRATT & WHITNEY AIRCRAFT (CANEL)

Material	Tensile Strength psi	Yield Strength psi	Eng. Strain Energy psi	True Strain Energy psi		DPH Hardness 1.1 Kg.	Elongation %	Area Reduction %	Elastic Modulus psi
304 SS	92,500	56,700	16,150	18,200	37,200	154	30.8	72.9	26.0×10^6
316 SS	72,400	52,300	18,050	17,700	38,000	203	30.4	78.2	26.0×10^6
T-111	101,800	100,800	15,100	10,700	50,900	218	13.8	86.2	27.0×10^6
T-222	133,800	133,800	12,850	12,900	67,800	286	10.9	71.5	27.0×10^6
T-222(A)	92,300	63,400	20,650	33,800	42,200	209	23.6	66.9	27.0×10^6
Mo-1/2Ti	84,100	79,700	10,700	11,000	44,400	207	15.0	75.9	43.0×10^6
Cb-1Zr	54,700	54,700	6,450	5,185	27,700	133	12.7	88.7	14.5×10^6
Cb-1Zr(A)	25,000	11,600	8,100	3,780	7,890	71	35.9	92.2	14.5×10^6

The mechanical properties data for the aluminum alloys, carbon steel, Plexiglas, and the Cu, Cu-Ni, Cu-Zn, and Ni materials were determined at room temperature in the Department of Chemical & Metallurgical Engineering laboratories at the University of Michigan and are reported elsewhere[18,30]. This data is presented here in Table XVI. The mechanical properties for carbon steel were also determined at 500°F and so noted in Table XVI.

Examination of the data in Tables XIV and XV indicates that several of the mechanical properties such as tensile strength, yield strength, strain energy, and hardness decrease in value for a given material as the temperature is increased. Such trends are indicative of the behavior of the cavitation resistance as a function of temperature, which has been discussed previously. Undoubtedly, it should be possible to correlate the cavitation resistance of the materials tested with the applicable mechanical properties data at the test temperatures. This is the subject of the next chapter.

TABLE XVI

MECHANICAL PROPERTIES DATA AT 70°F FROM UNIVERSITY OF MICHIGAN LABORATORIES

Material	Tensile Strength psi	Yield Strength psi	Eng. Strain Energy psi	True Strain Energy psi		DPH Hardness 1.1 Kg.	Elongation %	Area Reduction %	Elastic Modulus psi
1100-0 Al	12,250	7,600	4,950	4,320	22,600	27	44.5	85.5	10.0×10^6
2024 Al	72,000	57,900	13,300	13,600	31,050	171	20.0	34.5	10.0×10^6
6061 Al	45,300	40,000	25,800	9,840	38,620	127	19.4	56.7	10.0×10^6
Carbon Steel (70°F)	45,300	41,600	18,440	30,530	111,000	193	46.3	76.1	29.0×10^6
Carbon Steel (500°F)	62,510	18,400	19,225	20,900	66,650	125	37.2	63.6	28.0×10^6
Plexiglas	10,445	1,600	320	320	320	9	4.0	0.0	0.4×10^6
Cu	53,400	49,500	3,100	11,800	11,800	133	6.2	19.8	17.0×10^6
Cu-900°F	31,500	9,500	13,900	26,900	26,900	51	51.3	48.5	17.0×10^6
Cu-1500°F	30,700	5,000	6,100	11,800	11,800	41	32.5	33.2	17.0×10^6
Cu-Zn	93,900	82,000	4,700	55,400	55,400	197	5.3	40.7	16.0×10^6
Cu-Zn-850°F	47,600	20,000	28,600	57,000	57,000	71	62.6	60.9	16.0×10^6
Cu-Zn-1400°F	40,400	11,000	15,300	33,000	33,000	48	58.9	51.7	16.0×10^6
Cu-Ni	87,300	77,000	6,100	13,200	13,200	197	4.5	15.4	22.0×10^6
Cu-Ni-1300°F	57,900	20,000	3,100	36,200	36,200	96	34.9	43.5	22.0×10^6
Cu-Ni-1800°F	53,300	18,000	16,300	21,800	21,800	77	34.4	34.4	22.0×10^6
Ni	93,100	82,000	3,200	8,300	8,300	206	3.9	10.2	30.0×10^6
Ni-1100°F	50,500	13,000	18,300	48,300	48,300	67	43.8	51.6	30.0×10^6
Ni-1600°F	48,700	7,000	16,100	40,500	40,500	59	41.8	49.7	30.0×10^6

CHAPTER IX

CORRELATIONS OF CAVITATION DATA WITH MECHANICAL PROPERTIES DATA

A. Introduction

In order to fully investigate the dependence of cavitation resistance on the mechanical properties of the test materials and on the fluid properties, and to obtain a better understanding of the damage mechanisms involved, it is necessary to subject the experimentally-determined cavitation data and the appropriate mechanical and fluid properties data to a least mean squares fit by means of a suitable digital computer program. For these studies the University of Michigan IBM 7090 digital computer facility was utilized along with a very sophisticated least mean squares stepwise regression program which was first proposed by Westervelt[28] and later revised by Crandall.[29] Utilizing the first-order interaction form of the program, the problem at hand can be simply stated as follows: it is required to determine the appropriate coefficients and exponents in a predicting equation of the form:

$$Y = C_0 + C_1 X_1^a + C_2 X_2^b + C_3 X_3^c + C_4 X_4^d + \cdots\cdots\cdots + C_n X_n^q$$

where C_0, C_1, C_2, C_3, C_4, ..., C_n are constant coefficients; a, b, c, d, ..., q are constant exponents; the X's are the independent variables, in this case the mechanical properties of the materials and the fluid properties; and Y is the dependent variable, the average MDP rate. The independent variables are allowed to appear

in the predicting equation any number of times, each time raised to a different value of exponent and multiplied by an appropriate coefficient. The program allows great latitude on the possible exponents for the independent variables. The form of the program used in this investigation allows any or all of the independent variables to be raised to the following exponents: ± 1, ± 2, $\pm 1/2$, ± 3, $\pm 1/3$.

A predicting equation of the type noted above would be obtained by allowing only a "first-order interaction" of the possible terms, i.e., terms involving products of the independent variables would not be allowed. The program, however, does allow the option of a "second-order interaction", i.e., allows terms involving products of different independent variables. The choice must be made by the individual programmer.

In the present analysis (permitting only first-order interaction) the allowable mechanical properties (independent variables) were taken to be the tensile strength, yield strength, engineering strain energy,[30] true strain energy,[30] hardness, percentage elongation, percentage reduction in area, and modulus of elasticity. In addition one fluid property was included among the independent variables for all the correlations as a fluid coupling parameter to explain differences in cavitation resistance of a given material in different fluids. The fluid coupling parameters that were investigated included the ratio of acoustic impedances of test fluid and specimen material, density of fluid, surface tension, net positive suction head (NPSH), bulk modulus, and kinematic viscosity.. Hence in a given correlation there were 10 independent variables and

10 possible exponents for each independent variable. As a result a total of 100 terms are possible candidates for inclusion in the predicting equation plus a pure constant. From a physical point of view, it is hoped that a good statistical correlation will be possible with a minimum number of terms so that the predicting equation may hopefully be justified on physical grounds. This possibility would be unlikely if more than 5 or 6 terms were needed for the correlation.

A brief outline will be given here of the mechanics of the program. The interested reader is referred to the literature previously cited for the details. The major features of the program are as follows:

(1) Of the 100 possible terms that are candidates for inclusion in the predicting equation, the program randomly selects a subset of 40 terms to be analyzed.

(2) A correlation coefficient is computed for each of the 40 terms. The correlation coefficient is a measure of the ability of each term to individually explain the experimental data, i.e., predict the average MDP rate.

(3) The term with the greatest correlation coefficient is then included in the predicting equation, which at this point is of the form:

$$Y = C_0 + C_1 X_1^a$$

where C_0 and C_1 are constants to be determined.

(4) The constants C_0 and C_1 are computed using the least mean squares criterion.

(5) The initial 40 terms are then sorted into 2 subsets, those that are included in the predicting equation at this point, and those that are not.

(6) An importance factor is computed for each term now in the equation. The importance factor is a measure of the total contribution made by each term in explaining the experimental data.

(7) The importance factors of the terms in the equation are compared to a minimum level of importance set by the user. A typical range of values is 1% to 5%.

(8) Terms having an importance factor less than the minimum level are deleted from the equation.

(9) A potential importance factor is computed for each term not in the equation. The potential importance factor is a measure of the ability of each term not in the equation to explain the presently existing variance between the experimental data and the predicted data.

(10) The potential importance factors of the terms not in the equation are compared to a minimum level of importance set by the user. A typical range of values is 1% to 5%..

(11) Terms not in the equation having a potential importance factor greater than the minimum level are entered into the equation.

This procedure is used to examine the subset of 40 terms chosen randomly and is terminated either when all qualified terms have been entered into the equation or when certain statistical criteria (such as the coefficient

of determination and standard error in the dependent variable) set by the user have been satisfied. Whenever a new term is entered into the equation, the least mean squares criterion is used to compute a new set of coefficients. For a given problem it is possible to analyze several subsets of 40 terms, each chosen randomly from the set of 100 possible terms available. Such a procedure is advisable in that it increases the probability that the most significant terms contained in the initial set of 100 terms will enter the predicting equation.

The output from the program includes the terms in the predicting equation along with the appropriate exponents and coefficients, predicted MDP rates based on the correlation, experimental MDP rates, percent deviations, standard error in the dependent variable, coefficient of determination for the analysis, average absolute percent deviation for the analysis, etc. As a result it is possible to show graphically the statistical accuracy of the predicting equation by plotting the predicted MDP values versus the experimental points and noting the deviation from a 45° line which would signify a perfect fit.

B. Lead-Bismuth Correlations

Previously, cavitation-erosion studies were conducted in lead-bismuth alloy at 500°F and 1500°F in this laboratory. The experimental studies and preliminary mechanical properties correlations have been reported.[22] A summary of the complete correlation effort to date with the lead-bismuth data can now be presented.

The cavitation data obtained at 500°F and at 1500°F in lead-bismuth alloy was all submitted to the least mean squares regression

program previously discussed in an attempt to obtain a first-order interaction correlation that would be applicable at both temperatures, and, hence, would have the greatest generality allowed by the limited data. Ten mechanical and fluid properties were taken to be the independent variables with the average MDP rate being the dependent variable. The mechanical properties allowed in the analysis were the tensile strength, yield strength, engineering strain energy,[30] true strain energy (two values as explained before were considered, one taking into account the elongation of the test specimen, and the other the reduction in area),[30] hardness, percentage elongation, percentage reduction in area, modulus of elasticity, and ratio of the acoustic impedances of the test fluid and specimen material.* These properties were selected since previous investigators had attempted correlations with them and/or because many of the properties have been involved in hypothesized damage mechanisms.

Initially, an attempt was made to correlate the damage data with each mechanical property individually in order to determine the relative importance of each alone with respect to predicting the observed cavitation damage. Table XVII summarizes the results of this effort. The 10 properties considered, the statistically best predicting equations generated by the program for each property, the coefficient of determination (CD)** for the analysis, and the average absolute percent

---

* Chosen as a coupling parameter between fluid and material, and related to the ratio of reflected to transmitted energy as liquid shock waves or jets impinge on the solid.

** The coefficient of determination is a statistical quantity that can be interpreted as the proportion of the total variation in the dependent variable that is explained by the predicting equation. Its values range from 0 (no prediction) to 1.0 (perfect prediction).

TABLE XVII

SUMMARY OF SINGLE PROPERTY CORRELATIONS - LEAD-BISMUTH ALLOY

Property	Predicting Equation	CD*	AAPD**
1. True Strain Energy(TSER) (Based on Reduction in Area)	Avg. MDP Rate = $0.233 + 2.57\text{x}10^{4}(\text{TSER})^{-1}$	0.986	0.1
2. True Strain Energy(TSEE) (Based on Elongation)	Avg. MDP Rate = $1.106 + 4.08\text{x}10^{10}(\text{TSEE})^{-3}$	0.964	13.8
3. Reduction in Area (RA)	Avg. MDP Rate = $0.937 + 2.89\text{x}10^{5}(\text{RA})^{-3}$	0.907	37.9
4. Engineering Strain Energy (ESE)	Avg. MDP Rate = $0.324 + 8.77\text{x}10^{11}(\text{ESE})^{-3}$	0.878	5.7
5. Tensile Strength (TS)	Ang. MDP Rate = $0.675 + 7.41\text{x}10^{13}(\text{TS})^{-3}$	0.847	2.4
6. Hardness (H) (DPH - 1.1 Kg. Load)	Avg. MDP Rate = $0.451 + 1.72\text{x}10^{6}(\text{H})^{-3}$	0.794	2.9
7. Yield Strength (YS)	Avg. MDP Rate = $-4.139 + 2.14\text{x}10^{2}(\text{YS})^{-1/3}$	0.632	28.3
8. Acoustic Impedance Ratio (AI)	Avg. MDP Rate = $-2.321 + 12.22(\text{AI})$	0.546	40.9
9. Elastic Modulus (E)	Avg. MDP Rate = $-0.999 + 6.79\text{x}10^{7}(\text{E})^{-1}$	0.520	47.2
10. Elongation (ELON)	Avg. MDP Rate = $2.771 - 2.38\text{x}10^{3}(\text{ELON})^{-3}$	0.434	88.5

* Coefficient of Determination.

** Average Absolute % Deviation.

deviation (AAPD) for the analysis are noted. The predicting equations are arranged in order of decreasing statistical significance based on the coefficient of determination. It is seen that true strain energy based either on the reduction in area or elongation is quite successful as a single correlating parameter for all of the lead-bismuth data. The tensile strength, hardness, and engineering strain energy, although having much lower values of coefficient of determination, are also successful in this regard, based on the average absolute percent deviation. The other mechanical properties listed do not suitably account for the experimental data on an individual basis. It is further noted that the average MDP rate is inversely proportional to powers of true strain energy, engineering strain energy, tensile strength, and hardness in this analysis. Hence one might conclude that the cavitation resistance of a group of materials in lead-bismuth alloy could be at least qualitatively predicted on the basis of these mechanical properties.

Further attempts at complete correlations of the experimental data were conducted in which all ten mechanical properties noted previously, each raised to ten exponents, were possible terms in the predicting equation. Hence a total of 100 terms plus a pure constant were considered by the program. Table XVIII summarizes the statistically best predicting equations obtained under these conditions. The coefficient of determination and average absolute percent deviation are noted for each of the correlations presented. Note that all three equations contain terms involving the true strain energy based either on elongation or reduction in area. The tensile strength is also prominent in two of the equations.

TABLE XVIII

SUMMARY OF BEST CORRELATIONS WITH TEN PROPERTIES CONSIDERED - LEAD-BISMUTH ALLOY

(1)

$$\text{Avg. MDP Rate} = 0.713 + 3.12\times10^{4}(\text{TSER})^{-1} - 6.55\times10^{-4}(\text{TS})^{-1} + 2.97\times10^{21}(\text{E})^{-3}$$

Coefficient of Determination = 0.996

Average Absolute % Deviation = 0.4%

(2)

$$\text{Avg. MDP Rate} = 0.233 + 2.57\times10^{4}(\text{TSER})^{-1}$$

Coefficient of Determination = 0.986

Average Absolute % Deviation = 0.1%

(3)

$$\text{Avg. MDP Rate} = 0.682 + 3.24\times10^{10}(\text{TSEE})^{-3} + 1.09\times10^{9}(\text{TS})^{-2}$$

Coefficient of Determination = 0.986

Average Absolute % Deviation = 0.8%

These mechanical properties all enter the predicting equations in an inverse manner, as was the case with the single property correlations. The very best equation involves a combination of true strain energy, tensile strength, and elastic modulus, each entering in an inverse relationship.

In the analysis of the lead-bismuth data allowing all ten mechanical properties, the end result is a series of 15 predicting equations or correlations, each with a different statistical accuracy.

Obviously, the equation with the greatest statistical accuracy would result in the best fit between the predicted and experimental data. However, for the data submitted for analysis here, namely, the experimental cavitation information obtained at 500°F and at 1500°F in lead-bismuth alloy and the corresponding mechanical properties, it was found that the coefficient of determination for all the correlations was never less than 0.98, indicating extremely good agreement between the predicting equation values and the experimental data.

Figure 24 is a plot of the predicted values of average MDP rate based on Equation (1) in Table XVIII versus the corresponding experimental data points. Deviation from the 45° line noted on the plot is a measure of the error inherent in the correlation. The excellent agreement of the predicted values and experimental points is noted.

C. Mercury Correlations

The cavitation data obtained at 70°F and 500°F in mercury was also submitted to the least mean squares regression program in an attempt to obtain a first-order interaction correlation that would be applicable at both temperatures. The independent variables were the same as those discussed previously for the lead-bismuth correlations.

Initially, an attempt was made to correlate the damage data with each mechanical property individually. Table XIX summarizes the results of this effort. The ten properties considered, the statistically best predicting equation generated by the program for each property, the coefficient of determination for the analysis, and the average absolute percent deviation for the analysis are noted. The predicting

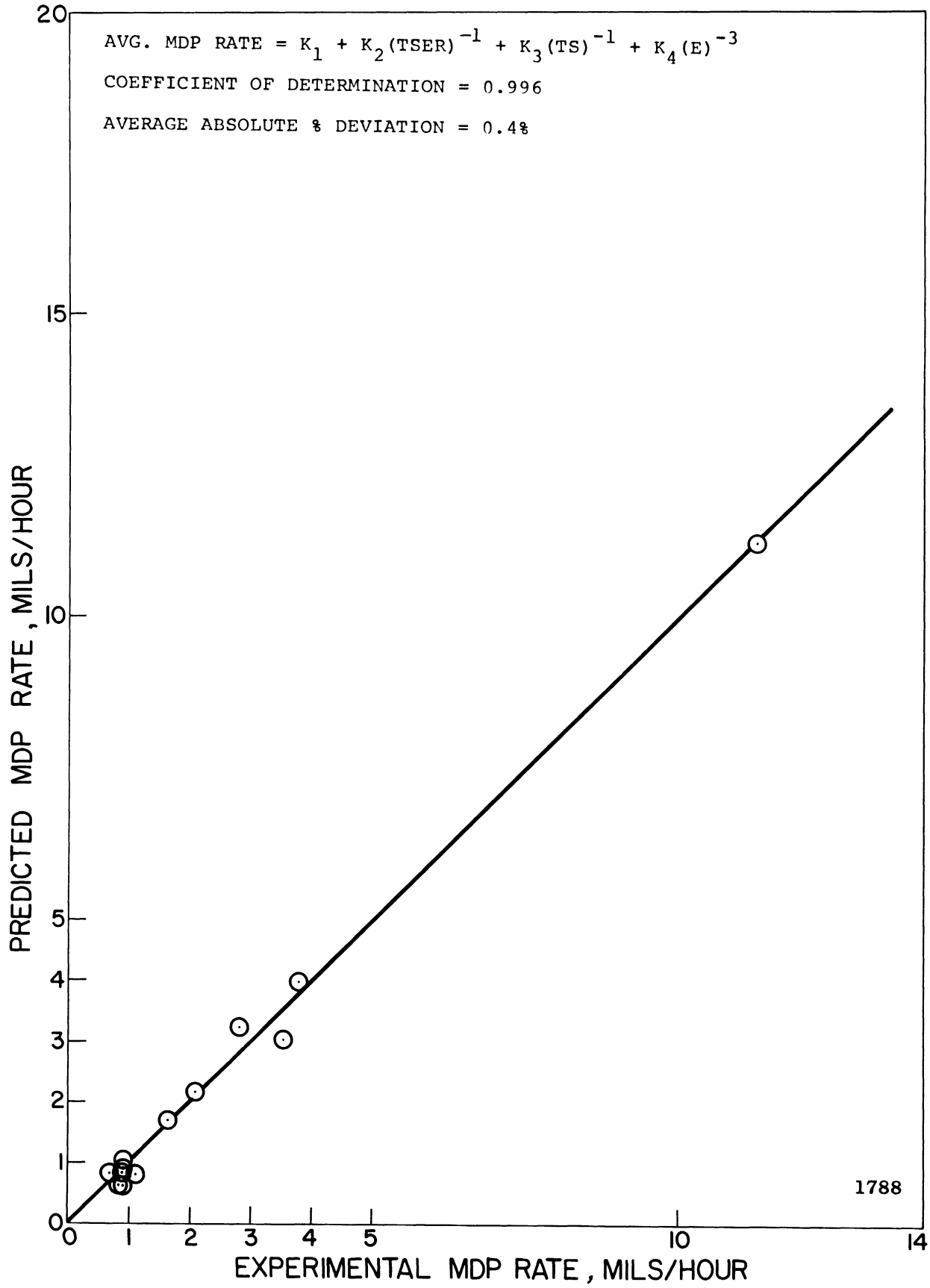

Figure 24. Comparison of Predicted MDP Rate and Experimental MDP Rate - Lead-Bismuth Alloy.

TABLE XIX

SUMMARY OF SINGLE PROPERTY CORRELATIONS - MERCURY

Property	Predicting Equation	CD*	AAPD**
1. True Strain Energy (TSEE) (Based on Elongation)	Avg. MDP Rate = $0.338 + 4.90 \times 10^{7}(TSEE)^{-2}$	0.965	8.5
2. Hardness (H) (DPH - 1.1 Kg. Load)	Avg. MDP Rate = $0.242 + 1.76 \times 10^{4}(H)^{-2}$	0.921	15.8
3. Tensile Strength (TS)	Avg. MDP Rate = $-0.385 + 9.59 \times 10^{4}(TS)^{-1}$	0.909	14.9
4. Yield Strength (YS)	Avg. MDP Rate = $0.178 + 3.82 \times 10^{4}(YS)^{-1}$	0.863	26.5
5. Elastic Modulus (E)	Avg. MDP Rate = $0.269 + 6.16 \times 10^{21}(E)^{-3}$	0.831	18.5
6. True Strain Energy (TSER) (Based on Reduction in Area)	Avg. MDP Rate = $0.657 + 1.40 \times 10^{12}(TSER)^{-3}$	0.824	35.1
7. Engineering Strain Energy (ESE)	Avg. MDP Rate = $-0.179 + 1.58 \times 10^{4}(ESE)^{-1}$	0.752	22.3
8. Acoustic Impedance Ratio (AI)	Avg. MDP Rate = $-0.186 + 4.91\ (AI)^{2}$	0.735	34.2
9. Reduction in Area (RA)	Avg. MDP Rate = $-0.237 + 2.52 \times 10^{-6}(RA)$	0.684	49.0
10. Elongation (ELON)	Avg. MDP Rate = $1.091 - 1.96 \times 10^{-6}(ELON)^{3}$	0.538	64.3

* Coefficient of Determination.

** Average Absolute % Deviation.

equations are arranged in order of decreasing statistical significance based on the coefficient of determination. It is seen that true strain energy based on elongation* and hardness are quite successful as single correlating parameters for all of the mercury data. The tensile strength, yield strength, and elastic modulus are only partially successful in this regard. The other mechanical properties listed do not suitably account for the experimental data on an individual basis. It is further noted that the average MDP rate is inversely proportional to some power of true strain energy, hardness, tensile strength, yield strength, and elastic modulus in this analysis. Hence one might conclude that the cavitation resistance of a group of materials in mercury could be at least qualitatively predicted on the basis of these mechanical properties.

Complete correlations in which all ten mechanical properties were allowed to enter the predicting equation were also conducted with the mercury data. Table XX summarizes the statistically best predicting equations obtained under these conditions. The coefficient of determination and average absolute percent deviation are noted for each of the correlations presented. Note that all three equations contain terms involving the true strain energy based on elongation, whereas, as previously mentioned, the true strain energy based on reduction in area was prominent in the lead-bismuth correlations. The hardness and tensile strength are also prominent. All of these properties are inversely proportional to the average MDP rate, and, hence, proportional to cavitation resistance. The statistically best correlation includes the true strain energy based on elongation and the hardness.

---

* Note that true strain energy based on reduction in area was a more successful parameter in the lead-bismuth correlations but is quite unsuccessful for the mercury tests. The reason for this disagreement is not known.

TABLE XX

SUMMARY OF BEST CORRELATIONS WITH TEN PROPERTIES CONSIDERED - MERCURY

(1)

$$\text{Avg. MDP Rate} = -0.577 + 1.39\times10^{11}(\text{TSEE})^{-3} + 16.49(\text{H})^{-1/2}$$

Coefficient of Determination = 0.966

Average Absolute % Deviation = 10.1%

(2)

$$\text{Avg. MDP Rate} = 0.338 + 4.90\times10^{7}(\text{TSEE})^{-2}$$

Coefficient of Determination = 0.965

Average Absolute % Deviation = 8.5%

(3)

$$\text{Avg. MDP Rate} = 0.232 + 1.41\times10^{11}(\text{TSEE})^{-3} + 2.89\times10^{4}(\text{TS})^{-1}$$

Coefficient of Determination = 0.961

Average Absolute % Deviation = 13.1%

Figure 25 is a plot of the predicted values of average MDP rate based on Equation (1) in Table XX versus the corresponding experimental data points. The excellent agreement of the predicted values and experimental points is noted.

The materials tested in lead-bismuth alloy and mercury were identical with the exception of the carbon steel and Plexiglas which were tested in mercury only. Single property correlations for each of the fluids indicate that a different form of true strain energy is successful as a correlating parameter, each raised to a different exponent. Hardness and tensile strength are also relatively successful in this regard for both fluids. Ten property correlations for each of the fluids

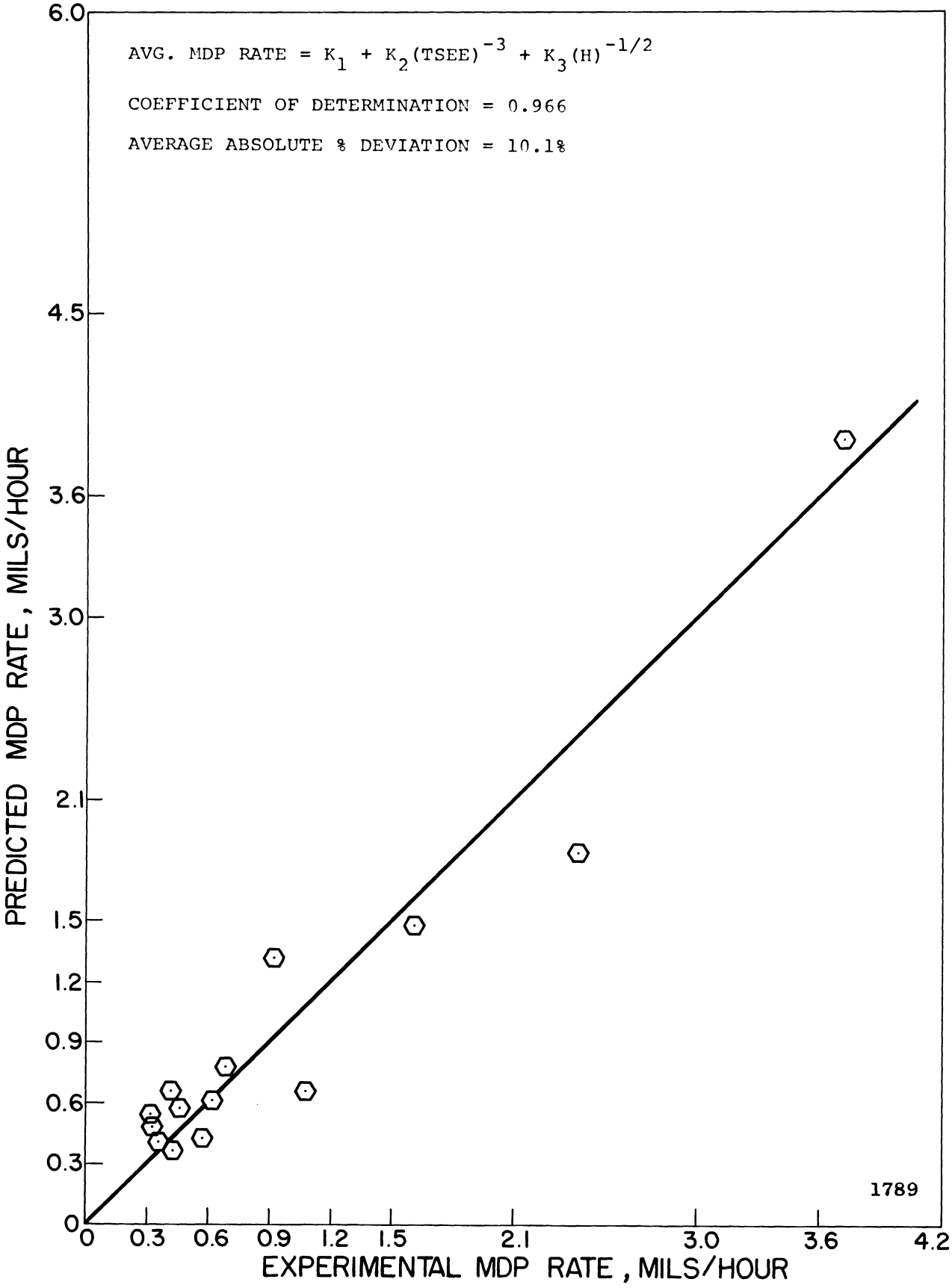

Figure 25. Comparison of Predicted MDP Rate and Experimental MDP Rate - Mercury.

show that a form of strain energy and also tensile strength appear in the predicting equations for each fluid. In general, it is seen for both fluids that mechanical properties that successfully correlate the experimental data individually are also prominent in the full ten property predicting equations, as expected.

D. Water Correlations - Subset 1

The cavitation data obtained at 70°F in water was analyzed in a manner similar to that employed for the lead-bismuth and mercury data. Since many more materials were tested in water than in the liquid metals, the materials were divided into three subsets for data analysis, as mentioned previously. Subset 1 consisted of those materials which were also tested in the liquid metals, whereas Subsets 2 and 3 were tested in water only. Separate correlations of the cavitation data in Subset 1, Subsets 2 and 3 combined, and the full water data set were carried out. Hence the effects of different fluids on the correlations can be determined by examining the individual correlations for the lead-bismuth data, mercury data, and Subset 1 of the water data. The materials tested in all three cases were identical. Further, by comparing the correlations of Subset 1 and the full water data set and by examining the correlation of Subsets 2 and 3 combined, it is possible to determine any significant differences that may exist in correlating parameters for the various subsets of water data.

Subset 1 was first correlated in terms of single properties. Table XXI summarizes the results of this effort. The ten properties considered, the statistically best predicting equation generated by

TABLE XXI

SUMMARY OF SINGLE PROPERTY CORRELATIONS - WATER - SUBSET 1

Property	Predicting Equation	CD*	AAPD**
1. Tensile Strength (TS)	Avg. MDP Rate = $0.006 + 8.38\text{x}10^{3}(TS)^{-1}$	0.953	0.2
2. Hardness (H) (DPH - 1.1 Kg. Load)	Avg. MDP Rate = $0.184 - 4.26\text{x}10^{-9}(H)^{3}$	0.934	4.8
3. Yield Strength (YS)	Avg. MDP Rate = $0.011 + 27.95(YS)^{-1/2}$	0.922	9.0
4. True Strain Energy (TSER) (Based on Reduction in Area)	Avg. MDP Rate = $0.108 + 7.50\text{x}10^{-17}(TSER)^{3}$	0.901	15.6
5. Acoustic Impedance Ratio (AI)	Avg. MDP Rate = $0.038 + 54.55(AI)^{2}$	0.897	10.8
6. Elongation (ELON)	Avg. MDP Rate = $0.147 - 5.62(ELON)^{-2}$	0.865	17.3
7. True Strain Energy (TSEE) (Based on Elongation)	Avg. MDP Rate = $0.115 + 1.26\text{x}10^{10}(TSEE)^{-3}$	0.860	16.8
8. Reduction in Area(RA)	Avg. MDP Rate = $0.087 + 7.13\text{x}10^{-6}(RA)^{2}$	0.857	18.3
9. Elastic Modulus (E)	Avg. MDP Rate = $0.041 + 1.80\text{x}10^{6}(E)^{-1}$	0.810	3.2
10. Engineering Strain Energy (ESE)	Avg. MDP Rate = $0.089 + 4.21\text{x}10^{2}(ESE)^{-1}$	0.782	4.9

* Coefficient of Determination.

** Average Absolute % Deviation.

the program for each property, the coefficient of determination for the analysis, and the average absolute percent deviation for the analysis are noted. It is seen that tensile strength, hardness, and yield strength are successful as single correlating parameters for Subset 1, each appearing in an inverse relationship. The acoustic impedance ratio is partially successful in this regard. The single property correlations of lead-bismuth data and mercury data also indicated that tensile strength and hardness were successful correlating parameters. However, the prominence of some form of true strain energy in the lead-bismuth and mercury cases has been reduced considerably in the correlations of the Subset 1 water data. It might also be noted here that the damage obtained in lead-bismuth alloy and mercury was very uniform, whereas the damage obtained in water on the materials in Subset 1 was somewhat more selective and was characterized by some individual, discrete craters.

Full ten property correlations of the Subset 1 data are summarized in Table XXII where only the statistically best predicting equations obtained are listed. We note that each predicting equation involves only a single mechanical property, namely, tensile strength, hardness, and acoustic impedance ratio, each of which was successful in the single property correlations. In fact, the predicting equation involving the tensile strength is identical to that obtained in the single property analysis.

Full ten property correlations of the lead-bismuth and mercury data also showed a strong dependence on tensile strength and hardness.

Figure 26 is a plot of the predicted values of average MDP rate based on Equation (1) in Table XXII versus the corresponding experimental data points and serves to indicate the extent of agreement obtained.

TABLE XXII

SUMMARY OF BEST CORRELATIONS WITH TEN PROPERTIES CONSIDERED - WATER - SUBSET 1

(1)

Avg. MDP Rate = $0.006 + 8.38 \times 10^{3}(TS)^{-1}$

Coefficient of Determination = 0.953

Average Absolute % Deviation = 0.2%

(2)

Avg. MDP Rate = $1.83(H)^{-1/2}$

Coefficient of Determination = 0.904

Average Absolute % Deviation = 14.9%

(3)

Avg. MDP Rate = $72.98(AI)^{2}$

Coefficient of Determination = 0.873

Average Absolute % Deviation = 28.9%

E. Water Correlations - Subsets 2 and 3

The materials contained in Subsets 2 and 3 (Plexiglas, aluminum, Cu, Cu-Ni, Cu-Zn, and Ni) were tested in water only. Single property correlations of the two subsets combined are summarized in Table XXIII.

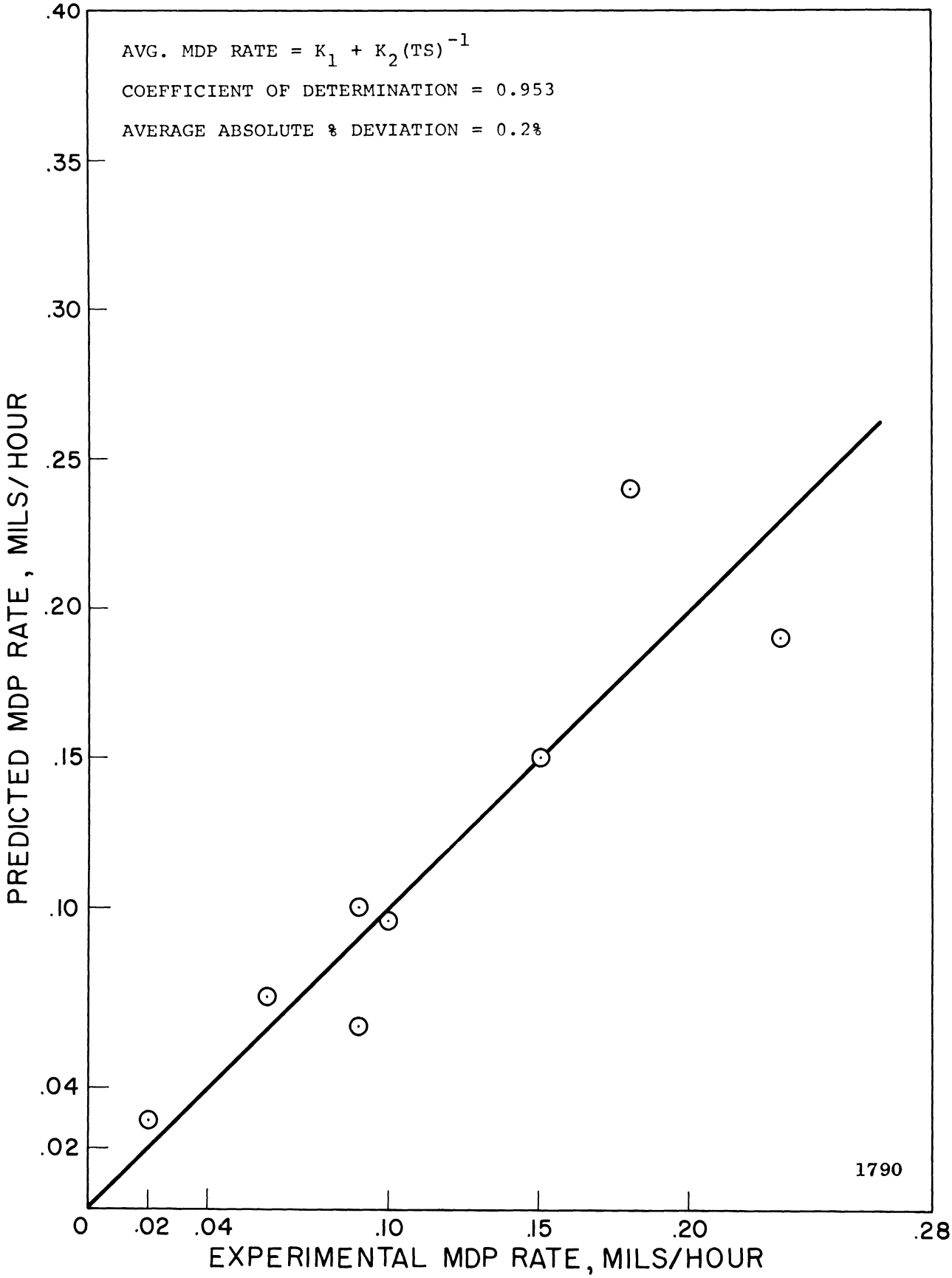

Figure 26. Comparison of Predicted MDP Rate and Experimental MDP Rate - Water - Subset 1.

TABLE XXIII

SUMMARY OF SINGLE PROPERTY CORRELATIONS - WATER - SUBSETS 2 & 3

Property	Predicting Equation	CD*	AAPD**
1. Hardness (H) (DPH - 1.1 Kg. Load)	Avg. MDP Rate = $1.038 - 3.96\times10^{4}(H)^{-3} - 1.02\times10^{2}(H)^{-1} + 5.35\times10^{3}(H)^{-2}$	0.966	6.1
2. Reduction in Area (RA)	Avg. MDP Rate = $1.383 + 4.54\times10^{-6}(RA)^{3} - 0.18(RA)^{1/2}$	0.950	8.0
3. Tensile Strength (TS)	Avg. MDP Rate = $-0.413 + 2.50\times10^{2}(TS)^{-1/2}$	0.910	5.4
4. Acoustic Impedance Ratio(AI)	Avg. MDP Rate = $1.505 - 3.31\times10^{-2}(AI)^{-1}$	0.794	15.4
5. Elastic Modulus (E)	Avg. MDP Rate = $-0.021 - 1.89\times10^{6}(E)^{-1} + 3.88\times10^{3}(E)^{-1/2}$	0.775	19.5
6. Yield Strength (YS)	Avg. MDP Rate = $0.198 + 15.80(YS)^{-1/3}$	0.768	17.6
7. True Strain Energy (TSER) (Based on Reduction in Area)	Avg. MDP Rate = $1.031 - 1.80\times10^{-10}(TSER)^{2}$	0.737	21.2
8. True Strain Energy (TSEE) (Based on Elongation)	Avg. MDP Rate = $0.447 + 6.91(TSEE)^{-1/3}$	0.737	21.9
9. Engineering Strain Energy(ESE)	Avg. MDP Rate = $0.641 + 13.80(ESE)^{-1/2}$	0.731	22.4
10. Elongation (ELON)	Avg. MDP Rate = $0.723 + 3.86\times10^{-3}(ELON)$	0.709	24.7

* Coefficient of Determination.

** Average Absolute % Deviation.

Hardness, reduction in area, and tensile strength are most suitable for correlation purposes, whereas the other properties listed are less successful in this regard. Tensile strength and hardness were also successful in the Subset 1 single property correlations, as well as in the corresponding lead-bismuth and mercury analyses.

Full ten property correlations of Subsets 2 and 3 combined are presented in Table XXIV. All three expressions listed have very high coefficients of determination and very low average absolute percent deviations, indicating excellent agreement between the experimental and predicted values. Hardness, tensile strength, and yield strength are prominent in these expressions. As noted previously, hardness and tensile strength were also successful as single correlating parameters.

TABLE XXIV

SUMMARY OF BEST CORRELATIONS WITH TEN PROPERTIES CONSIDERED - WATER - SUBSETS 2 & 3

(1)

$$\text{Avg. MDP Rate} = 0.392 - 12.0(YS)^{-1/3} - 3.82\times10^{7}(TSEE)^{-3} + 3.61\times10^{4}(TS)^{-1}$$

Coefficient of Determination = 0.991

Average Absolute % Deviation = 2.7%

(2)

$$\text{Avg. MDP Rate} = -0.822 + 6.22\times10^{2}(TS)^{-1/2} - 11.45(H)^{-1/2}$$

Coefficient of Determination = 0.985

Average Absolute % Deviation = 1.1%

(3)

$$\text{Avg. MDP Rate} = 0.163 - 3.41\times10^{3}(YS)^{-1} + 3.62\times10^{4}(TS)^{-1}$$

Coefficient of Determination = 0.984

Average Absolute % Deviation = 3.1%

Hence it appears that tensile strength and hardness are the most successful correlating parameters both for the Subset 1 water data and also the combined data in Subsets 2 and 3.

Figure 27 is a plot of the predicted values of average MDP rate based on Equation (1) in Table XXIV versus the corresponding experimental data points and serves to indicate the extent of agreement obtained. In this case the agreement is excellent.

F. Water Correlations - All Water Data

Finally, the complete set of water data was subjected to the regression analysis. The single property correlations are summarized in Table XXV. It is seen that the hardness, tensile strength, and yield strength are the most successful as correlating parameters among the ten properties, as expected. However, only hardness is reasonably successful from a statistical point of view. For the other properties, variations between experimental and predicted values are 40% and greater.

The statistically best ten property correlations of the water data are summarized in Table XXVI. Only Equation (1), involving a combination of tensile strength, hardness, and reduction in area, satisfactorily predicts the experimental data.

Figure 28 is a plot of the predicted values of average MDP rate based on Equation (1) in Table XXVI versus the corresponding experimental data points and indicates the extent of agreement obtained.

In summary, it is seen that the mechanical properties of hardness, tensile strength, and yield strength adequately predict the experimental water data on a single property basis. This is true either

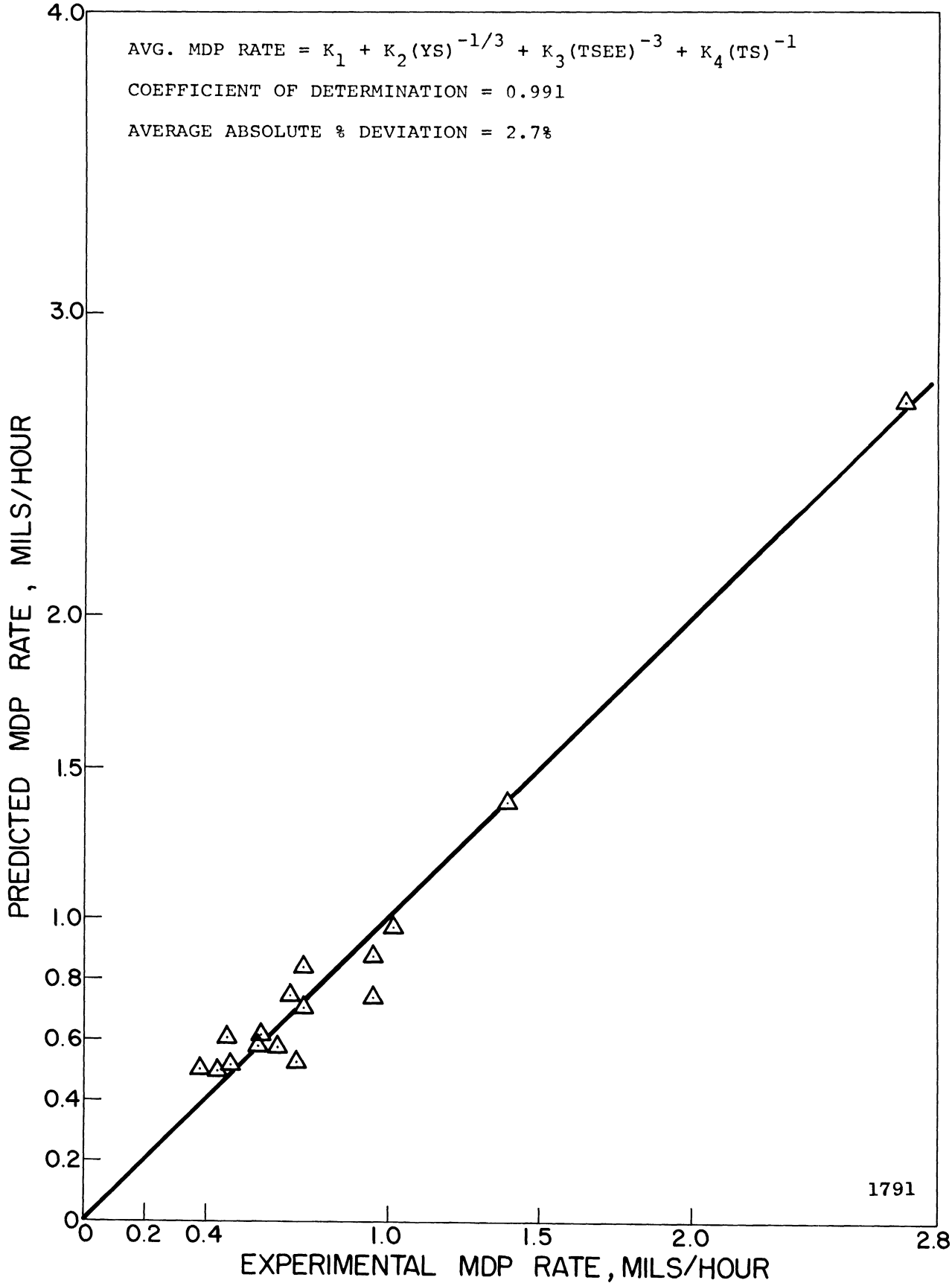

Figure 27. Comparison of Predicted MDP Rate and Experimental MDP Rate - Water - Subsets 2 and 3.

TABLE XXV

SUMMARY OF SINGLE PROPERTY CORRELATIONS - ALL WATER DATA

Property	Predicting Equation	CD*	AAPD**
1. Hardness(H) (DPH - 1.1 Kg. Load)	Avg. MDP Rate = $-6.023 + 1.30\times10^{4}(H)^{-2} + 53.63(H)^{-1/3} - 6.17\times10^{2}(H)^{-1} - 8.00\times10^{4}(H)^{-3}$	0.946	18.7
2. Tensile Strength(TS)	Avg. MDP Rate = $-0.619 + 2.69\times10^{2}(TS)^{-1/2}$	0.851	40.7
3. Yield Strength (YS)	Avg. MDP Rate = $-0.193 + 22.4(YS)^{-1/3}$	0.708	62.1
4. Acoustic Impedance Ratio(AI)	Avg. MDP Rate = $1.491 - 3.99\times10^{-2}(AI)^{-1}$	0.708	70.8
5. Elastic Modulus(E)	Avg. MDP Rate = $1.832 - 2.79\times10^{-4}(E)^{1/2}$	0.695	62.5
6. True Strain Energy(TSEE) (Based on Elongation)	Avg. MDP Rate = $0.053 + 10.70(TSEE)^{-1/3}$	0.627	92.6
7. Engineering Strain Energy(ESE)	Avg. MDP Rate = $0.084 + 10.39(ESE)^{-1/3}$	0.624	91.2
8. True Strain Energy(TSER) (Based on Reduction in Area)	Avg. MDP Rate = $0.295 + 7.95(TSER)^{-1/3}$	0.587	110.9
9. Reduction in Area(RA)	Avg. MDP Rate = $0.829 - 1.51(RA)^{-1/2}$	0.549	124.6
10. Elongation(ELON)	Avg. MDP Rate = $0.557 + 3.28(ELON)^{-2}$	0.538	120.9

* Coefficient of Determination.

** Average Absolute % Deviation.

for Subset 1, Subsets 2 and 3 combined, or the full water data set. In addition the elastic modulus is successful as a single correlating parameter for Subset 1. These same properties are the most prominent in the ten property water correlations.

In the case of lead-bismuth, tensile strength and hardness were also successful as single property correlating parameters, but the true strain energy was more successful in this respect. A similar comment applies to the single property mercury correlations.

In general, it is concluded that those properties most successful as single correlating parameters in a given fluid are the most prominent in the ten property correlations, as one would expect.

TABLE XXVI

SUMMARY OF BEST CORRELATIONS WITH TEN PROPERTIES CONSIDERED - ALL WATER DATA

(1)

$$\text{Avg. MDP Rate} = -0.068 + 3.07\times10^{8}(TS)^{-2} - 8.32\times10^{-7}(RA)^{3} - 2.03\times10^{3}(H)^{-3} + 1.49\times10^{2}(TS)^{-1/2}$$

Coefficient of Determination = 0.976

Average Absolute % Deviation = 0.5%

(2)

$$\text{Avg. MDP Rate} = -2.224 + 19.93(H)^{-1/3} - 2.22\times10^{2}(YS)^{-1/2}$$

Coefficient of Determination = 0.864

Average Absolute % Deviation = 28.5%

(3)

$$\text{Avg. MDP Rate} = -0.619 + 2.69\times10^{2}(TS)^{-1/2}$$

Coefficient of Determination = 0.851

Average Absolute % Deviation = 40.7%

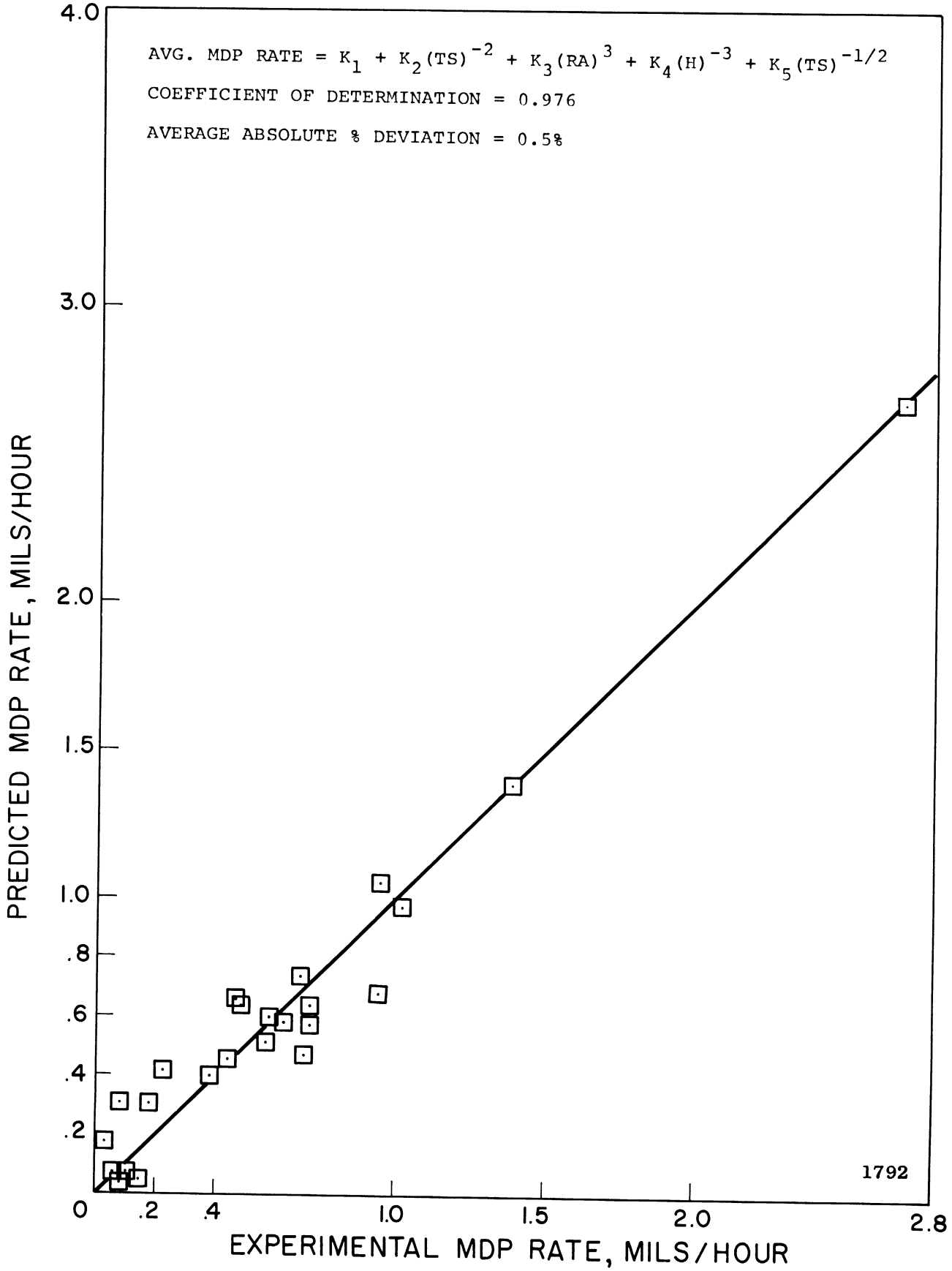

Figure 28. Comparison of Predicted MDP Rate and Experimental MDP Rate - All Water Data.

Thus far, the only property included in the regression analysis that is a function of the fluid has been the ratio of acoustic impedances of the test fluid and specimen material. This quantity did not successfully correlate either the lead-bismuth or mercury data and did not appear in the ten property correlations. In the case of the water data the acoustic impedance ratio was more successful as a correlating parameter.

It is noted at this point that whereas energy properties were quite important in the correlation of the data from the tests with high density liquid metals (lead-bismuth alloy and mercury), they are almost completely insignificant in the water tests. On the other hand, the strength properties (including hardness in this category) are predominant in the water tests. The same observations apply to the venturi tests, although the role of energy terms was not as great for the liquid metal venturi tests as for the vibratory liquid metal tests.(18)

Theoretical arguments have been advanced in the past to show that a correlation would involve both energy and strength terms.(36) According to these arguments only strength terms would be involved if the stresses imposed by the cavitating flow regime upon the materials were less than the fatigue limit for the materials. It would be expected that this limiting condition would apply more closely to the water tests (relatively low density fluid) than to the liquid metal tests. Thus this argument to some extent is consistent with the present experimental data.

G. Fluid Coupling Parameters

It is desired to obtain a predicting equation of high statistical accuracy valid for all the lead-bismuth, mercury, and water data combined. Since the dynamics of the bubble are controlled by the physical properties of the fluid, it is necessary to account for variations in fluid properties as the tests were conducted in three different fluids at several test temperatures. This can be done by including a suitable fluid coupling parameter among the several mechanical properties which are allowed to enter the predicting equation. The ratio of acoustic impedances of the test fluid and specimen material (previously discussed) is one such fluid coupling parameter. Others that have been suggested by various investigators include the fluid density, surface tension, net positive suction head, compressibility or bulk modulus, and kinematic viscosity. It is instructive to examine each of these with respect to definition, motivation, and any previous experimental history. All will be investigated as possible fluid coupling parameters in the comprehensive correlations described later.

(1) Acoustic Impedance Ratio (AI)

The acoustic impedance ratio is defined as:[31]

$$AI = \frac{\text{Acoustic Impedance of Test Fluid}}{\text{Acoustic Impedance of Test Specimen}} = \frac{R_1}{R_2}$$

$$AI = \frac{(\rho c)_{FLUID}}{(\rho c)_{MATERIAL}}$$

where:

AI = acoustic impedance ratio

ρ = density

c = velocity of sound in medium

R_1 = acoustic impedance of test fluid

R_2 = acoustic impedance of test specimen

Since the velocity of sound, c , can be expressed as:

$$c = (E/\rho)^{1/2} \text{ (for a solid)}$$

$$c = (B/\rho)^{1/2} \text{ (for a liquid)}$$

where:

E = elastic modulus (for a solid)

B = bulk modulus (for a liquid)

Thus:

$$AI = \frac{(B\rho)^{1/2}_{FLUID}}{(E\rho)^{1/2}_{SOLID}}$$

Physically, the acoustic impedance ratio is related to the ratio of reflected to transmitted energy as liquid shock waves or jets impinge on the solid test material. The transmission coefficient, α_t , which is defined as the fraction of acoustic energy incident upon an interface of two materials possessing dissimilar acoustic impedances that is transmitted across the interface, can be expressed as:[31]

$$\alpha_t = \frac{4 R_1 R_2}{(R_1+R_2)^2} \quad \frac{4(R_1/R_2)}{(R_1/R_2)^2 + 2(R_1/R_2) + 1}$$

where in our case R_1 and R_2 are the acoustic impedances of test fluid and test material, respectively. It is seen that as $R_1 \rightarrow R_2$, $\alpha_t \rightarrow 1$, and we have 100% transmission (both media have identical acoustic properties). Further, if a liquid jet is assumed to be the damaging mechanism in cavitation, then according to the most simplified "water-hammer" analysis, R_1/R_2 enters into the expression for the transient pressure generated on the surface by jet impact; i.e.,

$$\Delta p_{impact} = \frac{\rho_1 c_1 v}{1 + R_2/R_1}$$

where:

Δp_{impact} = pressure increase on surface due to impact

ρ_1 = density of fluid

c_1 = velocity of sound in fluid

v = velocity of liquid jet

R_1 = acoustic impedance of fluid

R_2 = acoustic impedance of test specimen

In the case of our experiment there are several reasons why one might select the acoustic impedance ratio as a suitable coupling parameter for the comprehensive cavitation damage correlations. First, acoustic energy in the form of sound waves is transmitted along the exponential horn assembly to which the test specimen is attached. This acoustic energy

is then propagated into the test fluid, but the amount of energy passing into the fluid is determined by the acoustic impedances of the test specimen and fluid. Hence, the formation of a bubble cloud at the specimen face is strongly dependent on suitable energy being transmitted into the fluid. Secondly, the bubble collapse gives rise to a shock wave or liquid jet that is propagated throughout the fluid. In order for damage to occur at the specimen surface, this energy in the form of the shock wave or liquid jet must be transmitted across the liquid-solid interface. Hence, one might expect the amount of damage to the test specimen to be a function of the amount of energy transmitted across this interface and actually reaching the specimen. Here again, the ratio of acoustic impedances or the transmission coefficient is the determining factor. Finally, the ratio is involved in the relation for pressure-loading of the surface in the case of jet impact, as previously stated. Thus, the ratio of acoustic impedances was chosen as a possible fluid coupling parameter. It is further postulated that the greater the acoustic impedance ratio, the greater the amount of damage sustained by the test specimen. This is reasonable since as $(R_1/R_2) \rightarrow 1$, $\alpha_t \rightarrow 1$, and we have complete transmission of the acoustic energy from transducer tip to fluid, and complete transmission of energy represented by shock waves or liquid jets from fluid to specimen surface,

causing maximum damage. In addition, the pressure generated by the impacting jet is also maximized for a given fluid condition.

(2) Density (ρ)

The density of the fluid may be a suitable coupling parameter since one would expect the pressure exerted on the specimen surface to be proportional to the density for fixed NPSH, compressibility, kinematic viscosity, etc. Hence, one would expect the damage to increase as the density was increased. Wilson and Graham[32] conducted cavitation tests on silver in a variety of fluids and showed experimentally that this was, indeed, the case.

(3) Surface Tension (σ)

The expected effect of surface tension on cavitation damage, based on the conclusions from dynamics of transient cavities, would be an increase in damage as the surface tension is increased, since collapse pressures would be higher with greater surface tension. This behavior was reported experimentally by Nowotny.[33] However, recent numerical calculations show that the effect of surface tension should be quite negligible.[36,37]

(4) Net Positive Suction Head (NPSH)

The net positive suction head, NPSH, is defined as:

$$NPSH = \frac{p-p_v}{\rho}$$

where:

p = local pressure of fluid

p_v = vapor pressure of fluid

ρ = density of fluid

It was shown by Nowotny[33] that damage was decreased as the vapor pressure increased for tests where p in the above relation was held constant, since the collapsing pressure differential was reduced for a given fluid, and, in addition, perhaps the additional vapor served to cushion the collapsing bubbles. As mentioned previously, the damage rate would be expected to increase as the density increased if the NPSH were held constant. In general, the damage should be inversely related to the NPSH. In our experiments the local static pressure, p, was varied by varying the argon cover gas pressure so that the difference between local static pressure and vapor pressure, $p - p_v$, was maintained constant. Then:

$$\text{NPSH} \propto 1/\rho$$

for these tests, based on static pressure. However, the dynamic head caused by the vibration of the horn would be the same for all fluids, assuming the fluid density and temperature do not affect the vibrating behavior of the horn (of course, this is not precisely true). Since the dynamic portion of the NPSH is probably predominant, these tests may well be closer to a constant NPSH condition than a constant

pressure suppression condition. If so, the collapse velocities would be similar for all fluids, and the imposed pressures on the surface would be proportional to the fluid density, so that damage should increase with increased fluid density. Clearly, more sophisticated and detailed analysis on this point is required to understand the complex relationships involved.

(5) Bulk Modulus (B)

The bulk modulus is the inverse of the compressibility. It might be a suitable coupling parameter since it affects the pressure exerted on the specimen surface. Hence, one would expect the damage to increase as the bulk modulus increased (compressibility decreased). This behavior was reported from experiments by Wilson and Graham.[32]

(6) Kinematic Viscosity (ν)

The kinematic viscosity, ν , is defined as:

$$\nu = \mu/\rho$$

where

μ = viscosity of fluid

ρ = density of fluid

Since bubble collapse pressures are theoretically greater[36,37] in fluids of low viscosity (although the effect is quite small),

one would expect cavitation damage to be inversely related to the viscosity, μ . Wilson and Graham[32] reported this effect from their experiments.

It is felt that each of the six quantities discussed above merits consideration as a fluid coupling parameter for the comprehensive lead-bismuth, mercury, and water correlations to be discussed.

H. Comprehensive Lead-Bismuth, Mercury, and Water Correlations

The major objective of the computer analyses described thus far is to deduce a single comprehensive predicting equation that would suitably explain the lead-bismuth, mercury, and water data. Such an equation would, of necessity, include at least one fluid coupling parameter to account for the variations in fluid properties for the three fluids considered and the corresponding test temperatures, since it has already been shown that the cavitation resistance of all the materials tested, and their relative rankings, depend on the fluid. The combined lead-bismuth, mercury, and water data was submitted to the regression program in an attempt to arrive at the required correlation of all experimental data in terms of mechanical and fluid properties. The mechanical properties allowed in these correlations were the same as previously employed: tensile strength, yield strength, engineering strain energy, true strain energy (two values based on elongation and reduction in area), hardness, elongation, reduction in area, and elastic modulus. In addition, each of the six fluid coupling parameters discussed previously, namely, acoustic impedance ratio, density, surface

tension, net positive suction head, bulk modulus, and kinematic viscosity, was combined separately with the group of nine mechanical properties. Hence, six comprehensive correlations were attempted, allowing a total of ten mechanical and fluid properties in each. It was hoped that such a procedure would indicate those fluid properties that were most successful as coupling parameters. The values of the fluid coupling parameters used in these correlations are listed in Table XXVII. A summary of the results of the six correlations follows.

(1) Acoustic Impedance Ratio (AI)

When the acoustic impedance ratio is used as the fluid coupling parameter and combined with the nine mechanical properties allowed to enter the predicting equation, the statistically best correlation obtained is:

$$\begin{aligned}\text{Avg. MDP Rate} = 8.97 &- 3.10\text{x}10^{2}(\text{TSER})^{-1/3} + 4.50\text{x}10^{4}(\text{TSER})^{-1} \\ &- .159(\text{TSER})^{1/3} - 1.20\text{x}10^{2}(\text{TSEE})^{-1/2} \\ &+ 1.71\ (\text{AI})^{1/3} - 7.40\text{x}10^{2}(\text{ESE})^{-1/2} \\ &- 3.49\text{x}10^{9}(\text{TSER})^{-3} + 3.22\text{x}10^{2}(\text{TS})^{-1/2} \\ &+ 8.88\text{x}10^{3}(\text{TSEE})^{-1} + 2.32\text{x}10^{2}(\text{ESE})^{-1/3}\end{aligned}$$

Coefficient of Determination = 0.980

Average Absolute % Deviation = 2.7%

Although the equation may appear formidable at first glance, it should be noted that 8 of the 11 terms present involve some form of the strain energy. If the allowable exponents were not restricted to positive and negative integers and

TABLE XXVII*

FLUID PROPERTIES DATA AT VARIOUS TEMPERATURES

Fluid Property \ Fluid	Water 70°F	Mercury 70°F	Mercury 500°F	Pb-Bi 500°F	Pb-Bi 1500°F
Acoustic Impedance (lbm./ft.^{2}sec.)	$.299 \times 10^6$	4.03×10^6	3.85×10^6	3.08×10^6	2.86×10^6
Density (ρ) (g./cc.)	1.0	13.55	12.98	10.38	9.64
Surface Tension (σ) (dynes/cm.)	72.8	465.0	419.0	397.0	367.0
Net Positive Suction Head (NPSH) (feet)	36.5	2.7	2.8	3.5	3.8
Bulk Modulus (B) (psi)	$.31 \times 10^6$	4.11×10^6	3.94×10^6	3.16×10^6	2.92×10^6
Kinematic Viscosity (ν) (ft.^{2}/hour)	.039	.0044	.0030	.0064	.0047

* Data obtained from References 34 and 35.

their reciprocals, the many strain energy terms, of which all three types are included, could undoubtedly be combined and reduced considerably. The appearance of the tensile strength in an inverse relationship is not surprising since it was successful as a single correlating parameter in each of the three fluids. The acoustic impedance ratio is also included, and it is noted that the damage rate increases as the acoustic impedance ratio increases, as postulated. One might conclude that the acoustic impedance ratio is successful as a fluid coupling parameter in these experiments.

(2) Density (ρ)

The density was next combined with the other nine mechanical properties allowed to enter the predicting equation, and the statistically best correlation obtained is:

$$\begin{aligned}\text{Avg. MDP Rate} = 2.44 &- 1.62(\rho)^{-1/3} + 4.82\times10^{2}(E)^{-1/3} \\ &+ 2.07\times10^{3}(TSEE)^{-1} - 1.99\times10^{13}(E)^{-2} \\ &+ 4.26\times10^{4}(TSER)^{-1} - 7.35\times10^{-2}(H)^{1/2} \\ &- 5.48\times10^{2}(TSER)^{-1/2} + 2.36\times10^{8}(TS)^{-2}\end{aligned}$$

Coefficient of Determination = 0.969

Average Absolute % Deviation = 9.7%

Three of the terms present in the equation involve the true strain energy and two terms are functions of the elastic modulus. The tensile strength and hardness are also present, each indicating that a decrease in damage rate would be

expected with increasing tensile strength or hardness. The density also appears as the fluid coupling parameter; and despite the negative exponent, increasing density would result in increased damage, since the coefficient of the term is negative. This is consistent with the observations in our own laboratory both in the venturi[18,24,25] and vibratory facilities, and has, of course, been postulated by other investigators.[32]

(3) Surface Tension (σ)

In a similar manner the surface tension was investigated as a possible fluid coupling parameter, and the statistically best predicting equation obtained is:

$$\text{Avg. MDP Rate} = 0.982 - 6.38(RA)^{-1/3} + 2.50\times10^{-6}(\sigma)^{2} - 1.28(ELON)^{-1/2} + 2.36\times10^{4}(TSER)^{-1} + 4.53\times10^{2}(ESE)^{-1} + 14.87(TSEE)^{-1/3} - 1.28\times10^{13}(E)^{-2}$$

Coefficient of Determination = 0.923

Average Absolute % Deviation = 2.4%

Again, three of the terms involve various forms of the strain energy. The surface tension enters with an exponent of 2, whereas the acoustic impedance ratio and density were each raised to the 1/3 power. The correlation indicates that increasing surface tension results in increased damage. This behavior was confirmed experimentally by Nowotny,[33] but is not consistent with numerical analyses of bubble collapse.[36,37] However, the simplified models used may in some way neglect the mechanism here involved.

(4) Net Positive Suction Head (NPSH)

Since the local pressure was varied in our experiments so as to maintain the difference between local pressure and vapor pressure constant, the static net positive suction head is inversely proportional to the density, but the dynamic NPSH applied by the horn is more closely constant, as already discussed. The correlation was carried out, and the statistically best predicting equation obtained is:

$$\begin{aligned}\text{Avg. MDP Rate} = &- 1.17\times10^{2} + 5.60\times10^{-3}(E)^{1/2} + 1.01\times10^{7}(TSEE)^{-2} \\ &- 3.68\times10^{2}(RA)^{-3} + 1.88\times10^{3}(TSER)^{-1/2} \\ &+ 5.81\times10^{4}(E)^{-1/3} + 2.76\times10^{4}(TS)^{-1} \\ &- 2.48\times10^{-2}(NPSH) - 45.21(TSEE)^{-1/2} \\ &- 5.12\times10^{2}(TSER)^{-1/3} - 5.17\times10^{5}(E)^{-1/2}\end{aligned}$$

Coefficient of Determination = 0.962

Average Absolute % Deviation = 5.0%

Two terms are functions of each of the forms of true strain energy used, while three additional terms involve the elastic modulus. The tensile strength appears in an inverse relationship, as expected, and the net positive suction head is present in a linear manner, but with negative coefficient. Hence, increasing net positive suction head results in a decrease in cavitation damage. However, this may be merely the density effect previously discussed.

(5) Bulk Modulus (B)

The statistically best predicting equation obtained when bulk modulus is introduced as the fluid coupling parameter is:

$$\text{Avg. MDP Rate} = 0.665 - 1.66\text{x}10^{2}(\text{TS})^{-1/2} - 2.59\text{x}10^{16}(\text{B})^{-3} + 5.27\text{x}10^{6}(\text{TSEE})^{-2} + 1.13\text{x}10^{4}(\text{H})^{-2} + 3.49\text{x}10^{7}(\text{TSER})^{-2} - 4.53\text{x}10^{5}(\text{H})^{-3} + 1.99\text{x}10^{13}(\text{TS})^{-3} + 9.02\text{x}10^{6}(\text{E})^{-1}$$

Coefficient of Determination = 0.975

Average Absolute % Deviation = 5.1%

The true strain energy, hardness, and tensile strength are each entered in the equation twice, while the bulk modulus is present with both a negative exponent and negative coefficient. Hence, as the bulk modulus is increased (compressibility decreased), the damage would increase, as expected theoretically,[36,37] and as often observed in field practice where damaging cavitation with petroleum pumps is virtually unknown as compared to water pumps. This trend has also been reported in a previous laboratory investigation using a vibratory facility.[32]

(6) Kinematic Viscosity (ν)

The final fluid coupling parameter investigated was the kinematic viscosity, ν . The statistically best predicting equation obtained in this case was:

$$\text{Avg. MDP Rate} = -0.294 + 6.91\text{x}10^{2}(E)^{-1/3} - 1.30\text{x}10^{2}(TSER)^{-1/3} + 3.13\text{x}10^{4}(H)^{-3} + 25.40(TSEE)^{-1/3} + 3.76\text{x}10^{4}(TSER)^{-1} - 5.95\text{x}10^{-3}(RA)^{1/2} - 6.30\text{x}10^{2}(\nu)^{2} + 0.243(ELON)^{1/3} - 2.54\text{x}10^{13}(E)^{-2} + 2.04\text{x}10^{-5}(\nu)^{-1}$$

Coefficient of Determination = 0.963

Average Absolute % Deviation = 2.2%

The true strain energy is involved in three terms while the elastic modulus appears in two. The hardness is also prominent in a strong inverse relationship. The kinematic viscosity, ν , appears in two terms, such that increasing kinematic viscosity results in a decrease in cavitation damage, as postulated.

A summary of the statistics applicable to the six comprehensive damage correlations discussed above are presented in Table XXVIII. The fluid coupling parameters considered are listed in an order determined by the coefficient of determination of the corresponding predicting equation. It is seen that the acoustic impedance ratio results in the predicting equation with highest coefficient of determination. However, all fluid properties considered as coupling parameters were quite successful in this regard. It should be emphasized that the acoustic impedance ratio involves both the density and bulk modulus of the fluid. All predicting equations had a value of coefficient of determination greater than 0.960, except when the surface tension was employed as the coupling parameter. In addition, the average absolute percent

TABLE XXVIII

SUMMARY OF STATISTICS FOR COMPREHENSIVE DAMAGE CORRELATIONS

Fluid Coupling Parameter	CD*	AAPD*
1. Acoustic Impedance Ratio (AI)	0.980	2.7
2. Bulk Modulus (B)	0.975	5.1
3. Density (ρ)	0.969	9.7
4. Kinematic Viscosity (ν)	0.963	2.2
5. Net Positive Suction Head (NPSH)	0.962	5.0
6. Surface Tension (σ)	0.923	2.4

* Coefficient of Determination
** Average Absolute % Deviation

deviation was less than 10% in all cases. As a result, it is difficult to make any recommendations as to an optimum fluid coupling parameter. All fluid properties considered in this study seem to be successful. The resulting predicting equations show a strong dependence on strain energy, hardness, tensile strength, and elastic modulus. In fact, the six predicting equations described above contained terms involving some form of strain energy 23 times (TSER-12, TSEE-8, and ESE-3), elastic modulus 9 times, tensile strength 5 times, hardness 4 times, reduction in area 3 times, and elongation 2 times. Of course, a coupling parameter was present in each equation, although it was by no means forced into the equation. It will be recalled that strain energy, tensile strength, and hardness were the most successful properties in the

single property correlations of lead-bismuth, mercury, and water separately. These mechanical properties along with the elastic modulus are also the most prominent in the comprehensive lead-bismuth, mercury, and water correlations.

The fact that all the forms of strain energy are sometimes involved and that their relative involvement depends on fluid, temperature, material, etc., may indicate that different modes of material failure are involved, depending upon the various test parameters, since it would be expected that TSER would most closely represent resistance to ductile failure while TSEE would be most closely involved with brittle failure.

Figure 29 is a plot of the predicted values of average MDP rate, computed using the comprehensive predicting equation with acoustic impedance ratio as the coupling parameter, versus the corresponding experimental data points, and indicates the extent of agreement afforded by this analysis.

J. Comparison with Venturi Facility Correlations

Previously[18], computer correlations of cavitation damage data generated in this laboratory's mercury and water venturi facilities were carried out and reported. It was found that no good correlation existed between any single mechanical property and the cavitation damage in the mercury tests. The ten property correlation of the mercury data showed that a combination of true breaking stress and tensile strength was significant. In the case of the ultrasonic investigations described above, true strain energy (based on elongation), hardness, and tensile strength were successful in the single property correlations. These same properties dominated the ten property correlations.

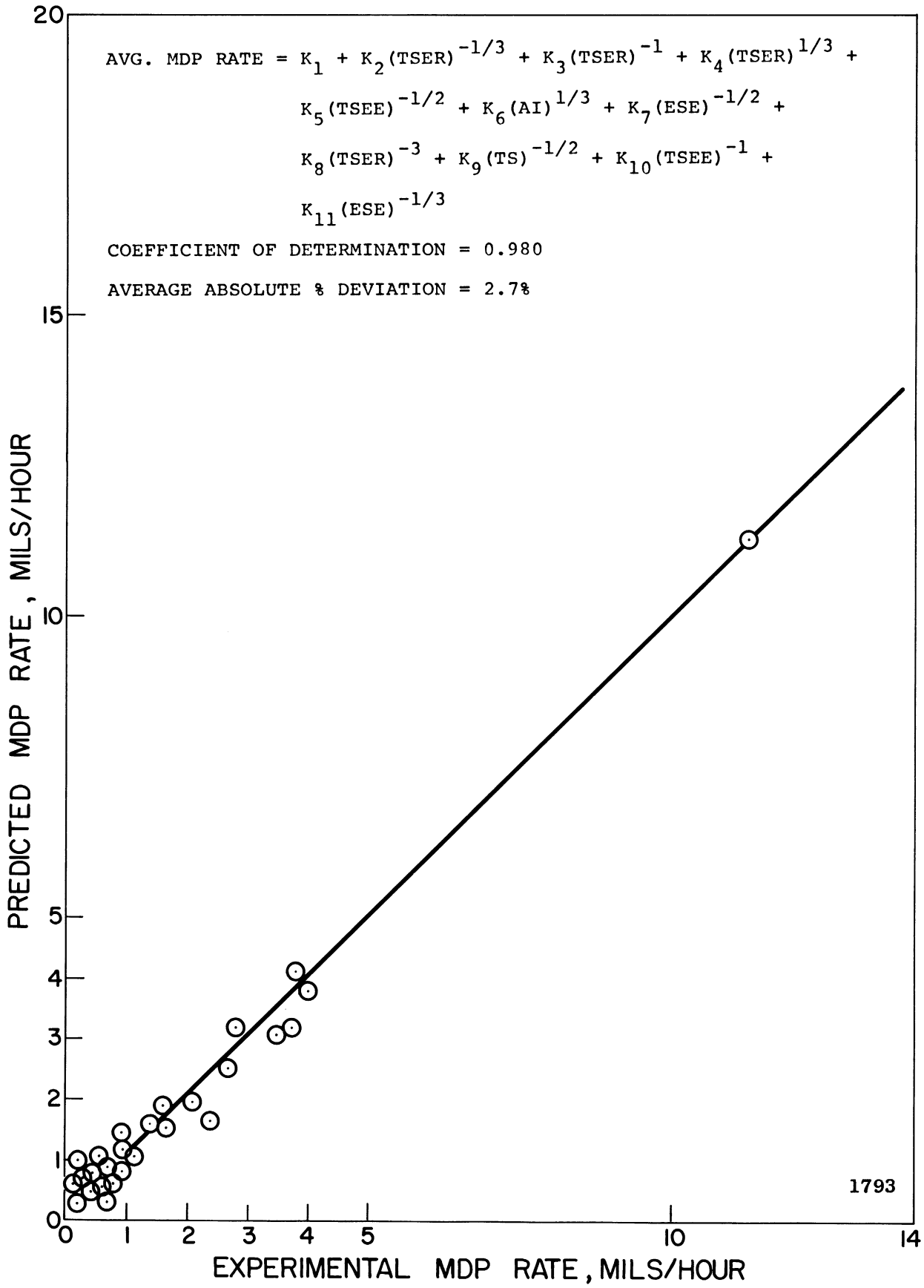

Figure 29. Comparison of Predicted MDP Rate and Experimental MDP Rate - All Lead-Bismuth, Mercury, and Water Data (Acoustic Impedance Ratio is the Fluid Coupling Parameter).

In the single property correlations of the full set of water data obtained in the venturi facility, it was found that the acoustic impedance ratio and the elastic modulus resulted in the best fit statistical expressions. The corresponding ultrasonic studies showed the hardness and tensile strength to be the most suitable.

Single property correlations of the subset of water data involving materials also tested in mercury were also carried out for the venturi facility. These materials correspond to Subset 1 of the acoustic results. It was found that elastic modulus and reduction in area result in good fits individually. Subset 1 of the water data in the ultrasonic facility was correlated well in terms of tensile strength, hardness, yield strength, or elastic modulus. Here there is some agreement among the two facilities.

The analysis of the remainder of the venturi water data (i.e., those materials tested in water only) on a single property basis shows that the correlation with elastic modulus and acoustic impedance ratio again is very good. This was also true with the full set of water data. These materials correspond to Subsets 2 and 3 of the acoustic water data where hardness, tensile strength, and reduction in area were successful as single correlating parameters.

The correlation of the full set of venturi water data and the two subsets resulted in predicting equations where the acoustic impedance ratio, elastic modulus, tensile strength, and true breaking stress were the most prominent properties. The corresponding ultrasonic

studies showed the tensile strength, hardness, and yield strength to be the predominant terms.

Correlations of the combined water and mercury venturi damage results are not yet available for comparison with the corresponding ultrasonic analysis.

In general, it is seen that the venturi results are best correlated in terms of true breaking stress, acoustic impedance ratio, elastic modulus, and tensile strength. The ultrasonic results correlate best in terms of tensile strength, hardness, elastic modulus, and strain energy. There is no explanation at this time as to the differences that exist. Undoubtedly, they are due to differences in the damaging mechanism itself in the two facilities.

CHAPTER X

SUMMARY AND CONCLUSIONS

Ultrasonic-induced cavitation studies have been conducted in mercury at 500°F and 70°F and in water at 70°F for a wide variety of materials including refractory alloys, steels, brasses, coppers, plastics, etc. The detailed results for the various fluid-material-temperature combinations are listed in the appropriate sections of the report. Various salient features include the following:

(a) All materials tested in mercury sustained greater damage at 500°F than at 70°F with the exception of the hot-rolled carbon steel. This is explained by the superior mechanical properties of this material at the higher temperature.

(b) Plexiglas was relatively much less cavitation-resistant in mercury than in water. This is consistent with previous observations from this laboratory in venturi tests.

(c) Detailed examination of the wetted but non-cavitated parts of the equipment indicates that corrosion effects in the absence of cavitation were not a factor in these investigations.

(d) For these tests wherein the applied static pressure above vapor pressure was held constant for the different tests, damage rates with mercury were 3 to 20 times greater than for water. No corresponding direct comparison was possible in the venturi tests[18], although generally damage with mercury was greater.

(e) In general, the damage rate was constant throughout the tests for the liquid metal tests and for most of the water tests. However, in some of the water tests the damage rate decreased markedly during the test. It is felt that this is a result of the very deep isolated pitting encountered in these tests. In general, water tests differed from the liquid metal tests in that quite uniform and relatively fine damage was encountered in the liquid metal tests as opposed to the water tests on the same materials. This may be a result of improper modeling of the fluid flow regime between the two fluids. The test durations were so adjusted that the total accumulative mean depth of penetration was always less than about 10 mils. It is within the range between zero and 10 mils MDP (ignoring the very early part of the test below perhaps 1.0 MDP) that the damage rates were substantially constant.

(f) Direct comparison of venturi and vibratory results from this laboratory shows that the rankings of materials for cavitation damage are quite similar, and particularly so for the mercury tests, but that the relative ratios between different materials are much greater in the venturi facility. The damage rates in the vibratory tests are of the order of 10^3 times those in the venturi, so that corrosive effects are much less important in the vibratory tests. This factor may be responsible for some of

the discrepancies in the comparisons of results from these two facilities.

Computer correlations of the cavitation damage data with applicable mechanical and fluid properties indicate the following important conclusions:

(a) There is no single material mechanical property which can be used to correlate the damage, even if coupling parameters to account for fluid property changes are included in the correlation.

(b) In general, the best correlations include one or more energy-type mechanical properties, one or more strength-type properties, and one or more fluid coupling parameters if the fluid properties are varied in the data set.

(c) The energy-type properties are more predominant in the tests with the high-density liquid metals, while the strength-type properties predominate for the water tests. This is consistent with theoretical expectations.

(d) No relatively simple single correlating equation applies well to all the data. If sufficient terms are allowed, of course, any degree of fit can be obtained. This lack of a single simple correlating equation may indicate that all important mechanisms in cavitation damage may not have been considered. For example, it may not be possible to explain cavitation damage in terms of properties which are

determined under semi-static conditions. Final conclusions in this regard must await the obtaining of additional data and more comprehensive correlations.

BIBLIOGRAPHY

1. Royal Society Discussion on Deformation of Solids Due to Liquid Impact, May 27, 1965; London, England.

2. Decker, O., "Cavitation Erosion Experience in Liquid Mercury Lubricated Journal Bearings," First Annual Mercury Symposium, November, 1965, Atomics International, Canoga Park, California, p. 14.

3. Shoudy, A. A., and Allis, R. J., "Materials Selection for Fast Reactor Applications," Proc. of Michigan ANS Fast Reactor Topical Meeting, April, 1965, Detroit, Michigan.

4. Wood, G. M., Kulp, R. S., and Altieri, J. V., "Cavitation Damage Investigations in Mixed-Flow Liquid Metal Pumps," Cavitation in Fluid Machinery, ASME, November, 1965, pp. 196-214.

5. Smith, P. G., DeVan, J. H., and Grindell, A. G., "Cavitation Damage to Centrifugal Pump Impellers During Operation with Liquid Metals and Molten Salt at 1050-1400°F, Journal of Basic Engineering, Trans. ASME, September, 1963, pp. 329-337.

6. Hunt, J. B., "Cavitation in Thin Films of Lubricant," The Engineer, January 29, 1965, pp. 22-23.

7. Hammitt, F. G., "Cavitation Damage and Performance Research Facilities," Symposium on Cavitation Research Facilities and Techniques, pp. 175-184, ASME Fluids Engineering Division, May, 1964. See also ORA Technical Report No. 03424-12-T, Department of Nuclear Engineering, The University of Michigan, November, 1963.

8. Plesset, M. S., and Ellis, A. T., "On the Mechanism of Cavitation Damage," Transactions ASME, Vol. 77, No. 7 October, 1955. pp. 1055-1064.

9. Thiruvengadam, A., and Preiser, H. S., "On Testing Materials for Cavitation Damage Resistance," Hydronautics, Inc. Technical Report 233-3, December, 1963.

10. Rheingans, W. J., "Accelerated Cavitation Research," Transactions ASME, Vol. 72, No. 5, July, 1950, pp. 705-719.

11. Kerr, S. Logan, "Determination of the Relative Resistance to Cavitation Erosion by the Vibratory Method," Transactions ASME, Vol. 59, July, 1937, pp. 373-397.

12. Preiser, H. S., Thiruvengadam, A., and Couchman, C. E., "Cavitation Damage in Liquid Sodium," Technical Report 235-1, Hydronautics, Inc., April 1, 1964.

13. Couchman, C. E., Preiser, H. S., and Thiruvengadam, A., "Cavitation Damage in Liquid Metals," Technical Progress Report 467-1 For the Period April 20, 1964, to December 31, 1964, Hydronautics, Inc., March 10, 1965.

14. Garcia, R., and Hammitt, F. G., "Ultrasonic-Induced Cavitation in Liquid Metals at 1500°F," Internal Report No. 05031-1-I, Department of Nuclear Engineering, The University of Michigan, February, 1965; also Transactions of the American Nuclear Society, Volume 8, No. 1, pp. 18-19, June, 1965.

15. Garcia, R., and Hammitt, F. G., "Ultrasonic-Induced Cavitation in Liquid Metals at 500°F," Internal Report No. 05031-3-I, Department of Nuclear Engineering, The University of Michigan, April, 1965.

16. Hammitt, F. G., "Observations on Cavitation Damage in a Flowing System," Journal of Basic Engineering, Transactions ASME, Series D, Vol. 85, 1963, pp. 347-359.

17. Hammitt, F. G., Barinka, L. L., Robinson, M. J., Pehlke, R. D., and Siebert, C. A., "Initial Phases of Damage to Test Specimens in a Cavitating Venturi as Affected by Fluid and Material Properties and Degree of Cavitation," Journal of Basic Engineering, Transactions ASME, June, 1965, pp. 453-464.

18. Robinson, M. John, "On the Detailed Flow Structure and the Corresponding Damage to Test Specimens in a Cavitating Venturi," Ph.D Thesis and ORA Technical Report No. 03424-16-T, Department of Nuclear Engineering, The University of Michigan, August, 1965.

19. Plesset, M. S., "The Pulsation Method for Generating Cavitation Damage," Journal of Basic Engineering, Transactions ASME, Vol. 85, Series D, No. 3, 1963, pp. 360-364. See also "Pulsing Technique for Studying Cavitation Erosion of Metals," Corrosion, Volume 18, No. 5, pp. 181-188, May, 1962.

20. Garcia, R., and Hammitt, F. G., "Ultrasonic-Induced Cavitation Studies," ORA Technical Report No. 05031-1-T, Department of Nuclear Engineering, The University of Michigan, October, 1964.

21. Mason, W. P., "Internal Friction and Fatigue in Metals at Large Strain Amplitudes," Journal of the Acoustical Society of America, Vol. 28, No. 6, pp. 1207-1218, November, 1956.

22. Garcia, R., and Hammitt, F. G., "Ultrasonic-Induced Cavitation Studies in Lead-Bismuth Alloy at Elevated Temperatures," ORA Technical Report No. 05031-2-T, Department of Nuclear Engineering, The University of Michigan, June, 1965.

23. Hammitt, F. G., "Observations on Cavitation Damage in a Flowing System," Journal of Basic Engineering, Transactions ASME, Vol. 85, September, 1963, pp. 347-359.

24. Hammitt, F. G., Barinka, L. L., Robinson, M. J., Pehlke, R. D., and Siebert, C. A., "Initial Phases of Damage to Test Specimens in a Cavitating Venturi as Affected by Fluid and Material Properties and Degree of Cavitation," Journal of Basic Engineering, Transactions ASME, June, 1965, pp. 453-464.

25. Hammitt, F. G., "Damage to Solids Caused by Cavitation," to be published Proc. Royal Society; presented at Royal Society Discussion on Deformation of Solids Due to Liquid Impact, May 27, 1965, London, England.

26. Plesset, M. S., and Devine, R. E., "Effect of Exposure Time on Cavitation Damage," ASME Paper No. 65-WA/FE-23; to be published Journal of Basic Engineering, Transactions ASME.

27. Personal Communication from Henry P. Leeper, Project Metallurgist, Pratt & Whitney Aircraft (CANEL), to F. G. Hammitt; February 26, 1965, and May 13, 1965.

28. Westervelt, Franklin H., "Automatic System Simulation Programming," Ph.D. Thesis, College of Engineering, The University of Michigan, November, 1960.

29. Crandall, Richard L., "The Mathematical and Logical Procedure of the Stepwise Regression Program with Learning," University of Michigan Computing Center Internal Report, 1965.

30. Harrison, Curtis A., Robinson, M. John, Siebert, Clarence A., Hammitt, Frederick G., and Lawrence, Joe, "Complete Mechanical Properties Specifications for Materials as Used in Venturi Cavitation Damage Tests," Internal Report No. 03424-29-I, Department of Nuclear Engineering, The University of Michigan, August, 1965.

31. Blitz, J., Fundamentals of Ultrasonics, Butterworth & Co., Ltd., London, England, 1963.

32. Wilson, R. W., and Graham, R., "Cavitation of Metal Surfaces in Contact with Lubricants," Conference on Lubrication and Wear, The Institution of Mechanical Engineers, London, England, October, 1957.

33. Nowotny, H., "Destruction of Materials by Cavitation," VDI-Verlag, Berlin, Germany, 84, 1942. Reprinted by Edwards Brothers, Inc., Ann Arbor, Michigan, 1946. English language translation as ORA Internal Report No. 03424-15-I, Department of Nuclear Engineering, The University of Michigan, 1962.

34. Liquid Metals Handbook, Richard N. Lyon, Editor-in-Chief, Second Edition, June, 1952.

35. International Critical Tables, Compiled by Clarence J. West and Callie Hull, McGraw-Hill Book Company, New York, 1933.

36. Ivany, R. D., "Collapse of a Cavitation Bubble in Viscous Compressible Liquid - Numerical and Experimental Analyses," Ph.D. Thesis, Department of Nuclear Engineering, The University of Michigan, Ann Arbor, Michigan, April, 1965; also available as ORA Technical Report No. 03424-15-T, The University of Michigan.

37. Ivany, R. D., and Hammitt, F. G., "Cavitation Bubble Collapse in Viscous Compressible Liquids - Numerical Analyses," ASME Paper No. 65-FE-16; to be published Journal of Basic Engineering, Transactions ASME.